KIET IJCE

KIET International Journal of Communications & Electronics

VOLUME 4, FIRST ISSUE, JAN-JUNE 2016, ISSN:2320-8996

Editorial Board

Editorial

Stable local feature detection and representation is a fundamental component of many image registration and object recognition algorithms. This issue gives an idea about examining (and improving upon) the local image descriptor used by SIFT. This also demonstrates the techniques that the more distinctive, more robust to image deformations, and more compact than the standard SIFT representation with increased accuracy and faster matching.

Recent advancement in wireless communications and electronics has enabled the development of Clustering routing protocols in wireless sensor network. Currently proposed clustering algorithms for Wireless Sensor Networks are examined. Comparisons on the performance between the various schemes in terms of the power and quality aspects is made. A review paper in the issue will provide the reader with a basis for research in clustering schemes for Wireless Sensor Networks.

Wireless communications services, cellular communication systems are going towards small cells with small transmit powers. Meanwhile device-to-device communication (D2D) is seen as a promising idea to increase the performance of wireless networks. In D2D, users in vicinity communicate directly without going through base station. A review on the concept of M2M (Machine-to-Machine) communications using D2D communications in cellular networks is given.

Quantum-dot cellular automata (QCA) technology has become an alternative to CMOS technology for future digital designs because it give low power dissipation, high density and no leakage current compared to CMOS Designs. Until now, parameters and area-delay cost functions are directly used from CMOS technology to compare QCA designs. This is not an appropriate approach because both the technologies are different. Therefore a comparative approach, several cost parameters are proposed which helps in evaluation of QCA Designs.

The microwave photonics can be defined as the study of optoelectronics devices and system operating at microwave frequency. The modulation and transmission in the frequency band between 100 GHz and 10THz is the area of interest. The transmission in microwave band has lot of loss and it can be compensated by using optical communication modulated by microwave frequencies. So combination of radio wave technology and photonics has become a necessity.

In this issue, a variety of anteena designs such as with vias and without vias are implemented and analysed to extend the bandwidth of proposed ZOR antenna which can be used for wireless applications like WLAN, WiMAX, Bluetooth etc. An ultra-wideband planar monopole antenna with tri notch along with a metamaterial structure has also been proposed with substrate height of 0.8mm.The antenna consist of semicircular radiating patch and a CSRR loaded ground plane. Another design of antenna for X-band and Wi-Max (Worldwide Interoperability for Microwave Access, 3.2–3.8 GHz) applications is also proposed. In proposed antenna slots created in ground plane and top patch provides wide bandwidth (4.6GHz) in X-band. This design approach is meant for satellite communication, amateur radio, military communication and middle band of Wi-Max applications. A metamaterial-inspired dual-mode antenna using rectangular type CSRR is proposed, and it is proposed that an increase in series capacitance will decrease the resonant frequency at which ZOR mode is achieved using rectangular type CSRR.

Preface

Dear Researchers,

We take this opportunity to welcome you all to the Volume No 4, Issue No. 1 of International Journal of Communications & Electronics (KIET - IJCE). This journal will provide a forum for in depth and substantial discussions on the theory, design and implementation of the emerging technologies in Communications, Networking, Microwave and Electronics techniques, thus providing solutions and strategies for business resilience.

It gives us an immense pleasure to have an amalgam of researchers from the fields of Communication Engineering, Electronics, and related technologies. The purpose of the Journal is to provide a platform to foster interdisciplinary communication among the delegates and to support the sharing process of diverse fields in various concepts and principles related to these domains.

Our appreciation also goes to entire team whose dedication and timeless efforts have gone for number of days for the second issue of the Journal.

Editors

Message

I am delighted to note that the Department of Electronics and Communication Engineering, KIET Group of Institutions, Ghaziabad is introducing Volume No 4, Issue No. 1 of International Journal of Communications and Electronics (KIET - IJCE).

I appreciate the efforts on the part of the Editorial Committee in bringing out an issue on Communications, Networking, Microwave and Electronics techniques.

I understand that the papers contributed for publication in the Volume No 4, Issue No. 1 are on almost all the current aspects of Communication Systems, Electronics systems, Microwave Engineering, Signal Processing & Applications, Networking Technologies and several others.

I have great pleasure in congratulating the Editors of this issue of KIET - IJCE for their untiring efforts in bringing out this third Volume No 3, Issue No. 1 of KIET-IJCE which will be a valued treasure for all who pursue research in Communications, Networking, Microwave and Electronics Engineering areas.

Let me close with warmest regards.

Dr. J. Girish
Director
KIET Group of Institutions

Message

It gives me immense pleasure in writing this foreword for the Volume No 4, Issue No.1 of the KIET International Journal on Communications and Electronics (KIET - IJCE). This journal is targeted towards researchers, professionals, educators and students to share innovative ideas, issues, recent trends and future directions in the fields of Electronics and Communication Engineering.

The Volume No 4, Issue No. 1 of the journal KIET-IJCE includes papers on the theory, design and implementation of the emerging technologies in the field of Communications, Networking, Microwave and Electronics techniques. Furthermore, it will enable the researchers in various domains to foster the exchange of concept, protypes, research ideas and the results of research work which could contribute to the academic arena and also befit business and industrial community.

Dr. Sanjay Sharma
Editor – in - chief
KIET - IJCE

FOURTH VOLUME

FIRST ISSUE

(JAN-JUNE 2016)

KIET IJCE KIET International Journal of Communications & Electronics
Volume. No. 4, Issue No. 1, January-June 2016, ISSN: 2320 - 8996

Object recognition using Robotic Vision

M.Umamurugan[1], C.S.Sundar Ganesh[2], R.T.Karthick[3]
[1]PG Student, Department of EEE,PSG College of Technology, Coimbatore
[3]Asst.Professor, Department of EEE, PSG College of Tecchnology, Coimbatore
[2]Asst.Professor, Department of RAE, PSG College of Tecchnology, Coimbatore
css@rae.psgtech.ac.in

Abstract—**Stable local feature detection and representation is a fundamental component of many image registration and object recognition algorithms. Mikolajczyk and Schmid recentlyevaluated a variety of approaches and identified the SIFT algorithm as being the most resistant to common image deformations. This paper examines (and improves upon) the local image descriptor used by SIFT. Like SIFT, our descriptors encode the salient aspects of the image gradient in the feature point's neighborhood; however, instead of using SIFT's smoothed weighted histograms, we apply Principal Components Analysis (PCA) to the normalized gradient patch. Our experiments demonstrate that the PCAbased local descriptors are more distinctive, more robust to image deformations, and more compact than the standard SIFT representation. We also present results showing that using these descriptors in an image retrieval application results in increased accuracy and faster matching.**

Index Terms—**SIFT, PCA, Feature Extraction, Matching and Euclidean distance.**

I. INTRODUCTION

Object can be recognized by appearance based method and feature based method. Appearance based methods use template images of the objects to perform recognition .In feature based method, a search is used to find feasible matches between object features and image features. The processing of object recognition has the following stages: feature extraction and feature matching. In computer vision, the Scale Invariant Feature Transform (SIFT) is an algorithm to identify and characterize local features in images. SIFT is well designed and derives distinctive image feature descriptors for image matching but it still suffers from its high cost of computation and high dimensionality. Yan ke presents a more distinctive and more compact feature descriptor, PCA-SIFT, which applies Principal Components Analysis (PCA) to the normalized gradient patch instead of using SIFT's smoothed weighted histograms which results in dimensionality reduction of the descriptors.

II. RELATED WORKS

There is a long history of research in object recognition that has modelled 3D objects using multiple 2D views. Thisincludes eigen space matching [7], which measures distance from a basis set of eigenvalue images; and histogram matching [9] which summarizes image appearance with histograms of selected properties. Earlier work [2] by the author (Lowe, 1999) extended the local feature approach to achieve scale invariance. Lowe [4, 2, 3] overcome such problems by detecting the points of interest over the image and its scales through the location of the local extrema in a pyramidal Difference of Gaussians (DOG). The Lowe's descriptor, which is based on selecting stable features in the scale space, is named the Scale Invariant Feature Transform (SIFT). In the paper [8], the dimensionality reduction of SIFT using Principal Component Analysis (PCA) on each object category is proposed to reduce computational complexity and memory requirement during training process and investigated under the proposed bag of feature object categorization framework. A new strategy to minimize the dimensionality of SIFT features is proposed [11] and the main idea is to do the Principal Component Analysis in the keypoint descriptor computation stage of the standard SIFT.

III. OVERVIEW OF SIFT ALGORITHM

SIFT (Scale Invariant Feature Transform) features are widely used in object recognition. These features are invariant to changes in scale, 2D translation and rotation transformations. To a limited extent they are also robust to 3D projection transformations. SIFT features have the following advantages. They are invariant to scale. They are invariant to 2D transformations like transformations and translation and rotation. Lowe [1], showed that practically these features are invariant to a limited amount of 3D projection

transformations. SIFT features are invariant to changes in illumination

The Scale-Invariant Feature Transform (SIFT) is an algorithm to identify and characterize local features in images. It allows for correct object identification with low probability of mismatch and is easy to match against a large database of local features. The representation of the image features has a direct impact on the performance of an object recognition system. Thus, the characterization and evaluation of SIFT's performance is important to advance the research on object recognition.

The SIFT algorithm finds extrema points in scale space, and extracts position, scale, rotation invariant feature vectors. The major stages of computation of SIFT descriptors are divided into four major stages [2]: (1) scale-space extrema detection (i.e., identifying keypoints); (2) keypoint localization; (3) orientation assignment; and (4) keypoint descriptor computation. These stages are used to produce the set of image features. The sections below provide details for these stages.

A) *Scale-Space Extrema Detection*

The first stage of calculation is to search over all scales and image locations. The difference-of-Gaussian function is used to detect stable key point locations in scale space. This stage attempts to find those locations and scales that are identifiable from different views of the same object. This can be efficiently achieved by using a scale space function. Furthermore, it has been shown under reasonable assumptions that it must be based on a Gaussian function. The scale space of a two-dimensional image is defined by equation (1) as shown below:

$$L(x, y, \sigma) = G(x, y, \sigma) * I(x, y) \quad \ldots\ldots\ldots(1)$$

Where * is the convolution operator, G(x, y, σ) is a variable-scale Gaussian, and I (x, y) is the input image. The parameter σ is the scale of the key point and is also the standard deviation of the Gaussian function, equation (2).

$$G(x,y,\sigma) = \frac{1}{2\pi\sigma^2} e^{-(x^2+y^2)/2\sigma^2} \quad \ldots\ldots\ldots(2)$$

The difference of Gaussians function, $D(x, y, \sigma)$, is used to detect stable keypoint locations in scale space; $D(x,y,\sigma)$ is computed by using the difference between two images, one with scale k times the other. Then, $D(x, y, \sigma)$ is given by equation (3).

$$D(x, y, \sigma) = (G(x, y, k\sigma) - G(x, y, \sigma)) * I(x, y)$$
$$= L(x, y, k\sigma) - L(x, y, \sigma) \quad \ldots\ldots\ldots(3)$$

To detect the local maxima and minima of $D(x, y, \sigma)$, each point is compared with its 8 neighbors at the same scale, and its 9 neighbors up and down one scale. If this value is the minimum or maximum of all these points then this point is an extrema. The extrema is used as a SIFT key point.

B) Key point Localization

In order to enhance the stability of the follow-up image feature matching and increase the algorithm's anti-noise ability, we need to remove the low-contrast and unstable key points. This stage attempts to eliminate these unstable key points from the final list of key points by finding those that have low contrast or are poorly localized on an edge. This may be achieved by calculating the Laplacian value for each keypoint found in stage one. The location of extrema, z, is given by equation (4).

$$z = -\frac{\partial^2 D^{-1}}{\partial x^2}\frac{\partial D}{\partial x} \quad \ldots\ldots\ldots(4)$$

C) Orientation Assignment

This step aims to assign a consistent orientation to the key points based on local image properties. The key point descriptor can then be represented relative to this orientation, achieving invariance to rotation. The gradient magnitude, m, and orientation, μ, of (x, y) are given in equations (5) and (6)

$$m(x,y) = \sqrt{(L(x+1,y) - L(x-1,y))^2 + (L(x,y+1) - L(x,y-1))^2} \quad \ldots(5)$$

$$\mu(x,y) = \tan^{-1}((L(x,y\mp1) - (L(x,y-1)/(L(x+1,y) - L(x-1,y))) \quad \ldots(6)$$

D) Key point Descriptor Calculation

The local image gradients are measured at the selected scale in the region around each key point. These are transformed into a representation that allows for significant levels of local shape distortion and change in illumination. The local gradient data, used above, is also used to create key point descriptors. The gradient information is rotated to line up with the orientation of the key point and then weighted by a Gaussian with a variance of 1.5 * the key point scale. These data are then used to create a set of histograms over a window centered on the key point. Key point descriptors typically use a set of 16 histograms, aligned in a 4×4 grid, each with 8 orientation bins, one for each of the main compass directions and one for each of the mid-points of these directions. This process results in a feature vector containing 128 elements.

IV. NEED FOR PCA

SIFT features are invariant to scale and 2D transformations like transformations and translation and rotation. These features are also invariant to a limited amount of 3D projection transformations. However SIFT has its own problems. First, the number of SIFT features that are generated from an image cannot be controlled. The second problem is computational as SIFT features are of high

dimension. Thus the major problem in SIFT is its very high dimension. The large computational effort associated with matching all the SIFT features for recognition tasks, limits its usage to many applications.

There are two main reasons that we take the PCA-SIFT descriptor instead of the SIFT descriptor in this paper. First, the standard SIFT feature vector will contain a great number of redundant information, which are undesirable for describing the objects. PCA-SIFT will apply the PCA method to minimize this redundancy which is mainly derived from the background features in the local image patches. Also the shows the dimensionality is reduced for PCA SIFT compared to other methods [2].

V.PRINCIPAL COMPONENT ANALYSIS

Principal Component Analysis (PCA) is a standard technique for dimensionality reduction and has been appliedto a broad class of computer vision problems, including feature selection object recognition and face recognition. While PCA suffers from a number of shortcomings such as its implicit assumption of Gaussian distributions and its restriction to orthogonal linear combinations, it remains popular due to its simplicity. The contribution of this paper lies in rigorously demonstrating that PCA is well-suited to representing key point patches and that this representation significantly improves SIFT's matching performance.

The first three stages of PCA SIFT is same as that of SIFT algorithm. The difference arises in the third stage which is the key point descriptor stage. PCA-SIFT applies Principal Components Analysis (PCA) to the normalized gradient patch instead of using SIFT's smoothed weighted histograms. This algorithm for local descriptors accepts the same input as the standard SIFT descriptor: the sub-pixel location, scale, and dominant orientations of the key point. We extract a 41×41 patch at the given scale, centered over the key point, and rotated to align its dominant orientation to a canonical direction.

VI. PCA SIFT DESCRIPTION

PCA-SIFT can be summarized in the following steps: (1) pre-compute an Eigen space to express the gradient images of local patches; (2) given a patch, compute its local image gradient; (3) project the gradient image vector using the Eigen space to derive a compact feature vector. This feature vector is significantly smaller than the standard SIFT feature vector, and can be used with the same matching algorithms. The Euclidean distance between two feature vectors is used to determine whether the two vectors correspond to the same keypoint in different images.

A) Computation of local image gradient for patches

PCA enables us to linearly-project high-dimensional samples onto a low-dimensional feature space. For our application, this projection (encoded by the patch Eigen space) can be pre-computed once and stored. The input vector is created by concatenating the horizontal and vertical gradient maps for the 41×41 patch centered at the key point. Thus, the input vector has 2×39×39=3042 elements.

More precisely, each of the patches satisfies the following properties: (1) it is centered on a local maximum in scale-space; (2) it has been rotated so that one of the dominant gradient orientations is aligned to be vertical; (3) it only contains information for the scale appropriate to this key point – *i.e.*, the 41×41 patch may have been created from a much larger region from the original image. The remaining variations in the input vector are mainly due to the "identity" of the keypoint or to unmodeled distortions. These remaining variations can be reasonably modelled by low-dimensional Gaussian distributions, enabling PCA to accurately represent them with a compact feature representation.

B) *Projection of gradient image vector*

More importantly, projecting the gradient patch onto the low-dimensional space appears to retain the identity related variation whilediscarding the distortionsinduced by other effects. Each was processed as described above to create a 3042-element vector, and PCA was applied to the covariance matrix of these vectors. The matrix consisting of the top n eigenvectors was stored on disk and used as the projection matrix for PCA-SIFT. The images used in building the Eigen space were discarded and not used in any of the matching experiments.

C)Feature representation

To find the feature vector for a given image patch, we simply create its 3042-element the normalized image gradient vector and project it into the feature space using the stored Eigen space. It is empirically determined good values for the dimensionality of the feature space, n to be 20. The standard SIFT representation employs 128-element vectors whereas PCA SIFT results in significant space benefits. Thus the PCA SIFT feature descriptor obtained is dimensionally reduced compared to that of SIFT descriptor.

VII. IMAGE FEATURE MATCHING

Image matching, also referred to as image correspondence, plays an important role in many aspects of computer vision. For instance, objects recognition, image retrieval, stereo correspondence, building panoramas and so on. Two main problems prevent us from matching progress. First, the number of elementary primitives in an image is large. The other problem is the possible variance between matching image pairs. Translations, rotations, scales and luminance changes can cause the difference of two pictures. It is virtually

impossible to compare two images using traditional methods such as a direct comparison between grey values. Two methods enabling a more reliable comparison have been developed: correlation-based methods and feature-based methods. The correlation-based methods still involve all the pixels in images but all pixels will be grouped as windows with certain sizes. On the contrary, feature-based methods just focus on sparse sets of features.

Feature point matching is done as follows. Given an interest feature point in one image, the matches of that point in other image are to be found. The definition of match depends on the matching strategy. The distance between the descriptors is the main similarity criterion. The results for distance threshold-based matching reflect the distribution of the descriptors in space, so this strategy is used. If the distance between the particular pair of feature points falls below the chosen threshold t, this pair is termed as a match.

The Euclidean distance between two feature vectors is calculated to determine whether the two vectors belong to the same keypoint in different images. For each descriptor in image A the distance to all descriptors in image B is calculated. If ratio of the distance of the second closest distance to the closest is greater than or equal to 1.5 (threshold), the descriptor from A is matched to the one from B, otherwise the descriptor in A is not at all matched. This criterion is to avoid having too many false matches for points in image A which are not present in image

VIII. EXPERIMENTAL RESULTS

The matching is performed for real images pairs using both SIFT and PCA SIFT by distance ratio method for various thresholds. Also under different transformations, including rotation, jpeg compression and noise added. For every catalogue, a pair of images are taken in the range from small image transformations to large ones and the transformations are significant enough to illustrate the features of SIFT and PCA SIFT. The test images are illustrated in Figure 2a and Fig 2b.

Fig. 2a Image used for test

Fig. 2b Image used for test.

The number of keypoints obtained for the original and transformed image pairs for various transformations are shown in the table 2.

Image	Keypoints Detected
Giraffe	1528
Rotated giraffe	1421

Table 2. Number of Keypoints obtained for image pairs

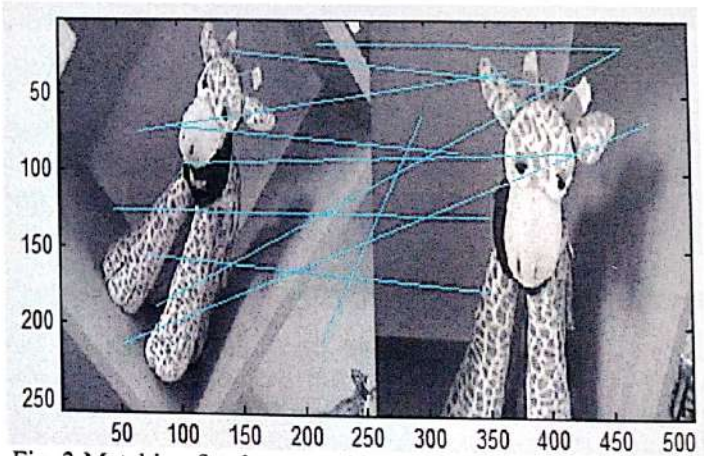

Fig. 3 Matching for the rotated image pair for threshold of 0.8 . Matches obtained by PCA SIFT

	SIFT	PCA SIFT
Dimensionality	High	Low
Dimension Value	128	20 or less
Computation	Less	Low
Memory Requirement	High	Low

Table3. Comparison between SIFT and PCA SIFT

IX. CONCLUSION

In this paper, local feature descriptor matching based on SIFT and PCA SIFT are done. By implementing PCA in SIFT, the dimensionality of the features is reduced. The matching points are also increased so as the accuracy as shown in the table 3. The performance evaluation and the matching local image descriptors by Singular Value Decomposition method instead of Euclidean distance method are considered to be the future work.

REFERENCES

[1] C. Schmid, R. Mohr, "Local Gray value Invariants for Image Retrieval", IEEE Transactions on Pattern Analysis and Machine Intelligence, Vol.19,PP.530-534,1997

[2] D.G. Lowe, "Distinctive Image Features from Scale Invariant Keypoints", Int'l J. Computer Vision, vol. 2, pp. 91-110, 2004

[3] D.G. Lowe, "Local Feature View Clustering for 3D Object Recognition", Proc. of the IEEE Conference on Computer Vision and Pattern Recognition, Hawaii, 2001 ,pp.682-688.

[4] D.G. Lowe, "Object Recognition from Local Scale Invariant Features", Proc. Seventh Int'l Conf. Computer Vision,Kerkyra, 1999,pp. 1150-1157.

[5] H. Bay, T. Tuytelaars, L. Van Gool, "SURF, Speeded Up Robust Features", Journal of Computer Vision and Understanding,Vol. 110, pp. 346-359, May 2006

[6] K. Mikolojczyk and C. Schmid, "A Performance Evaluation of local descriptors", IEEE Transaction on Pattern Analysis and Machine Intelligence, 2005, pp.1615-1630

[7] Murase, Hiroshi, and Shree K. Nayar, "Visual learning and recognition of 3-D objects from appearance", International Journal of Computer Vision, Vol. 14, pp. 5-24,1995

[8] N. Watcharapinchai , S. Aramvith , S. Siddhichai and S. Marukatat, "Dimensionality Reduction of SIFT using PCA for Object Categorization", International Symposium on Intelligent Signal Processing and Communication Systems, Bangkok, Feb 2008,pp. 1-4.

[9] Schiele, Bernt, and James L. Crowley, "Recognition without correspondence using multidimensional receptive field histograms", International Journal of Computer Vision,Vol.36,pp. 31-52, 2000 .

[10] Sai K. Vuppala, Sorin M. Grigorescu, DanijelaRistic, and Axel Graser, " Robust color Object Recognition for a Service robotic Task in the System FRIEND II", 10th International Conference on Rehabilitation Robotics - ICORR'07,Noordwijk,June 2007,pp. 704-713.

[11] Y. Ke and R. Sukthankar, "PCA-SIFT: a more distinctive representation for local image descriptors", IEEE Computer Society Computer on Computer Vision and Pattern Recognition, June 2004, pp. 506-513.

KIET IJCE KIET International Journal of Communications & Electronics
Volume. No. 4, Issue No. 1, January-June 2016, ISSN: 2320 - 8996

Microwave Photonics: - Analytic Study

Rishabh Rai,
Assistant Professor, Department of Electronics & Communication Engineering
Vidyadaan Institute of Technology & Management, Ariaon, Buxar, Bihar, 802119
rishabh.rahul001@gmail.com

Abstract – **Optoelectronics/photonics is integrated with microwave signals for their transmission and processing because low loss wide bandwidth capability of optoelectronics system has become an attractive technology for microwave transmission. The microwave photonics can be defined as the study of optoelectronics devices and system operating at microwave frequency. The key components require for microwave photonics applications include optical sources which can be modulated by high frequency, high speed photo detector, optically control microwave devices and suitable transmission media. Directly modulated semiconductor lasers are used to modulate frequency up to 40 GHz whereas external modulator are used for modulator frequency up to 100 GHz while photo detector operating at 10 THz modulation frequency has been realized. The modulation and transmission in the frequency band between 100 GHz and 10THz is the area of interest. The transmission in microwave band has lot of loss and it can be compensated by using optical communication modulated by microwave frequencies. So combination of radio wave technology and photonics has become a necessity.**

Government of India has installed a national broadband facility in which optical fiber communication is used to transmit data from National Capital to 6000 block centers passing through State headquarters and various cities but there is no solution to connect blocks with Panchyat in various villages. Microwave photonics can provide the above connectivity solution by transmitting data from block centers to various Panchyat through radio waves.

Keywords: Optoelectronics, Microwave, Photonics

I. INTRODUCTION

Microwave signal is modulated using optical carrier frequency for low loss wideband transmission. The signal at the transmitted end is again converted into radio waves & transmitted or else, microwave signal can be transmitted directly to the receiver using single mode/multimode optical fibers.

In one case, the radio waves at receiver end are detected & sent using optical fiber cables over long distances and reconverted at the end into audio/video/data. In another case, the optical carrier is directly sent at receiver end & reconverted into required output such as audio/video/data & text. The block diagram of basic structure of system of microwave photonics is given in figure 1.

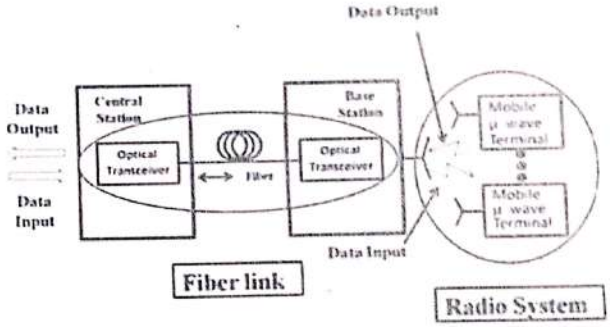

Figure 1. Basic block diagram.

Typical radio-wave application system is illustrated in Fig. 2. Wireless communication link consists of a transmitter (Tx) and a receiver (Rx) as shown in Fig. 2(a), and some kind of object is placed between the Tx and Rx in applications to measurement, testing, and sensing as shown in Fig. 2(b). Now, what happens when we introduce photonic technologies in Tx and Rx?

Figure 3 shows a block diagram of MWP-based transmitter, that is, a photonically assisted radio-wave transmitter. First, the optical (O) signal, whose intensity is modulated at microwave (MW) and/or millimeter-wave (MMW) frequencies, is generated by the optical MW/MMW signal source, and is

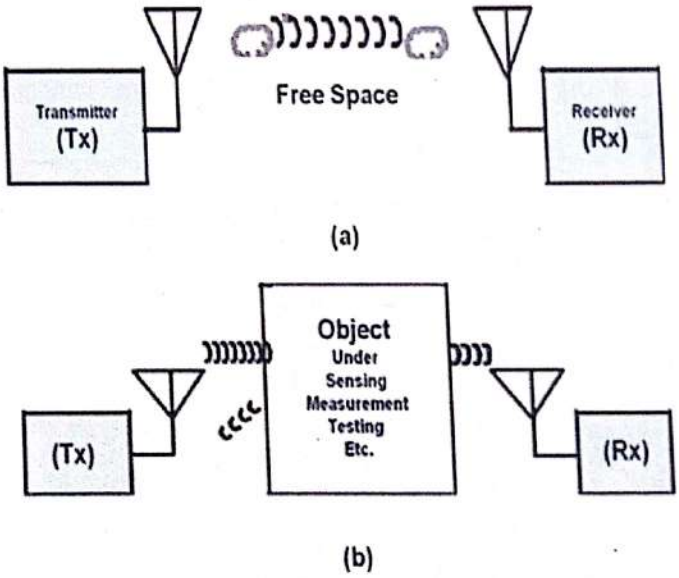

Figure 2. Radio-wave system (a) communication and (b) Measurement

delivered through optical fiber cables, and converted to the electrical (E) signal by a high-frequency O-E converter such as a photodiode. The converted signal is followed by a power amplifier and/or a frequency multiplier, and is finally radiated into free space by an antenna. The antenna unit can be separated and remotely controlled by optical fiber cables.

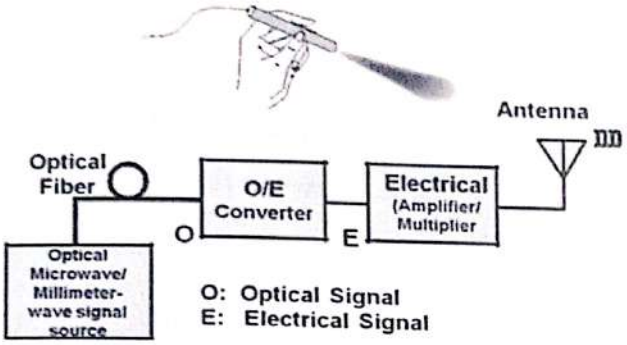

Figure 3. Photonically-assisted MW/MMW Transmitter.

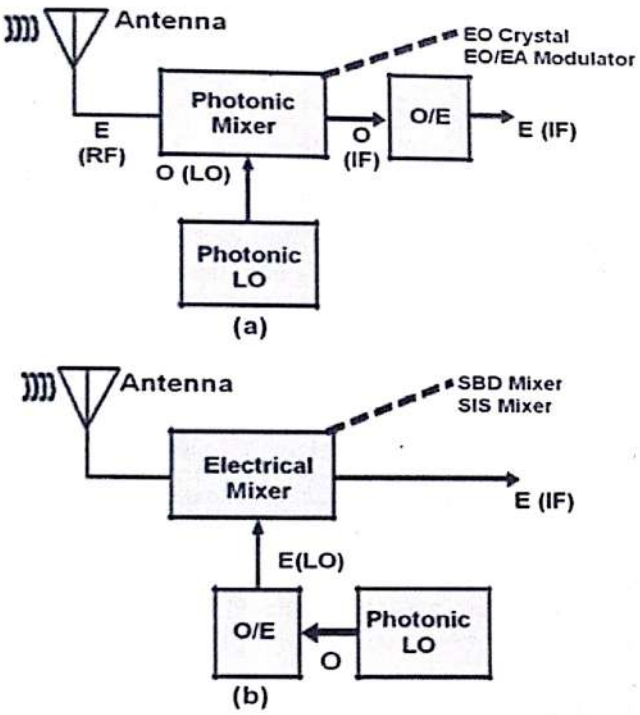

Figure 4. Photonically-assisted MW/MMW receiver.

Figure 4 shows two types of photonically-assisted radio-wave receivers; one employs a photonic mixer pumped by photonic local oscillator (LO) signals. Typical photonic mixer is a bulk electro- optic (EO) crystal, and optical modulator devices such As Electro-absorption (EA) modulator. Here, the optical intermediate frequency (IF) signal is converted to as a LiNbO waveguide EO modulator and a semiconductor the electrical IF signal by a slow photodiode. The other type is based on a nonlinear electrical mixer such as a Schottky-diode mixer, and a superconducting (SIS) mixer. The LO signal is generated by a high-frequency photodiode followed by the optical MW/ MMW signal source, as is used in the transmitter (Fig. 3).

II. ENABLING DEVICE TECHNOLOGIES

As for the optical MW/MMW source in Fig. 3, there are lots of options such as optical heterodyning using two frequency-tunable laser diodes, optical heterodyning using two modes filtered from a multi-frequency (wavelength) optical source or optical frequency comb generator (OFCG), the combination of a continuous-wave (CW) laser with an external modulator, and semiconductor mode-locked lasers (Fig. 5). Low-phase-noise and frequency-tunable optical MMW generators based on the optical heterodyning technique is shown in Fig. 6 [2].

Method	Frequency	Tunability	Stability/ noise
Heterodyning two LDs	Excellent >10 THz	Excellent >10 THz	Bad *frequency drift large linewidth*
CW LD + External modulator	Fair <100 GHz	Fair <100 GHz	Excellent *determined by electronics*
Mode-locked laser diode (passive/active)	Good Passive >1 THz Active 240 GHz	Bad <1 GHz	Excellent *only for active*
Optical comb (OFCG) + Filter	Excellent > 1THz	Excellent >1 THz	Excellent *determined by electronics*

Figure 5. Comparison of CW optical MW/MMW sources.

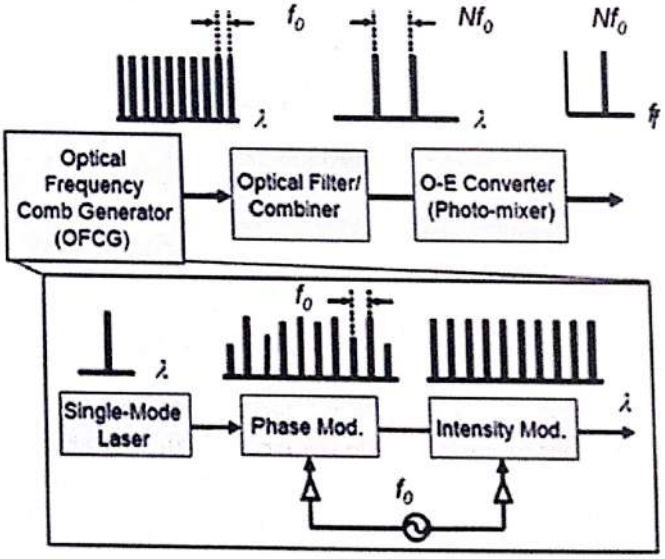

Figure 6. Example of Optical Heterodyning Techniques.

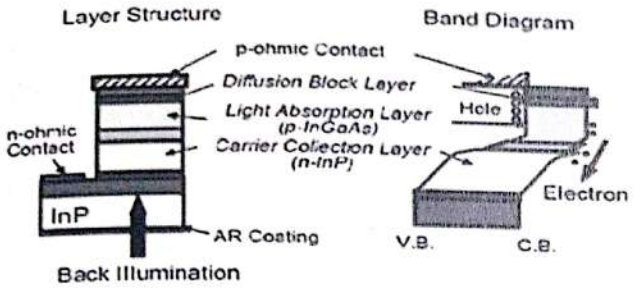

Figure 7. Structure of UTC-PD.

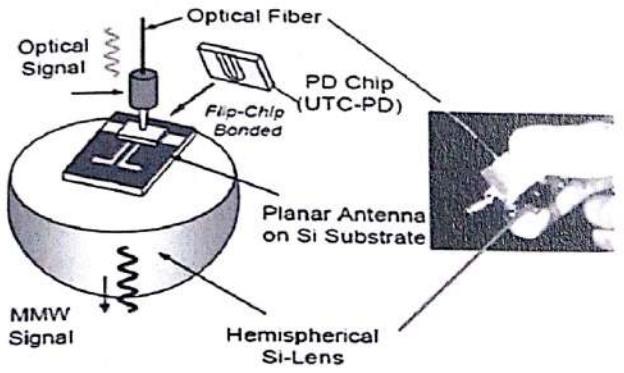

Figure 8. Example of Photonic MMW Emitter.

An O-E converter is a key device in the system. Since optical amplifiers with a high gain of over 30 dB and a large bandwidth of over 1 THz are now readily available, a high-power O-E converter to boost the signal generator performance is needed. An ultrafast photodiode called a uni-traveling-carrier photodiode (UTC-PD), whose band diagram is shown in Fig. 7 [3] is used. Fig. 8 depicts an example of photonic MMW emitter, where the UTC-PD and the antenna are integrated [4].

As a good example of the photonic MMW receiver or detector, the electro-optic (EO) sensor made of a bulk EO crystal offers the largest bandwidth extending to the terahertz frequency region. The operation of the EO sensor is analogous to that of the down-converter in the electronic mixer operation as shown in Fig. 9(a). Fig. 9(b) shows the EO sensor attached to the optical fiber [5]. Highly sensitive EO materials used at an optical wavelength of 1.55 μm are CdTe and DAST. This EO sensor is also applicable to microwave regions, and is proven to be useful in the specific absorption rate (SAR) measurement at cellular phone frequency (1.5 GHz ~ 2 GHz) [5].

III. SYSTEM APPLICATIONS

The photonic MMW transmitter is applied to the 120-GHz-band wireless link system to realize a 10-Gbit/s transmission (> 1 km) transmission. The wireless link can support the optical network standards of both 10 GB/s (10.3 Gbit/s) and OC-192 (9.95 Gbit/s) with a bit error rate of 10^{-12}. The above is successful demonstrated in the wireless transmission of 6-channel uncompressed high-definition television (HDTV) signals using the link.

capacity [6]. Fig. 10 shows a block diagram of the wireless link. A high-gain Cassegrain antenna is used for a long distance

The ultralow-noise characteristics of the photonically generated MMW/THz-wave signal have been verified through their application to the LO for superconducting mixers in receivers used for radio astronomy. Radio-astronomical signals from the universe have been successfully observed using a 97.98-GHz photonic LO [7].

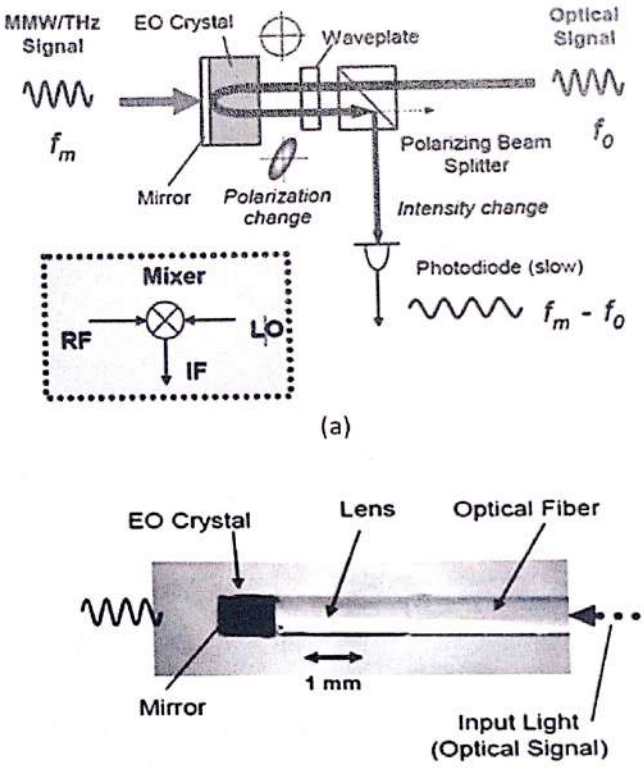

Figure 9. Electro-optic sensor as photonic MMW down-converter, (a) Block diagram, (b) example of EO sensor.

A great advantage of photonic LOs in spectroscopic measurement systems is their wide tun-ability. For this purpose, a wideband receiver has been tested with the same combination of superconducting mixers and a photonic LO at frequencies from 260 to 340 GHz [8]. MMWs/THz waves generated by

the optical heterodyning using the OFCG and UTC-PD are successfully applied to the spectroscopy measurement [9,10].

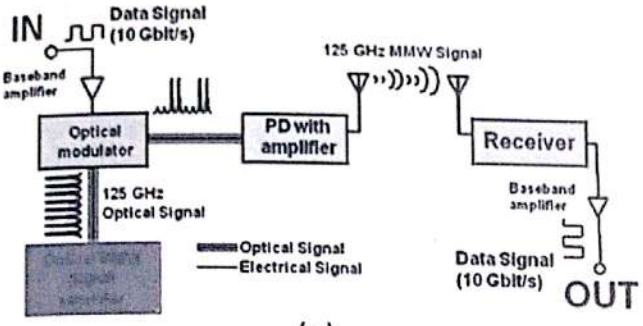

(a)

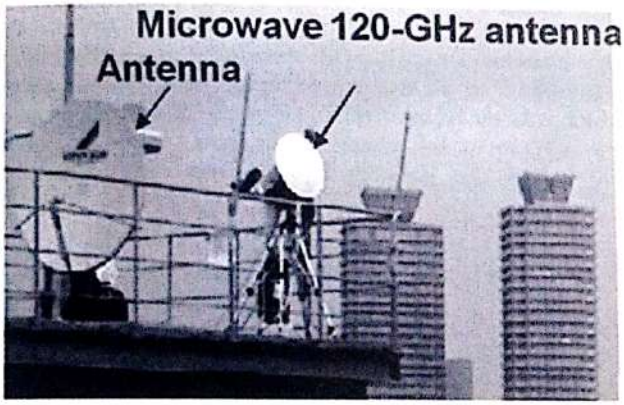

(b)

(c)

Figure 10. (a) Block diagram of 120-GHz-band wireless link. Photographs of (b) field trial and (c) application scene.

IV. CONCLUSION

A brief overview of microwave and millimeter-wave photonics systems is described along with key devices incorporated in the system. The fusion of wireless and optical-fiber-based wired telecommunications technologies will continue to steadily. The Technology for the optical generation and detection of radio waves will become essential for various fields of measurement, as it facilitates the handling of ultra-high-frequency radio waves, which has been difficult with previoustechnologies.

V. REFERENCES

[1] A. Seeds, Development of Microwave Antenna at 120 GHz, *IEEE Trans. Microwave Theory and Tech.*, Vol. 50, 2002, pp 877-887.

[2] A. Hirata *et al.*, Integration of Microwave and photonics Technology, *IEICE Trans. Electron.*, Vol. E88-C, 2005, pp 1458 -1464.

[3] H. Ito *et al.*, Long Range Communication using optical fibers and RF wave Technology, *IEEE J. Light wave Technology*, Vol. 23, 2005, pp 4016 – 4021.

[4] A. Hirata *et al.*, Microwave and Millimeter wave Communication link using photonics, *IEEE Trans. Microwave Theory Tech.*, Vol. 49, 2001, pp 2157-2162.

[5] H. Togo et al., Spectroscopy Measurement at RF and MM Wave Frequencies, IEICE Trans. Electron., Vol. E90-C(2), 2007, pp 436 – 442.

[6] A. Hirata et al., Limitations of Microwave Technology in Long Range Communication, IEEE Trans. Microwave Theory Tech., Vol. 54, 1937 - 1944, 2006.

[7] S. Takano et al., Traffic Optimization in WDM Optical Networks, Publ. Astron. Soc. Japan, Vol. 55, 2003, pp L53 – L56.

[8] S. Kohjiro et al., trends in Optical Communication in Terahertz Frequency Range, Tech. Digest of Intern. Workshop on Terahertz Technology, 18B-6, 2005, pp 119 -120, Osaka.

[9] H.J. Song et al., Advancements in Microwave Photonics, Tech. Digest of IEEE/LEOS Summer Topicals 2007, TuC4.3, July 2007.

[10] N. Shimizu *et al.*, Convergence of Microwave & Photonics Technology, *Tech. Digest of IRMMW/THz 2007*, Sept. 2007, pp 895- 896.

KIET IJCE KIET International Journal of Communications & Electronics
Volume. No. 4, Issue No. 1, January-June 2016, ISSN: 2320 - 8996

Cost Comparison Parameters for Quantum-Dot Cellular Automata Designs

Nidhi[1], Rashmi Chawla[2]

EE Department, YMCA University
Faridabad, India

[1]nidhu060792@gmail.com
[2]rashmi.chawla@rediffmail.com

***Abstract*— Quantum-dot cellular automata (QCA) technology has become an alternative to CMOS technology for future digital designs because it give low power dissipation, high density and no leakage current compared to CMOS Designs. Many circuits are studied in QCA technology. But how to examine that which QCA Design is better than any other QCA design is not considered yet. Until now, parameters and area-delay cost functions are directly used from CMOS technology to compare QCA designs. This is not an appropriate approach because both the technologies are different. Therefore in this paper, several cost parameters are proposed which helps in evaluation of QCA Designs. And through these parameters it is found that the number of QCA logic gates, the delay and the number and type of crossovers, are the main parameters which effect QCA designs and must be considered before choosing any design for an application.**

***Keywords*— Quantum-dot cellular automata (QCA), cost functions, parameters.**

I. INTRODUCTION

Quantum-dot cellular automata (QCA) [1] technology have become possible replacement to CMOS technology. QCA provides various advantages like fast speed, low power consumption and high density, which have the capability to maintain the trend of Moore's Law. Many novel approaches are offered by QCA in computation and communication which are "processing-in-wire" and "memory-in-motion" [2] and so it is used as an nanoscale technology for the development of digital systems.

Until now, the circuits having only local interaction in QCA have been implemented Designs. In this interaction both electrostatic interaction (molecular, semiconductor, and atomic) and magnetic interaction QCAs have been implemented and investigated. At present semiconductor QCA can only work at low temperatures. However, as the technology is developing, the temperature range may vary. Arithmetic circuits, memory, and simple processors have been designed and analyzed with QCA Designer [2]. But the manner in which to compare and analyze QCA designs are not studied.

As addition is considered as the heart of computer arithmetic calculation, and a designer would like to make the best adder in their designs, but what defines the "best" adder in QCA technology? In previous research it was found that multilayer QCA circuits are preferred over the coplanar circuits because they offer better area, latency, and the number of cells [3], which are directly used from CMOS parameters. But the difference between both the multilayer crossovers and coplanar crossovers is not considered and there are no parameters provided for their comparison. Multilayer crossovers consume less area compared to coplanar crossovers and the cost of fabrication of multilayer crossovers is more compared to that of coplanar crossovers. As CMOS and QCA technologies are both different so previous parameters and area-delay cost functions can't be used for true comparison. So, new parameters and specific cost functions for the QCA circuits need to be investigated that can help in guiding the optimization of the QCA circuit designs.

In this paper, the evolution of the cost parameters of CMOS technology is considered so that the ideas are generated for the cost parameters of QCA Designs. Based on this analysis of all present parameters, a group of new QCA cost functions is proposed. The proposed cost functions can be used to examining the performance of any QCA circuit. Adder designs are selected in QCA Designs because adder designs are the heart of the computer calculations. Than in future QCA adders are compared based on these parameters and then examined with both the CMOS area-delay cost function and proposed QCA cost functions in terms of the overall cost. And final comparison results show that the selection of the "best" adder is based on the design of application and also differs between technologies. This paper is a first step to evaluate the overall cost of QCA circuit design and it is anticipated that further consideration of cost functions for QCA designs will be inspired by this paper.

The remainder of the paper is organized as follows. Section II presents the QCA basics. In Section III, several comparison parameters are studied. Section IV provides the proposed QCA cost functions. Conclusions are given in Section V.

KIET IJCE KIET International Journal of Communications & Electronics
Volume. No. 4, Issue No. 1, January-June 2016, ISSN: 2320 - 8996

II. QCA BASICS

A. QCA Cell

A basic QCA cell that is made of four quantum dots which can bind electron within it is shown in Fig. 1(a). All the dots are connected with each other via a tunneling wire through so that electron can tunnel among all four dots. First two extra free electrons are added within QCA cell and as the electron repulsive force between them are placed at antipodal position within QCA cell. Depending on this position of electrons two different structures of QCA cell may exist, called polarization of the QCA cell and denoted. P=+1 and P=-1 indicates the binary logic values '1'and '0'respectively and P=0 specifies an un-polarized cell in Fig. 1(b) i.e., contains no information. The rotated cells are used for coplanar crossings as shown in Fig. 2.

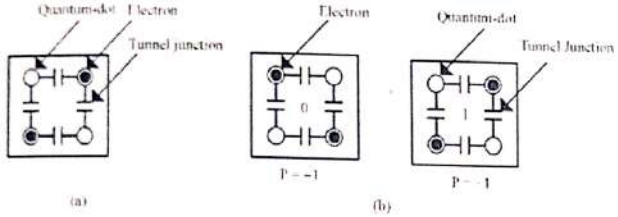

Fig 1. QCA Regular cell polarization

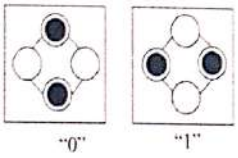

Fig 2. QCA Rotated Cell

B. QCA Wire and Logic Gates

In contrast to a physical wire, a QCA "wire" is a chain of cells where the cells are placed adjacent to each other as shown in Fig. 3. The QCA logic gates are three-input majority gates and inverters. An inverter is designed by diagonally placing cells from each other and different structures are also present as shown in Fig. 4(b). Inverters can usually be included in the interconnections and do not provide any additional delay. A three-input majority gate consists of five QCA cells which have the function of $M(a, b, c) = a\,b + b\,c + a\,c$ as shown in Fig. 4(a). A 2-input OR gate or a 2-input AND gate can be implemented by fixing one of the majority gate inputs to "1" or "0", respectively. In combination with inverters, these two logic components can be used for implementation of logic function.

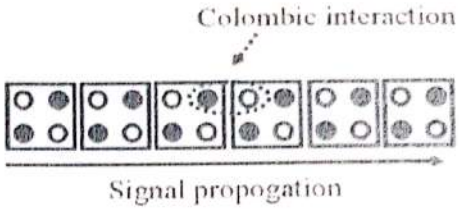

Fig 3. QCA Wire

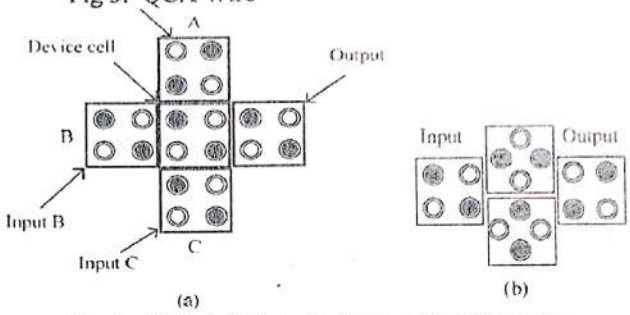

Fig 4. QCA (a) Majority Gate and, (b) Inverter

C. QCA Wire and Logic Gates

QCA clocking is made of four phase shift by 90° as shown in fig.4 which creates a new path to design nano-circuits. The clock signals of QCA circuits are generated by an electric field which is applied to the QCA cells to modulate the tunneling barrier between dots (i.e., inter dot barrier). The physical raising and lowering of the barriers depends on the actual phase of technology. Four phases of clock are as follows:

Switch phase— the barrier between dots of QCA cell is increased. The quantum dots are influenced by the electron of its neighboring and electron starts tunneling between dots. So the QCA cell becomes in polarized state.

Hold phase— barrier of the cell remains high and electron can't tunnel between dots and the cell maintains its current states (fixed polarization).

Release phase— barrier between dots are decreased, electron can tunnel through dots and QCA cell become in un-polarized state.

Relax phase— barrier stay at lowered and cell remains in un-polarized state.

The smallest unit of delay in QCA is a clocking zone delay that is quarter of a clock cycle.

Two types of clocking floorplans can be used in QCA circuit implementations, namely columnar regions and zone regions as shown in Fig. 5. The columnar approach is considered to be more practical for physical implementation than that of zone approach. However, it has difficulty in realizing high circuit densities and short feedback loops. On the other hand, the zone approach can achieve all this. Smaller zones are more difficult to implement, but are considered as

more area efficient. Using large clocking zones reduces the clock speed for reliable operation and increases the delay of the circuit.

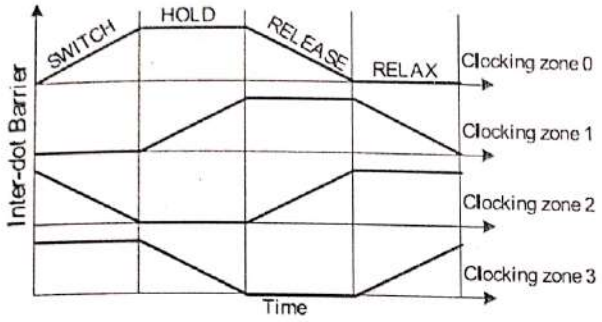

Fig 5. QCA clocking Scheme

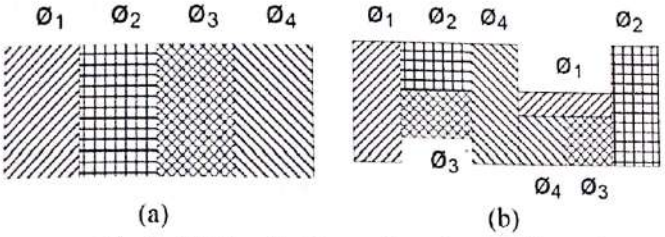

Fig 6. QCA clocking floorplans: (a) columnar Region and (b) zone Region.

Therefore, there is a tradeoff between the size of clocking zones and the circuit stability and efficiency. For semiconductor QCA, it is possible to clock QCA cells individually. As a result, small zones can be used for clocking. However, for magnetic and molecular QCA, columnar clocking zones are generally used. This study is based on semiconductor QCA. Therefore, small zones are used for the QCA designs.

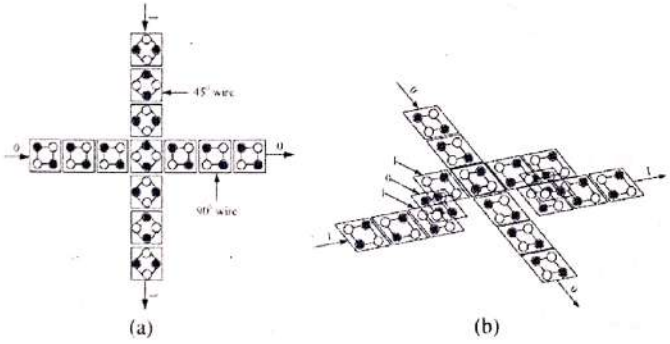

Fig 7. Crossovers in QCA: (a) Coplanar crossovers and, (b) Multilayer crossovers.

D. QCA Wire Crossings

In semiconductor QCA technology, two wire crossing options are available, that are multilayer crossovers and coplanar crossings. A coplanar crossing was proposed [4] as a unique property of a QCA layout which implements the crossovers by using only one layer, as shown in Fig. 7(a). A coplanar crossing can use both regular and rotated cells that do not interact with each other when they are properly aligned. The other alternative is multilayer crossing , which uses more than one layer of cells as shown in Fig. 8(b). However, multilayer crossovers are not easy to fabricate due to the structure of multiple layer. The cost of fabricating a multilayer crossover is expected to be significantly greater than that of a coplanar crossing because of difficulty to fabricate it.

III. Cost Parameters

Area, delay, and power consumption are considered as the main parameters for CMOS circuits and on the basis of these parameters the quality of CMOS circuits are measured. In the past, the main concern of a CMOS circuit was as the area of circuits because it was directly related to the cost of the design. But as the feature size is decreased very much due to the advancement in the fabrication technology and now area is not the major concern and the main goal has changed to the speed and performance of the device. Thompson has proposed various models of the area-time [7] and he proposed the CMOS cost function as:

$$\text{Cost Area–Delay} = A \times T^n \ , 0 \leqslant n \leqslant 2 \qquad (1)$$

Where A is the area and T is the delay of a CMOS circuit. Based on Mead and Rem's VLSI model theory of bisection problem Lower bounds of cost functions were derived [9]. For a QCA also a minimum unit of time is needed to transmit information in QCA wires, which is a clocking zone delay (equal to a quarter of a clock cycle) . This suggests that the models of (1) may also be applicable to QCA technology. Transistor size can improve the speed of a circuit while at the same time it increases the power dissipation. Therefore, cost functions that involve power delay are as follows :

$$\text{Cost Power–Delay} = P^m \times T^n \qquad (2)$$

Where P is the power dissipation and it is determined by dynamic power dissipation in CMOS technology. The dynamic power dissipation is given as:

$$P_{\text{Dynamic}} = \alpha \, C_L \, (V_{dd})^2 f \qquad (3)$$

Where α is the activity factor, C_L is the load capacitance, V_{dd} is the supply voltage, and f is the clock frequency. As irreversible power dissipation from bit erasures (which is negligible in CMOS) dominates the total power dissipation in QCA, the power dissipation issue is different from that of

CMOS must also be considered. Similar to CMOS, the cost metrics for QCA circuits need to be carefully investigated as these can significantly affect the choice of QCA designs. In this section, some new metrics including the number of logic gates, the irreversible power dissipation, and the number of crossovers are investigated.

A. Delay

Delay is considered as an vital parameter for assessing the performance of circuits. Various circuits are applied with the same clock rate, so the number of clocking zones present in the circuit is considered as the measure of the latency i.e Delay. And it is determined as the number of clocking zones times the clock period along its path of information flow and better QCA circuit designs use fewer clocking zones. Therefore, the delay of a QCA circuits should also be included in a cost function. The minimum delay in QCA is a clocking zone delay and it is 1/4 of a clock cycle.

B. Area/Complexity

The number of cells in QCA circuits is similar to the number of transistors in CMOS circuits. In a QCA circuit logic components and connecting wires are both combination of QCA cells. Therefore, the number of cells in a QCA circuit is considered to be directly proportional to its area and including both the logic components and the QCA wires would result in a double weighted area parameter [4]. So, any one of them can be used to measure the complexity of a QCA circuit. The area of QCA designs is mainly dependent on types of crossovers present in the circuit. Therefore, if only area is considered for comparison of QCA Designs it will lead to wrong result. Therefore to measure the complexity of a QCA circuit, the numbers of logic gates and crossovers are best parameters. Therefore, the circuit complexity in QCA is actually the sum of the three elements: majority gates, inverters and crossovers.

C. Irreversible Power Dissipation

In integrated circuits the major limiting factors is the power dissipation. Even the power dissipation in QCA designs is very small, but QCA circuits have thermal problems due to high density. Bit erasures generate "irreversible dissipation" which is negligible in the traditional technology, it becomes a major limitation in computers with ultrahigh density at nanoscale integration. It has been proved experimentally that the power dissipated in the clocking wires is small [4].

QCA "wires", are combination of QCA cells, and each cell can be considered as shift registers which stores the values and which have one input and one output and due to this it is reversible cell and therefore it dissipates little power [5]. Similarly, the inverter gate is also a logically reversible unit, which consumes less power. The irreversible dissipation mostly occur in the three-input majority gate, because it have three input but only one output so there is no balancing between input and output and due to this there is significant information loss and unavoidable power dissipation, which is equivalent to the activity factor (α). Different algorithms and architectures use different numbers of majority gates, which leads to different activity factors. Therefore, majority logic reduction methods should be employed in QCA designs so that less cost efficient design is obtained [5].

D. Number of Crossovers

Crossover refers to the two separate signal wires in the circuit at the same point and it also very important parameter in QCA technology. The coplanar crossings use only one layer, but require careful alignment of cells during fabrication and the other crossing is the multilayer crossover. Gin etal discovered the original idea of multilayer QCA circuits, which is applied to multilayer crossovers in many QCA designs.

For a multilayer crossover, minimum of three layers are required to implement the crossings and the distance between two vertical neighboring layers needs to be arranged properly so that the kink energy is matched to that of normally adjacent cells, which is difficult to obtain. As a result, complexity increases in fabrication of multilayer crossovers compared with coplanar crossings.

To do clocking in both crossover types is very difficult during operation. For coplanar crossings, very fine clocking zones are required for signal propagation. The clocking of multilayer crossovers is also very difficult. Thus, when more crossovers are used in a QCA circuit, it becomes more difficult to fabricate the circuit [10].

And the cost of a multilayer crossover is greater than that of a coplanar crossing, which suggests a cost model as follows:

$$C_{ml} = m \times C_{cp} \qquad (4)$$

Where, C_{ml} is the cost of a multilayer crossover, C_{cp} is the cost of a coplanar crossing, and m is a coefficient to reflect the higher cost of a multilayer crossover to coplanar crossing. If a multilayer crossover uses at least three single layers, m is assumed to be 3 or more. Minimizing the number of crossovers is always desirable in QCA circuit design [10]. Thus, the number of crossovers is very important parameter in QCA that must be included in QCA cost functions.

IV. Proposed QCA Cost Parameters

Based on the above cost parameters either the number of cells or the area can be used as the cost function for comparison of the designs. So to measure the complexity of a

QCA circuit, the numbers of logic gates and crossovers are considered as the parameters. The majority gates have irreversible power dissipation and crossovers are associated with fabrication difficulty. Therefore, they should have higher weightings. Delay is always important due to the performance considerations. For these reasons, the delay, number of logic gates, and number of crossovers are used as a measure of the performance, complexity, irreversible power dissipation, and the fabrication difficulty of a QCA circuit. A generalized QCA cost function is as follows:

$$\text{Cost QCA} = (M^k + I + C^l) \times T^p,\ 1 \leqslant k, l, p \qquad (5)$$

Where, M is the number of majority gates, I is the number of inverters, C is the number of crossovers, T is the delay of the circuit, and k, l, p are the exponential weightings for majority gate count, crossover count and delay, respectively. A constant weighting of "1" is assigned to the number of inverters, as inverters only affect the complexity of QCA circuits. These cost functions are similar to the CMOS area-delay cost functions as in (1). The cost functions prioritize different parameters according to the weightings k, l, and p. For example, if speed is a primary concern, more weight can be given to the delay parameter, i.e., a higher value of p. If fabrication cost is more important, the value of l should be higher than that of p and k and so on. Therefore, the weight values can be adjusted depending on the overall design optimization goal.

V. Conclusions

Many cost related parameters are specified in QCA circuits which must be considered while comparing the QCA designs. Based on the above analysis, the delay, the number of majority gates, and the number of crossovers are the important parameters of a QCA design can be used as cost function for circuits. A family of cost functions was proposed, Cost = $(M^k + I + C^l) \times T^p$, for the comparison of QCA circuits. Based on these cost functions the performance, complexity, irreversible power dissipation, and the fabrication difficulty of a QCA circuit can be measured. And this can be used as the basis for telling which QCA Designs are optimized according to need of the application.

VI. References

[1] C. Lent and P. Tougaw, "A device architecture for computing with quantum dots," Proc. IEEE, vol. 85, no. 4, pp. 541–557, Apr. 1997.

[2] E. E. Swartzlander Jr., H. Cho, I. Kong, and S. Kim, "Computer arithmetic implemented with QCA: A progress report," in Proc. Conf. Rec. 44th Asilomar Conf. Signals, Syst. Comput., 2010, pp. 1392–1398.

[3] Vikramkumar Pudi and K. Sridharan, Senior Member, IEEE, "low complexity designripple carry and brent-kung adders in QCA", IEEE Transactions on nanotechnology, vol. 11,no. 1, January 2012.

[4] Timothy J. Dysart, Member, IEEE, "Modelling of electrostatic QCA wires", IEEE Transactions on nanotechnology, vol. 12, no. 4, January 2013.

[5] Ravi K. Kummamuru, Alexei O. Orlov, Rajagopal Ramasubramaniam, Craig S. Lent, Gary H. Bernstein, and Gregory L. Snider, Senior Member, IEEE, "Operation of quantum dot cellular automata shift registers and analysis of erros", IEEE transactions on electron devices, vol. 50, no. 9, September 2003.

[6] Srivastava, S.; Sarkar, S.; Bhanja, S., "Estimation of Upper Bound of Power Dissipation in QCA Circuits," in Nanotechnology, IEEE Transactions on , vol.8, no.1, pp.116-127, Jan. 2009.

[7] C. Thompson, "A complexity theory for VLSI," Ph.D. dissertation, Carnegie Mellon University, Pittsburgh, PA, USA, 1980.

[8] Ahmad, F., Bhat, G.M. and Ahmad, P.Z.,"Novel Adder Circuits Based on Quantum-Dot Cellular Automata (QCA)",Circuits and Systems, 5, 142-152,2014.

[9] C. Mead and M. Rem, "Cost and performance of VLSI computing structures," IEEE Trans. Electron Devices, vol. 26, no. 4, pp. 533–540, Apr.1979.

[10] K. Walus, G. Jullien, and R. Budiman, "QCA coplanar wire-crossing and multi-layer networks," in Proc. iCore Banff Summit, 2004.

KIET IJCE KIET International Journal of Communications & Electronics

Volume. No. 4, Issue No. 1, January-June 2016, ISSN: 2320 - 8996

Designing of Zeroth Order Antenna with Extended Bandwidth

Samarika Mehta[1] and Monika[2]

B.Tech Student[1], Assistant Professor[2]

Department of Electronics and Communication Engineering, Jaypee Institute of Information Technology, Noida - 201307, India

[1]samarika1593@gmail.com, [2]moniktronics@gmail.com,

Abstract- **This paper represents the designs and analysis of epsilon negative zeroth order resonant antenna. In this paper, design with vias and without vias are implemented and analysed to extend the bandwidth of proposed ZOR antenna which can be used for wireless applications like WLAN, WiMAX, Bluetooth etc. ZOR phenomena is used to reduce the physical size of proposed antenna (0.27λ x 0.53 x 0.017λ).**

Keywords: **zeroth order resonanace(ZOR), extended bandwidth, epsilon negative transmission line (ENG-TL), microstrip.**

I. INTRODUCTION

Nowadays, microstrip patch antennas are widely used and its study has made great progress in recent years It has a wide number of applications like GPS, Bluetooth, missile systems, military purpose, WiMAX, WLAN, WiFi etc. due to its less complexity, less sensitivity, low volume, small size, light weight, affordable cost and easy implementation. And we are designing for wireless applications like WiMAX, Bluetooth, 3G, 4G, WLAN.

Metamaterials are those materials whose properties are defined from their internal structure rather than the matter of which it is composed of. It allow us to manipulate the wave propagation by changing its internal structure in different ways, either mechanically or electrically. They exhibits some unique properties like antiparallel phase and group velocities, and a zero propagation constant [2],[4],[5].

The zeroth order resonant antenna are based on CRLH transmission lines or epsilon negative transmission lines. Since the resonant frequency is independent of antenna size, we have an advantage of size reduction of ZOR antenna. But ZOR antennas suffer narrow bandwidth and low radiation efficiency which is bane for its wide applications. However, bandwidth depends on shunt inductance and capacitance and hence on manipulating these shunt elements bandwidth can be improved. As a result we get the better bandwidth for our wireless applications like WiMAX, Bluetooth, 3G, 4G, WLAN .

II. GENERAL ENG THEORY

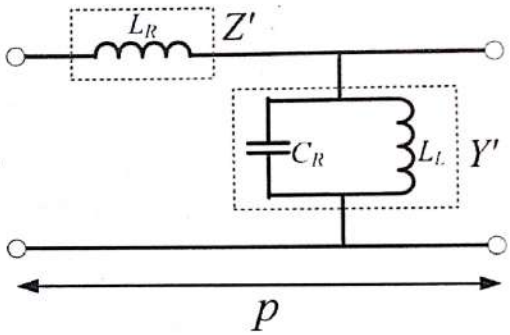

Figure 1 : Circuit Model of an ENG-TL

An equivalent circuit model of an ENG-TL is shown in Fig. 1, which consists of series inductance L_R , shunt capacitance C_R and shunt inductance L_L . The immittances of the ENG-TL are given by

$$Z' = j\omega L_R \qquad (1)$$

$$Y' = j(\omega C_R - \frac{1}{\omega L_L}) \qquad (2)$$

The same theory is presented in [1] where the extension of bandwidth of both ZOR and FOR antenna takes place.

By applying Bloch and Floquet theory to the unit cell of periodic structures, the dispersion relation is determined by

$$\beta_p = cos^{-1}(1-\frac{\omega^2}{2\omega_R^2}+\frac{\omega_{sh}^2}{2\omega_R^2}) \quad (3)$$

Where,

$$\omega_R = \frac{1}{\sqrt{L_R C_R}} \quad (4)$$

$$\omega_{sh} = \frac{1}{\sqrt{L_L C_R}} \quad (5)$$

β is the propagation constant for Bloch waves, and is the length of the unit cell. The resonance of the ENG-TL for resonance modes can be obtained by the following condition:

$$\beta_{np} = \frac{n\Pi p}{l} = \frac{n\Pi}{N} \quad (6)$$

Where N and l are the number of unit cells and the total physical length of the resonator, respectively. Considering an open-ended boundary condition, the resonant frequency is given by[1],[3],[5]:

$$\omega = \sqrt{\frac{1}{C_R}(\frac{1}{L_L}+\frac{2}{L_R}(1-cos\frac{n\Pi}{N}))}$$

(where n=0,1,2,….,N-1) (7)

When n is zero, the propagation constant becomes zero and zeroth-order resonance occurs.

$$cos^{-1}(1-\frac{\omega^2}{2\omega_R^2}+\frac{\omega_{sh}^2}{2\omega_R^2}) = 0 \quad (8)$$

$$\omega = \omega_{sh} \quad (9)$$

The resonant frequency of the ZOR is given as

$$\omega = \frac{1}{\sqrt{L_L C_R}} \quad (10)$$

When n=1, first-order resonance occurs and propagation constant is:

$$\beta_p = \Pi \quad (11)$$

Hence,

$$1 - \frac{\omega^2}{2\omega_R^2}+\frac{\omega_{sh}^2}{2\omega_R^2} = -1 \quad (12)$$

$$\frac{\omega^2}{2\omega_R^2}+\frac{\omega_{sh}^2}{2\omega_R^2} = 2 \quad (13)$$

the resonant frequency is given by:

$$\omega = \sqrt{\frac{1}{C_R}(\frac{1}{L_L}+\frac{4}{L_R})} \quad (14)$$

When n is zero, the wavelength becomes infinite and the resonant frequency of the zeroth-order mode becomes independent of the size of the antenna, while the shortest length of the conventional open ended resonator is one half of the wavelength. Thus, an antenna with a more compact size can be realized.

III. ANTENNA DESIGN & SIMULATIONS

According to the ENG-TL theory, the resonant frequencies are only determined by the ENG circuit parameters. In this work, it fully consider the balances of L_R L_L and C_R . Introducing a large L_L and small Cr can extend the bandwidths of the ZOR. Since the gain bandwidth product is constant hence the gain is reduced.

For design and simulation of the antenna, we selected the FR4 substrate with ε = 4.4 and tanδ = 0.02.

Dimensions: L=26mm, W=50mm, W_f = 6.3mm, W_s = 2.6mm , g_1 = 2mm, g_2 = 0.6mm, l_1=1.8mm, l_2 = 4.6mm, l_3= 20.5mm, Ls=16mm, p=5mm, d_1=0.3mm, S_1=0.3mm

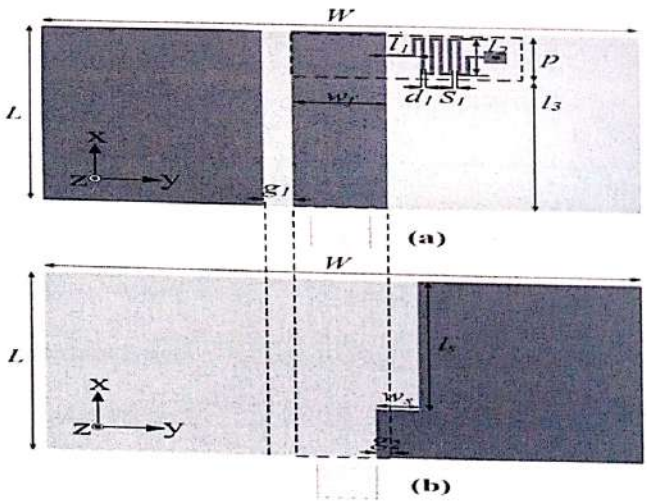

Figure 2: Dimensions of proposed ZOR antenna with vias: (a) Top view (b) Bottom view

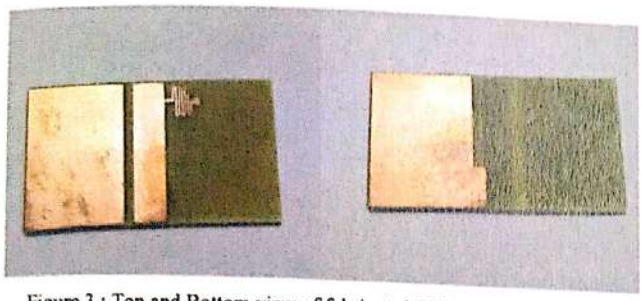

Figure 3 : Top and Bottom view of fabricated ZOR antenna with vias

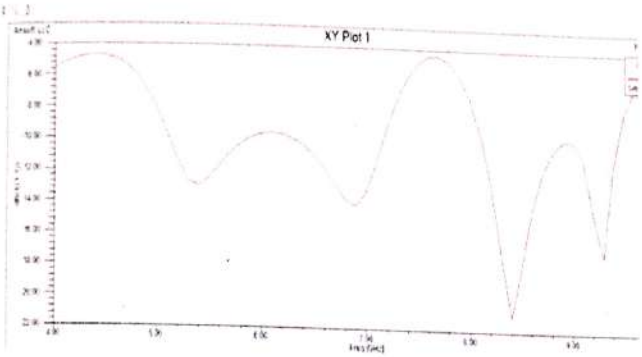

Figure 4: simulated S_{11} graph of proposed ZOR antenna with vias.

At f=5.4Ghz, the radiation efficiency of proposed ZOR anrenna with via is 85.47% with radiated power and accepted power are 810.45 mW and 948.2 mW respectively, where the normalized peak gain and normalized peak directivity are 0.39917 and 0.46702 respectively.

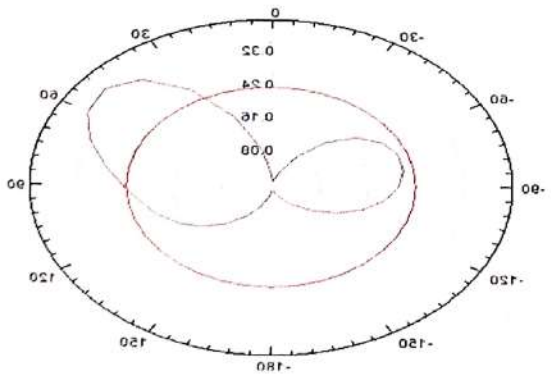

Figure 5: simulated 2-D Radiation Pattern of proposed ZOR antenna with vias at f=5.4GHz

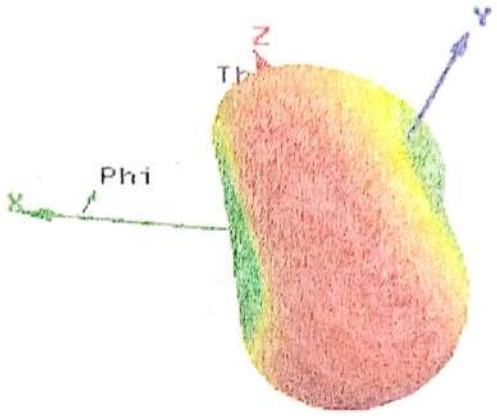

Figure 6: simulated Polar Plot of proposed ZOR antenna with vias at f = 3.2 GHz

The overall size of radiation aperture is 0.46λ x 0.90 λ x 0.028 λ (26mm x 50mm x 1.6 mm) at f=5.4 GHz.

According to [1], the presence of harmonic resonances which interfere the designed ZOR and FOR which is the only drawback of meander lines.

Table 1: Frequency Parameters of Proposed ZOR Antenna with Single Via

PARAMETERS	VALUES
Peak Directivity	0.46702
Peak Gain	0.39917
Peak Realized Gain	0.3785
Radiated Power	0.81045 W
Accepted Power	0.9482 W
Incident Power	0.99998 W
Radiation Efficiency	0.85472
Frequency	5.4Ghz

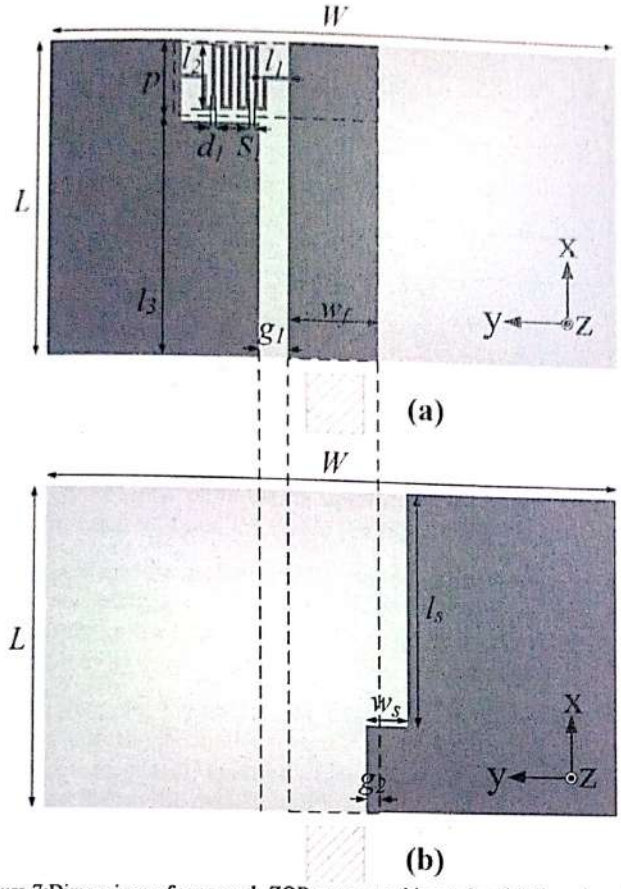

Figure 7:Dimensions of proposed ZOR antenna without vias: (a) Top view , (b) Bottom view

Dimensions: L=26mm, W=50mm, W_f = 6.3mm, W_s = 2.6mm , g_1 = 2mm, g_2 = 0.6mm, l_1=1.8mm, l_2 = 4.6mm, l_3= 20.5mm, Ls=16mm, p=5mm, d_1=0.3mm, S_1=0.3mm

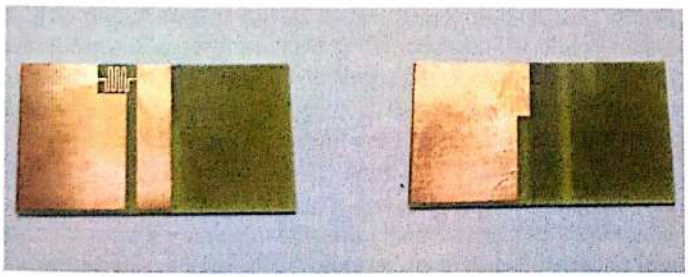

Figure 8: Top and Bottom view of fabricated ZOR vialess antenna

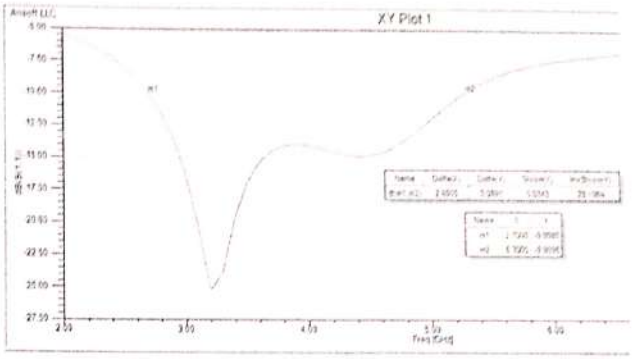

Figure 9: simulated S_{11} graph of proposed ZOR vialess antenna.

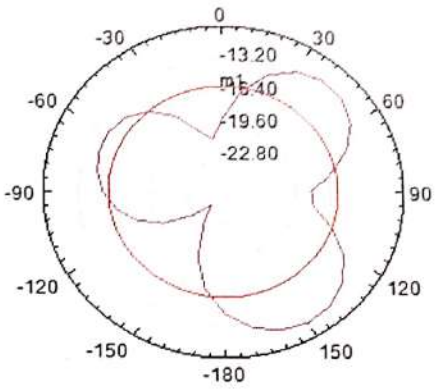

Figure 10: simulated 2-D Radiation Pattern of proposed vialess ZOR antenna at f=3.2GHz

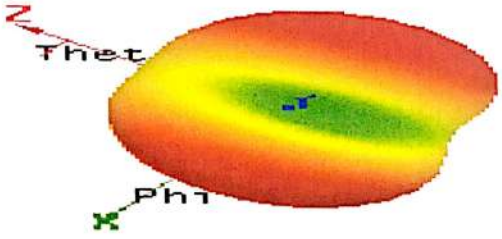

Figure 11: simulated Polar Plot of proposed vialess ZOR antenna at f = 3.2 GHz

Table 2 Frequency Parameters of Proposed Vialess ZOR Antenna

PARAMETERS	VALUES
Peak Directivity	0.076717
Peak Gain	0.071518
Peak Realized Gain	0.071361
Radiated Power	0.93016 W
Accepted Power	0.99779 W
Incident Power	0.99997 W
Radiation Efficiency	0.93222
Frequency	3.2Ghz

The overall size of radiation aperture is 0.27λ x $0.53\ \lambda$ x $0.017\ \lambda$ (26mm x 50mm x 1.6 mm) at f=3.2 GHz.

At f=3.2Ghz, the radiation efficiency is 93.22% with radiated power and accepted power are 930.16 mW and 997.79 mW respectively, where the normalized peak gain and normalized peak directivity are 0.071518 and 0.076717 respectively.

ZOR does not depend on the physical size, this makes it is possible to design a smaller resonant antenna than the traditional microstrip resonator antenna. The design without via gives better result than the design with via.

This antenna has a zeroth-order resonant frequency at f_0 = 3.2GHz and radiation efficiency was approximately 93.22%. The proposed antenna is fabricated on a FR4 substrate with a dielectric constant of 4.4 and thickness of 1.6 mm.

IV. CONCLUSION

In this paper, it is demonstrated the bandwidth enhancement of proposed ZOR antenna. The size of proposed antenna can be reduced because of its zeroth order resonance. The circuit model of proposed ZOR antenna was derived and analyzed inorder to study the bandwidth enhancement. The bandwidth is enhanced because of the merging of zeroth order resonance and first order resonance. Here zeroth order resonance makes the antenna compact and first order resonance increases the directivity and gain. Also as the bandwidth increases gain decreases simultaneously. Since the proposed theory and results show good agreement with each other hence the proposed antenna can be used for modern wireless communication system.

V. REFERENCES

[1]. Bing-Jian Niu, Quan-Yuan Feng "Epsilon Negative Zeroth- and First-Order Resonant Antennas With Extended Bandwidth and High Efficiency" *IEEE Transactions On Antennas And Propagation, VOL. 61, NO. 12, DECEMBER 2013*

[2]. T. Jang, J. Choi, and S. Lim, "Compact Coplanar Waveguide (CPW)-fed Zeroth-Order Resonant Antennas with Extended Bandwidth and High Efficiency on Vialess Single Layer," *IEEE Ttrans. Antennas Propag., Vol. 59, NO. 2, PP. 363–372, FEB. 2011.*

[3]. J. H. Park, Y. H. Ryu, J. G. Lee, and J. H. Lee, "Epsilon Negative Zerothorder Resonator Antenna," *IEEE Trans. Antennas Propag., Vol. 55, NO.12, PP. 3710–3712, DEC. 2007.*

[4]. Lai, T. Itoh, and C. Caloz, "Composite Right/Left-Handed Transmission Line Metamaterials," *IEEE MICROW. MAG., VOL. 5, NO. 3, PP. 34–50.*

[5]. Lai, K. M. K. H. Leong, and T. Itoh, "Infinite Wavelength Resonant Antennas With Monopolar Radiation Pattern Based On Periodic Structures," *IEEE TRANS. ANTENNAS PROPAG., VOL. 55, NO. 3, PP. 868–876, MAR. 2007.*

KIET IJCE KIET International Journal of Communications & Electronics

Volume. No. 4, Issue No. 1, January-June 2016, ISSN: 2320 - 8996

A Survey on Clustering Protocols for Energy efficiency of sensors nodes in Wireless Sensor Network

[1]Rakesh Kumar Saini, [2] Dr.Ritika
Astt.Professor and PhD Research Scholar, Department of MCA, DIT University, Dehradun
Associate Professor and Head Department of MCA, DIT University, Dehradun
[1]rk.saini@dituniversity.edu.in, [2]riti_79@rediffmail.com

Abstract-**Recent advancement in wireless communications and electronics has enabled the development of Clustering routing protocols in wireless sensor network. The Wireless sensor networks can be used for various application areas (e.g., health, military, home).For different application areas; there are different technical issues that researchers are currently resolving. In this review paper, we examine currently proposed clustering algorithms for Wireless Sensor Networks. We will briefly discuss the operations of these algorithms, as well as draw comparisons on the performance between the various schemes. Specifically, we will examine the performance in terms of the power and quality aspects of these schemes. This review paper should provide the reader with a basis for research in clustering schemes for Wireless Sensor Networks.**

Index Terms - **Clustering algorithms, Energy efficient clustering, Network lifetime, Wireless sensor networks.**

I. INTRODUCTION

A wireless sensor network is a collection of sensor nodes interconnected by wireless Communication channels. Each Sensor node is a small device that can collect data from its surrounding area, carry out simple Computations, and communicate with other Sensors or with the base station (BS). [2] Such networks have been realized due to recent advances in micro-electromechanical systems and are expected to be widely used for applications such as environment monitoring, home security, and earth quake warning. Wireless sensor networks consist of a large number of low power multifunctional sensor nodes with sensing, limited computation and Wireless communications capabilities. Recent advances in sensor technology have enabled the development of small, low-cost and low power sensors that can be connected via a Wireless networks.[5] In wireless sensor networks, Sensors are densely deployed so that it can be Applicable to a variety of fields that include surveillance, military, national security, and chemical or biological detection. Many routing protocols have been proposed for wireless sensor networks. The main goal the routing protocols in wireless sensor networks is to find ways for improvement of energy efficiency and reliable transmission of sensed data to the Sink. Almost all of the routing protocols can Be classified according to the network structure as flat, hierarchical, or location based. And hierarchical routing protocols can be classified again according to the clustering tactics as distributed or centralized fashion. For example, LEACH (Low-Energy Adaptive Clustering Hierarchy), HEED (Hybrid Energy-Efficient Distributed clustering) use distributed tactics and LEACH-C (LEACH-Centralized) use centralized tactics. The main goal of cluster-based routing protocol is to efficiently maintain the energy consumption of sensor nodes by involving them in multi-hop communication within a cluster and by performing data aggregation and fusion in other to decrease the number

of transmitted messages to sink and transmission distance of sensor nodes.

II.CLUSTERING

The grouping of sensor nodes into clusters has been widely pursued by the research community in order to achieve the network scalability objective.[6] Every cluster would have a leader, often referred to as the cluster-head (CH). Although many clustering algorithms have been proposed in the literature for ad-hoc networks, the objective was mainly to generate stable clusters in environments with mobile nodes. Many of such techniques care mostly about node reach ability and route stability, without much concern about critical design goals of WSNs such as network longevity and coverage. Recently, a number of clustering algorithms have been specifically designed for WSNs. These proposed clustering techniques widely vary depending on the node deployment and bootstrapping schemes, the pursued network architecture, the characteristics of the CH nodes and the network operation model. A CH may be elected by the sensors in a cluster or pre-assigned by the network designer. A CH may also be just one of the sensors or a node that is richer in resources. The cluster membership may be fixed or variable. CHs may form a second tier network or may just ship the data to interested parties, e.g. a base-station or a command center.

III.CLUSTERING OBJECTIVE

Many protocols have been proposed for energy-efficiency in WSN in the last few years. Clustering based schemes are believed to be the most energy efficient routing protocols for wireless sensor networks. As defined previously, Clustering is grouping of similar objects, or the process of finding a natural association among some specific objects or data. [5] The structure of a general cluster scheme is shown in the following Figure1. In each cluster, one node is elected as the cluster-head (CH) while the rest of the nodes are member nodes. Member nodes in their respective clusters sense the ambient conditions in the environment and transmit the measured data to their corresponding cluster-head.

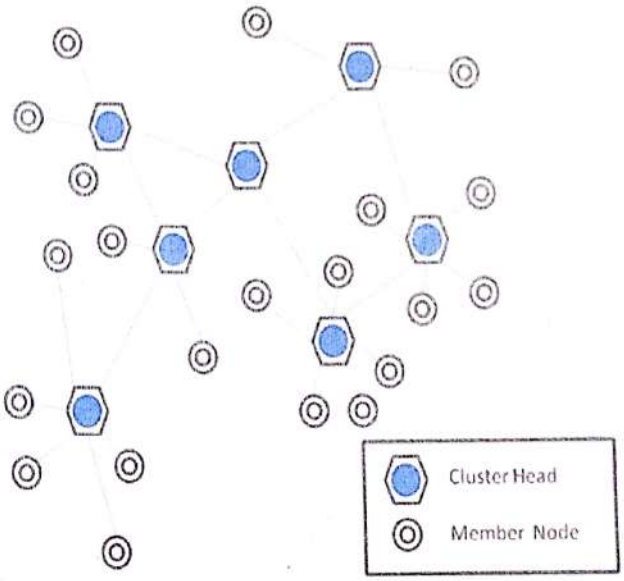

Figure1.Clustering in Sensor Network

Cluster-heads handles the responsibilities to collect data from their member nodes, to aggregate them, and finally to forward the aggregated data either to neighboring cluster-head (multi hop) or directly (single hop) to sink/base station. Clustering leverages the advantages of small transmit distances for most of nodes, requiring only a few nodes to transmit far distances to the sink/base station. Thus clustering along with the reduction in energy consumption improves the network life-time. Along with clustering, the concept of hierarchical clustering also plays a very important role in developing energy efficient schemes for WSN.Clustering has many objectives which are:

1. Allows Aggregation
2. Limits data transmission
3. Load balancing
4. Fault-tolerance
5. Increased connectivity and reduced delay
6. Minimal cluster count
7. Maximal network longevity
8. Facilitates the reusability of the resources
9. Gives impression of smaller and stable networks
10. Reduces network traffic and contention for the channel

11. Forms virtual backbones for inter cluster routing using CHs and gateway nodes

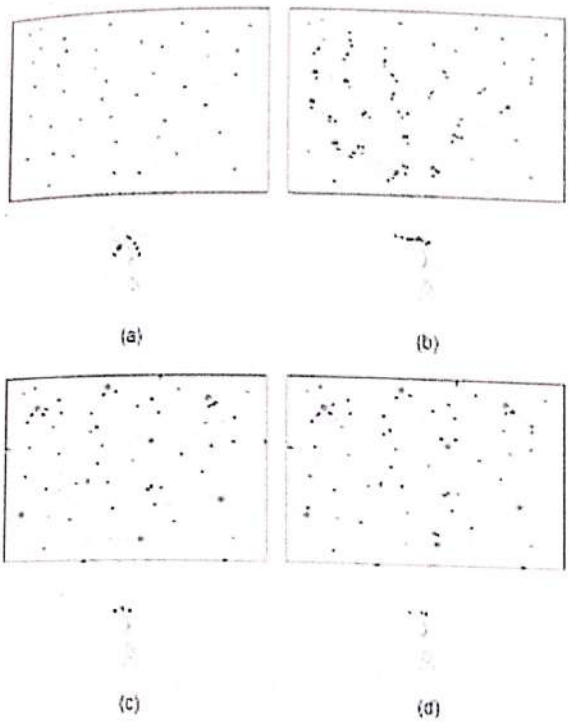

Figure2: Sensor information forwarding with and without clustering and aggregation (a) Single hop without clustering (b) Multihop without clustering (c) Single hop with clustering(d) Multihop with clustering.

In figure 2(a) Show single hop without Clustering, there is sensor direct communicate with the base station but in figure 2(b) sensors communicate first with other sensor nodes and finally communicate with base station, there is without clustering all sensor nodes communicate with base station. In figure 2(c) Clustering is shown, there is a area is divided into many clusters and every cluster has a cluster head, all sensor nodes communicate with cluster head first and then cluster head of every cluster communicate with base station, there is cluster head communicate with base station directly. In figure 2(d) all cluster head communicate with each other and finally send data to base station. Hierarchical clustering is an efficient way for lowering energy consumption within a cluster. It is mainly a two-level routing where one level is used to select cluster heads and other is for routing. Lower energy consumption within a cluster is achieved by data aggregation and fusion to decrease the number of transmittable messages. Also clustered Network allows coverage of large area of phenomenon and additional load balancing without degrading the performance of the network.

IV.CLUSTERING PROTOCOLS

A. LEACH-Distributed

Low-Energy Adaptive Clustering Hierarchy (LEACH) was proposed by Heinzelman [1] and is one of the first cluster-based routing approaches for WSNs. LEACH has inspired many subsequent cluster-based routing schemes. The main goal of LEACH is to select sensor nodes as cluster heads by rotation, so that high energy dissipation in communicating with the base station is spread to all sensor nodes in the network. The nodes organize themselves into local clusters, where one node acts as the local base station or cluster head. LEACH also performs local data compression, reducing the amount of data sent from the clusters to the base station, which further reduces energy dissipation and enhances system lifetime. Sensors elect themselves as local cluster heads with a certain probability at any given time. These cluster-head nodes then broadcast their status to all the other sensors in the network. The sensor nodes then determine which cluster they want to join by choosing the cluster head that requires the minimum communication energy. After all the nodes are organized into clusters, each cluster head creates a schedule for the nodes in its cluster. Once the cluster head has the data from its nodes, the cluster head aggregates the data and then transmits the data to the base station. This is a high-energy transmission because the base station is far away. Because being cluster head drains the battery of that node, the cluster heads are not fixed, so that energy usage can be spread over multiple nodes. The operation of LEACH breaks down into rounds. Each round has two phases: the setup phase and the steady-state phase. During the setup phase, clusters are organized; during the

steady-state phase, data transmission is performed. LEACH is a totally distributed approach and requires no global information.

Advantages of LEACH

(1) Each node has an equal chance to become a cluster head but cannot be selected as cluster head in a subsequent round so the load is shared between nodes.

(2) Because LEACH uses Time Division Multiple Access (TDMA), it keeps cluster heads from unnecessary collisions.

(3) LEACH can avoid a lot of energy dissipation by opening and closing members' communication interfaces in conformity with their allocated time slots.

Limitations of LEACH

(1) Because LEACH uses single-hop communication, it cannot be deployed in networks spread over large distances.

(2) Because cluster heads are elected only on the basis of probability, not taking energy into consideration, LEACH cannot provide actual load balancing.

(3) Because cluster heads are elected on the basis of probability, uniform distribution cannot be ensured. So, there is a chance that the elected cluster heads are concentrated in one part of the network and some nodes might not have any cluster heads in their vicinity.

(4) The idea of dynamic clustering brings extra overhead.

B. HEED

Hybrid Energy-Efficient Distributed (HEED) clustering was introduced by Younis and Fahmy.[2] The main goal of HEED is to prolong network life. The main difference between HEED and LEACH is cluster head election; cluster head election in HEED is not random. The construction of clusters is based on residual energy of the node and intra-cluster communication cost. Cluster heads have higher average residual energy than the member nodes. The communication technique of HEED is the same as LEACH.

Advantages of HEED

(1) HEED is a fully distributed cluster-based routing technique.

(2) HEED achieves load balancing and uniform cluster head distribution due to lower power levels of clusters.

(3) HEED achieves high energy efficiency and scalability by communicating in a multi-hop fashion.

Limitations of HEED

(1) Energy consumption is not balanced because more cluster heads are generated than the expected number.

(2) As with LEACH, massive overhead is created due to multiple rounds.

(3) HEED also has additional overhead owing to several iterations being done to form clusters.

C. PEGASIS

Power-Efficient Gathering in Sensor Information Systems was proposed by Lindsey *et al.*[12] and is an improved version of LEACH. The main idea behind PEGASIS is that each node communicates only with its close neighbors and becomes the leader for transmission to the sink, one by one. The nodes are randomly located, and each sensor node has capabilities for data detection, wireless communication, data fusion, and positioning. Energy load is evenly distributed among all the sensor nodes in the network. In PEGASIS, the

nodes are organized into a chain, which can either be assigned by the sink and then broadcast to all the nodes or accomplished by the nodes themselves using a greedy algorithm. If the nodes form the chain themselves, the nodes can first get the location data of all nodes and locally form the chain using the same greedy algorithm.

Advantages of PEGASIS

(1) PEGASIS has the ability to outperform LEACH because it reduces the overhead due to dynamic cluster formation, and decreases the number of data transmissions due to the chain of data aggregation.

(2) The energy load is distributed uniformly in the network. To make sure that the fixed sensor node is not selected as the leader and thus to prevent the

Volume. No. 4, Issue No. 1, January-June 2016, ISSN: 2320 - 8996

subsequent early death of this sensor node, all sensor nodes take turns acting as leader.

Limitations of PEGASIS

(1) PEGASIS is not suitable for networks with time-varying topologies. In PEGASIS, it is essential to have a complete view of the topology at each and every node for chain construction.

(2) It is assumed by PEGASIS that every sensor node is able to communicate with the sink directly, whereas in real life nodes use multi-hop communications to communicate with the sink.

(3) Communication has very long delays, which can cause a node to become a bottleneck.

(4) The network is not very scalable because all the nodes must have global knowledge of the network and use the greedy algorithm.

D. *LEACH-Centralized*

Low-Energy Adaptive Clustering Hierarchy-Centralized was proposed by Heinzelman [13].LEACH offers no guarantee about the placement and/or number of cluster heads. In, an Enhancement over the LEACH protocol was proposed. The protocol, called LEACH-C, uses a centralized clustering algorithm and the same steady-state phase as LEACH. LEACH-C protocol can produce better performance by dispersing the cluster heads throughout the network. During the set-up phase of LEACH-C, each node sends information about its current location and residual energy level to the sink. In addition to determining good clusters, the sink needs to ensure that the energy load is evenly distributed among all the nodes. To do this, sink computes the average node energy, and determines. The sink finds which nodes have energy below this average. Clusters using the simulated annealing algorithm to solve the NP-hard problem of finding k optimal clusters. This algorithm attempts to minimize the amount of energy for the ordinary nodes to transmit their data to the cluster head. Once the cluster heads and associated clusters are found, the sink broadcasts a message that obtains the cluster head ID for each node. If a cluster head ID matches its own ID, the node is a cluster head; otherwise the node determines its TDMA slot for data transmission and goes sleep until it's time to transmit data. The steady-state phase of LEACH-C is identical to that of the LEACH protocol. Although LEACH and LEACH-C protocols act in a good manner, they also suffer from many drawbacks like the following.

(i) CHs' selection is random, which does not take into account the residual energy of every node or need the support of BS.

(ii) The high frequency of reclustering wastes a certain amount of energy.

(iii) It cannot cover a large area.

(iv) CHs are not uniformly distributed, where CHs can be located at the edge of the cluster.

E. *EEPSC*

Energy-Efficient Protocol with Static Clustering) was proposed by Amir Sepasi Zahmati [6] and it is a hierarchical static clustering based protocol, which eliminates the overhead of dynamic clustering and engages high power sensor nodes for power consuming tasks and as a result prolongs the network lifetime. In each cluster, EEPSC chooses the sensor node with maximum energy as the cluster-head (CH); thus, not only there is always one CH for each cluster, but also the overhead of dynamic clustering is removed. EEPSC is a modified version of the Low-Energy Adaptive Clustering Hierarchy (LEACH) protocol presented in LEACH uses the paradigm of data fusion to reduce the amount of data transmitted between sensor nodes and the base station. Data fusion combines one or more data packets from different sensors in a cluster to produce a single packet. It selects a small number of CHs by a random scheme which collects and fuses data from sensor nodes and transmits the result to the base station. LEACH uses randomization to rotate the CHs and achieves a factor of 8 improvement compared to the direct approach before the first node dies.

The main difference between EEPSC and LEACH are described below:

(i) EEPSC benefits a new idea of using temporary-CHs and utilizes a new setup and responsible node selection phase.

(ii) EEPSC utilizes static clustering scheme, therefore eliminates the overhead of dynamic clustering

V. COMPARISON BETWEEN CLUSTERING PROTOCOLS

Table 1 Highlight the comparison between cluster-based routing protocols on the basis of energy efficiency, cluster stability, scalability, delivery delay, load balancing.

Protocol Name	Cluster Stability	Scalability	Delivery Delay	Energy Efficiency	Load Balancing
LEACH	Medium	Very Poor	Very Small	Very Poor	Medium
HEED	High	Medium	Medium	Medium	Medium
PEGASIS	Poor	Very Poor	Very Large	Poor	Medium
LEACH-C	High	High	Medium	Medium	Medium
EEPSC	High	High	Very Large	High	High

Table 1: Comparison between clustering protocols

VI. CONCLUSIONS

In this paper we have examined the current state of proposed clustering protocols. In wireless sensor networks, the energy limitations of nodes play a crucial role in designing any protocol for implementation. In this paper, we present an overview of cluster-based routing algorithms in WSNs. We discuss the advantages and taxonomy of cluster-based routing algorithms in WSNs. In addition, we compare different approaches on the basis of various performance measures. It is clear that the different cluster-based routing algorithms mentioned above can be used to improve the performance of WSNs.

VII. REFERENCES

[1] W. R. Heinzelman, A. Chandrakasan, and H.Balkrishnan,"Energy-Efficient Communication Protocol for Wireless Micro sensor Networks", in Proceedings of 33rd Hawaii International Conference on System Science, Vol. 2, Jan. 2000, pp.1-10.

[2] O. Younis and S. Fahmy, "HEED: A Hybrid Energy-Efficient Distributed Clustering Approach for Ad hoc Sensor Networks", IEEE Transaction on Mobile Computing, Vol. 3, No. 4, 2004, pp. 660-669.

[3] Ameer Ahmed Abbasi, Mohamed Younis, "A survey on clustering algorithms for wireless sensor networks", Computer communication 30(2007)2826-28410

[4] W. R. Heinemann, J. Kulik, and H. Balakrishnan, "Adaptive Protocols for Information Dissemination in Wireless Sensor Networks," Proc. ACM MobiCom '99, Seattle, WA, 1999, pp. 174–85.

[5] Mao ye,Chengfali,Guihaichen and jiewu "An Energy efficient clustering scheme in Wireless sensor network"Ad Hoc and Sensor wireless Networks,vol3 pp.99-119,April 2006.

[6] Amir Sepasi Zahmati ,Bahman Abolhassani ,Ali Asghar Behesti Shirazi and Ali Shojaee Bakhtiari,"An Energy-Efficient protocol with Static clustering for Wireless Sensor Network", proceedings of world academy of science, Engineering and Technology volume 22 July 2007 ISSN 1307-6884.

[7] I.F. Akyildiz et al., Wireless sensor networks: a survey, Computer Networks 38 (2002) 393–422.

[8] C-Y. Chong, S.P. Kumar, Sensor networks: evolution, opportunities, and challenges, Proceedings of the IEEE 91(8) (2003) 1247–1256.

[9] S. Naeimi, H. Ghafghazi, C.-O. Chow, and H. Ishii, "A survey on the taxonomy of cluster-based routing protocols for homogeneous wireless sensor networks." *Sensors*, vol. 12, no. 6, pp. 7350–7409, 2012. Article (CrossRef Link)

[10] P. Kumar, M. P. Singh, and U. S. Triar, "A Review of Routing Protocols in Wireless Sensor Network," *International Journal of Engineering Research & Technology(IJERT)*, vol. 1, no. 4, pp. 1–14, 2012.

[11] X. Liu and J. Shi, "Clustering Routing Algorithms In Wireless Sensor Networks: An Overview," *KSII Transactions on Internet and Informaiton Systems*, vol. 6, no. 7, pp. 1735–1755, 2012.

[12] S. Lindsey, C. Raghavendra, and K. M. Sivalingam, "Data Gathering Algorithms in Sensor Networks Using Energy Metrics," *IEEE Transactions on Parallel and Distributed Systems*, vol. 13, no. 9, pp. 924–935, 2002. Article (CrossRef Link)

[13] W. B. Heinzelman et al., "An Application-Specific Protocol Architecture for Wireless Microsensor Networks," *IEEE Transactions on Wireless Communications* Volume 1, No. 4, Oct 2002,pp.660 - 670.

KIET IJCE KIET International Journal of Communications & Electronics

Volume. No. 4, Issue No. 1, January-June 2016, ISSN: 2320 - 8996

Review on M2M Communications Using D2D Communications in Cellular Networks

[1]Sudhir B. Lande, [2]Smita K. Mankar

Department of electronics & Communication, Kavikulguru Institute of Technology & Science,Ramtek, India.

[1]landeeed@yahoo.co.in, [2]smitamankar19@gmail.com,

***Abstract*—Machine-to-Machine (M2M) communications enable networked devices and services to exchange information and perform actions seamlessly without the need for human intervention. They are viewed as a key enabler of the Internet of Things (IoT) and applications, like mobile healthcare, telemetry, or intelligent transport systems. Wireless communications services, cellular communication systems are going towards small cells with small transmit powers. Meanwhile device-to-device communication (D2D) is seen as a promising idea to increase the performance of wireless networks. In D2D, users in vicinity communicate directly without going through base station. In this paper we review the concept of M2M communications using D2D communications in cellular networks. We use full duplex D2D communication with up-link and down-link required in D2D in cellular systems.**

Keywords*— *Device-to-Device (D2D) communications, full-duplex, Machine-to-Machine (M2M) communications, up-link, down-link

I. INTRODUCTION

Increasing demand for wireless communication is leading to congestion of radio spectrum, which is an expensive and scarce resource. So better utilization of radio spectrum becomes more important and new technologies are required for this purpose. Device-to-Device communication is seen as a new technology component which can improve the spectral efficiency of the cellular systems.

In device-to-device communication, users directly communicate with each other instead of going through base station. UE1, UE2, UE3 are the users. Since now a days users require high data rates specially for local connectivity services like gaming, video sharing, offloading the data transfer from base station and establishing direct communication between users will be highly beneficial for the system. Fig.1 shows the general idea of D2D communication.

D2D is categorized into two groups, in-band and out-band shown in Fig. 2. In out-band, D2D links use unlicensed band such as ZigBee or Wi-Fi, while in-band, D2D link uses licensed cellular bands. The connection is establishing in out-band D2D which is called autonomous out-band or by the base station which is called controlled out-band [2].

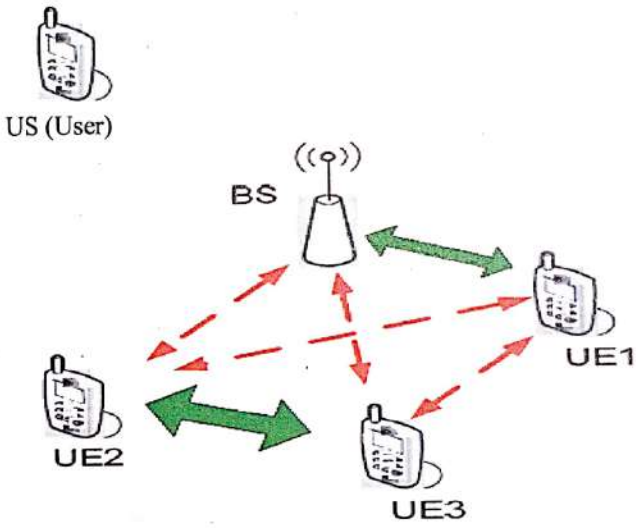

Fig. 1 Device-to-Device (D2D) Communications [1]

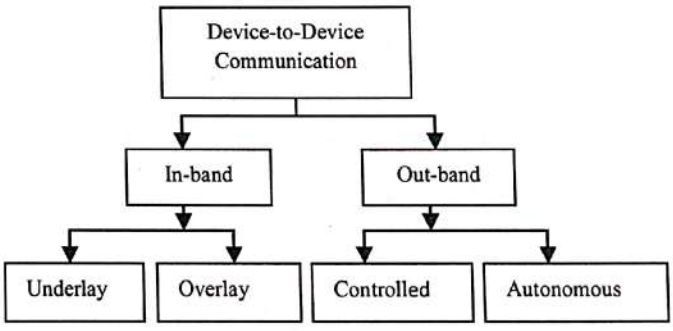

Fig. 2 Device-to-Device (D2D) Classification

In-band D2D also has two categories, D2D users can have share the same resources as some of the cellular users which is called as underlay in-band or dedicated radio resources, which is called overlay in-band.

The problem of deciding on whether D2D users should communicate through base station (cellular mode) or directly (D2D mode) is an important issue. The problem of

deciding on whether D2D users should communicate through BS (cellular mode) or directly (D2D mode) is an important issue.

During the last two decades, the trend in wireless communication technologies has shifted from the traditional voice-centric "man-to-man" mobile communications to data-centric "man-to-machine" mobile communications and further shift towards "machine-to-machine". A typical example of machine-to-machine mobile communications is car-to-car (C2C) or vehicle-to-vehicle (V2V) communications. As the name refers, in M2M communication systems, all entities in the network are in motion. These entities can either be mobile users or vehicles [3].

Fig. 3 Machine-to-Machine Communication [4]

Machine-to-Machine (M2M) communication describes algorithms, mechanisms and technologies that enables networked devices, wired and wireless, and services to exchange information or control data without explicit human intervention. M2M communication is an important aspect of traffic control, remote control, logistic services, supply chain management and telemedicine. It forms the basis for a concept known as the Internet of Things (IoT). Key components of an M2M system include RFID, sensors, a Wi-Fi cellular communications link and autonomic software programmes to help a networked device interpret data and make decisions.

Telemetry is the most well-known type of M2M communication, which has been used since the early part of the last century to transmit operational data. In Fig. 3 shows, M2M communications, all machines like mobile, van, home, laptop, computer, ambulance etc are first send the signals to the BS and then they are communicate with each other. In this paper, we communicate two devices directly without send the data to BS and later into M2M communication in cellular networks.

II. LITERATURE REVIEW

Mobile M2M communications face many technical challenges despite the promising benefits in terms of revenue opportunities and cost reductions in maintenance and resources. M2M devices are usually small in size and not expensive, introducing energy, bandwidth, computation, and storage constraints to communications [5].

A.D2D Supports in Cellular Networks

Now day's cellular networks offer wide coverage areas, high data rate, and decreasing latency, and therefore they are a key enabler of D2D communications. D2D communication is considered to be one of the key technologies in future wireless systems to increase spectral Efficiency. Providing direct communication between devices will decreases latency and also offload data from base station. The problem of radio spectrum congestion due to increasing demand for wireless communications services, cellular communication systems which have small transmit power and are going implemented in device-to-device communication are investigated and it was shown by results that currently available full-duplex radios can be used in device-to-device communication. Power control, resource allocation and interference-limited-area are used to deal with the interference that is the result of resource sharing [2].

B. D2D Communications and Network Coding

In 2009, the author Afif et al. [1] Introduced two concepts which have not been present in cellular systems for IMT-Advanced so far-Device-to-Device (D2D) communication and network coding. Both of these concepts are used to increase the efficiency of cellular communication systems, especially from a network point of view. The result is to achieved sufficient SINRs multi-antenna receivers are required that allow device-to-device communication when the D2D connections re-use cellular resource within the cell. The author shown that user grouping in a multi-user networks improves substantially the capacity of network coding. As a solution, introduced a low complexity user grouping strategy and showed that when applied with a window size of 6, the user grouping algorithm provided mean capacity gains of 34% and 16% as compared to random network coding.

C. Cooperative D2D Communications

Shalmashi et al. proposed a cooperative device-to-device

communications in order to combat the problem of congestion in crowded communication areas such as shopping mall and open air festivals.

The idea is allowed a D2D transmitter which is act as an in-band relay for a cellular link and at the same time transmits its own data in the downlink. It observed that the D2D receiver is able to cancel the cellular user signal which can improve the achieved data of the D2D link in most cases [6].

D. Formation of Devices

The device-to-device communications have several benefits. The author Pankil et.al.Discussed what can be their blocking probability in cellular cells as well as formation of D2D group [7]. The blocking probability describes for D2D communication which devices are ready for communicate with each other. It was concluded that the all devices get connected it means there is no blocking of the devices for communication when the traffic load is less. As the load increases, the blocking probability also increases.

E. Survey on D2D

The surveyed literature showed that D2D communication can improve the spectrum efficiency greatly. The authorArash Asadi et.al categorised D2D communication in two major groups, namely, in-band and out-band [8]. He faced the major issue in underlay D2D communication is the power control and interference management between D2D and cellular users. Overlay D2D communication does not have the interference issue because D2D and cellular resource do not overlap. And the interference level of the unlicensed spectrum which is called as out-band is uncontrollable, hence QoS is a challenging task in highly saturated wireless areas.

F.M2M Support in Wireless Networks

M2M devices using radio technologies have some problems from cellular networks and wireless networks. In mobile-to-mobile cooperative communication systems, the author Batool Talha introduced the analysis of a large variety of M2M fading channels and presents the state-of-the-art regarding the modelling in cooperative systems. In this, the author modelled and analysed narrowband M2M fading channels in cooperative network systems under line-of-sight (LOS) as well as non-line-of-sight (NLOS) propagation conditions. The performance of dual-hope-multi-relay cooperative systems introduced over M2M fading channels with Equal Gain Combining (EGC) and line-of-sight propagation conditions was evaluated. It is concluded that, in a dual-hope-relay-system with Equal Gain Combining (EGC), improves the systems performance of line-of-sight components in the transmission links [9].

G. M2M Support in Cellular Networks

The cellular networks offer wide coverage areas which have high data rate, and decreasing latency, and therefore they are enabler of M2M communications. Marwat et al. [10] argue that, even in the presence of regular mobile M2M traffic and LTE traffic cannot be considered negligible, and it can have some impact like dramatic impact on the LTE network performance in terms of Quality of Service (QoS).

H. Energy Efficient and Reliable M2M

Now a days energy efficient communications are extremely important in challenging areas where access to mains power is difficult. Andrius et al. proposed a new approach which is called as Clone-to-Clone (C2C) has the potential to reduce the traffic between end points, improve network performance and reduce power consumption of device. In [11], it was shown that, the M2M communication is much more powerful than that and C2C is an new approach to solve the issues hindering development of the network applications in the next generation.

The author Andrius et al, introduced Energy Efficient and Reliable (EER) and all research issues related with the deployment of M2M architecture of M2M communication. "Green Allocation with Zone Algorithm" (GAZA), this algorithm used to achieve Energy efficient and Reliable M2M system for energy efficient and dynamic traffic grooming in WDM networks [12].

I. M2M in Vehicular Networks

In [3], the author Booysen et al. shown that M2M communications in the vehicular networking context and he was investigated areas where M2M principles can improve vehicular networking. Since connected vehicles are network of machines that are communicating with each other, preferably autonomously, vehicular networks can benefit a lot from M2M communications support. Then they highlighted the specific applications, requirements and protocols relating to M2M based vehicular networks.

Finally, they performed analysis of the challenges faced by M2M systems. The standardization of communication interfaces in a network was the most significant challenge with high mobility and variability of components. Managing privacy and security in such a dynamic network requires further attention.

III. European Telecommunication Standards Institute(ETSI) M2M ARCHITECTURE

The European Telecommunication Standards Institute (ETSI) M2M architecture is currently the reference architecture for global, end-to-end, M2M service level communications, and is being adopted by main European telcos [13]. The system architecture is based on current network and application domain standards, and it is limited extended with M2M Applications and Service Capabilities layers (SCLs). SCLs are Service Capabilities (SCs) on the Network domain, M2M Device, or M2M Gateway. SCs provide functions to be shared among different M2M applications. The functions of a SCL include, but are not limited to, registration of applications, provision of means for storage, policy-based selection of communication means for information delivery, support for multiple management

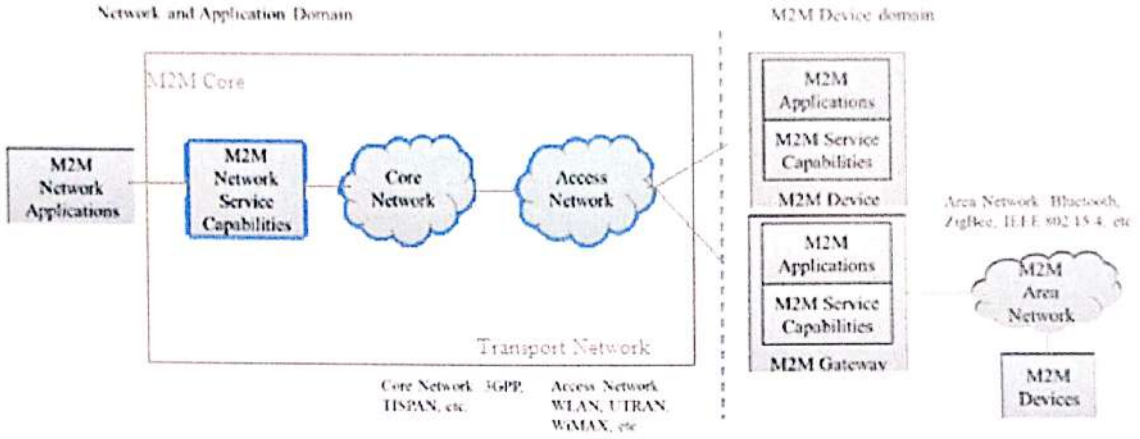

Fig. 4 European Telecommunications Standards Institute (ETSI) Machine-to-Machine (M2M) high level system overview [15]

protocols, or support of remote management of gateways and devices [14]. Fig. 4 shows the high level ETSI M2M system architecture as defined in ETSI Technical Standard (TS) [15]. the key entities in M2M are

A.M2M Gateway: - M2M devices interconnection to the network and their inter-operability.

B. M2M Device:- a device that runs application using M2M capabilities and network domain functions.

C.M2M Area Network: - it provides connectivity between the M2M devices, ETSI M2M gateways, compliant and non-compliant with ETSI M2M.

D.M2M Applications: - applications that use Service Capabilities accessible via open interfaces and run the service logic.

E.M2M Network and Application Domain: - it provides connectivity between M2M applications and M2M gateways.

F.M2M Network Applications:- applications, in the Network and applications domain, that use Service Capabilities accessible via open interfaces and run the service logic.

The Network and Application Domain is formed by the Transport Network, the M2M Core, and the Access Network. The Access Network provides connectivity between the M2M Device.

The Transport Network, Domain and Core Network provides connectivity within the Application Domain and the Network. Satellite, UTRAN, UWB, WLAN, or WiMAX technologies are used in the Access Network. The M2M Cores are composed by the M2M Network SCs and Core Network (CN). The Core Network provides IP connectivity, roaming capabilities within the M2M Core. The technologies provided by TISPAN or 3GPP can be used in the CN.

The M2M Device domain is formed by M2M Area Network, M2M gateways and M2M devices. The M2M devices are connected directly to the network and application domain using the Access Network, or they can connect first to an M2M gateway using the M2M Area Network. In first case, the devices are run an M2M applications and an SCL, and provides access to Access Network for the M2M Device, since the M2M Device has only an M2M Application running, but no SCL, and it is not compliant with ETSI. The Area Network provides connectivity between M2M gateways and M2M devices, and can be built on Bluetooth, ZigBee, M-BUS, UWB or IEEE 802.15.4 technologies.

To better illustrate some entities, the author described a map and storyboard in M2M. Fig. 5 shows an high-level view of storyboard [13]. In an M2M ecosystem, Jonathan, a user, connect his smartphone which acting as an M2M Gateways, to collect information from sensor, M2M devices, over Bluetooth using an M2M Application.

The M2M Gateway send the data to a Network SCL

(NSCL) using 3G, which have main function is to manage the data. In this case, for the backup storage purpose , the NSCL stores the data and send the content to a medical Network Application.

The M2M Management functions are all the functions required to manage M2M SCs and M2M applications in the Network and Applications Domain, and the Network Management functions have functions required to manage the access, transport networks and core. The management functions include the configuration management, performance management, fault management and software upgrading management. M2M Application life cycle

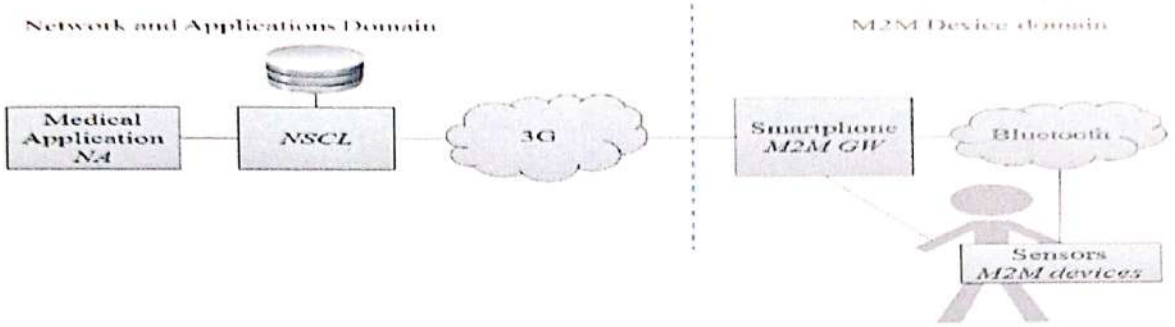

Fig. 5 High-level view of the storyboard [13]

management includes removing, upgrading and installing applications in the M2M Gateway or Device. The M2M Device management includes the configuration management of the M2M Gateways or Devices. The M2M Area Network management includes configuration management for the M2M Area Networks.

IV. PROBLEM FORMULATION

Many papers are published related to D2D and M2M communications separately. And more research also carried out in these two different topics. Now, in this paper we combine D2D and M2M communications. First we communicate two devices directly instead of going to base station, increase the spectral efficiency and then they are communicate with M2M in cellular network.

V. FULL-DUPLEX D2D COMMUNICATION WITH

A. UP-LINK RESOURCE

Consider that D2D users are using the same radio resources as uplink transmissions in the cell. In this case, base station receives interference from D2D transmissions. D2D receivers will also receive interference from uplink transmissions of the cellular users that share the same resources as D2D link. In $A_1$and $A_2$are interferencelimited areas for D2D users D1 and D2, and radius of these areas are $d_1$and d_2 respectively refer Fig.6. Throughput of the system in the presence of D2D link is increased, the amount of this gain depends on the resource allocation and power control methods. On other hand, while using full-duplex radios, throughput is affected by the residual of self-interference. Z_T is total throughput of the system when D2D link is activated

For half-duplex (HD) D2D:

$$Z_{T,HD} = Z_C + Z_{Cj,HD} + Z_{D,HD} (1)$$

For full-duplex (FD) D2D:

$$Z_{T,FD} = Z_C + Z_{Cj,FD} + Z_{D,FD} (2)$$

In the above equation, $Z_C$is throughput of cellular users that are not sharing resourceswith D2D users,$Z_{Cj,HD}$and $Z_{Cj,FD}$rate of cellular users that exploit thesame resources as D2D users in half-duplex and full-duplex mode respectively. Rate of half-duplex D2D link is $Z_{D,HD}$ and for full-duplex D2D denote the rate by$Z_{D,FD}$.

We consider γi to be the SNR of CUi at BS, $\gamma_{j,HD}$ and $\gamma_{j,FD}$ to be the SINR of the cellular users that share the same resources as D2D users while D2D is in half-duplex and full-duplex mode. So the rates for cellular and D2D users are

$$Z_C = \sum_{i=1,i\neq j}^{M} \log_2(1+\gamma_i) \qquad (3)$$

$$Z_{Cj,HD} = \sum_{j=1}^{M} \log_2(1+\gamma_{j,HD}) \qquad (4)$$

$$Z_{Cj,FD} = \sum_{j=1}^{M} \log_2(1 + \gamma_{j,FD}) \quad (5)$$

When D2D users operate in half-duplex mode, D2D user D_2 is transmitting and D2D user D_1 is receiving. Denote the SINR of D2D user D_1 as γ_{DI}. Rate of the D2D link is

$$Z_{D,HD} = \log_2(1 + \gamma_{DI}) \quad (6)$$

When D2D users use full-duplex mode, both of D2D

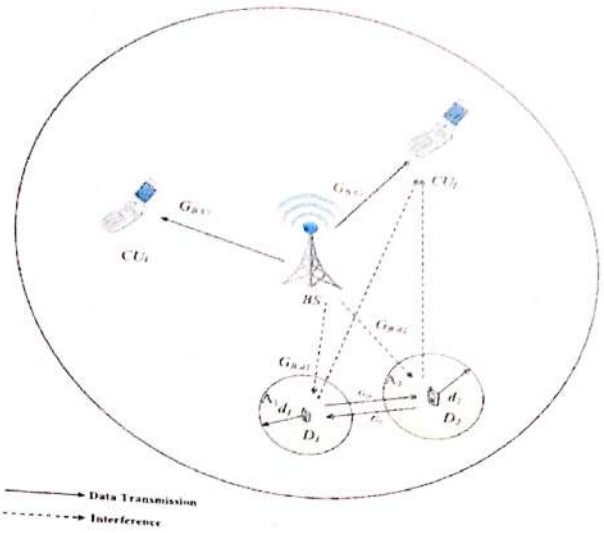

Fig. 6 D2D System Model [2]

users transmit and receive at the same time and the throughput of FD D2D link rate is

$$Z_{D,FD} = \sum_{I=1}^{2} \log_2(1 + \gamma_{DI}) \quad (7)$$

In SINR equations for cellular transmissions, we consider P_{Ci} to be the transmit power of CU_i and $G_{Ci,BS}$ channel gain between CU_i and BS. P_j is the transmit power of cellular user that is using the same resources as D2D users and $G_{Cj,BS}$ is the channel gain between CU_j and BS, and $I_{Di,Cj}$ is interference from D2D transmissions to CU_j.

SINR for half-duplex mode is

$$\gamma_{j,HD} = \frac{P_{Cj} \cdot G_{Cj,BS}}{N_0 + I_{D2,Cj}} \quad (8)$$

SINR for full-duplex mode is

$$\gamma_{j,FD} = \frac{P_{Cj} \cdot G_{Cj,BS}}{N_0 + I_{D1,Cj} + I_{D2,Cj}} \quad (9)$$

N_0 is additive white Gaussian noise in all the equations.

B. DOWN-LINK RESOURCE

In this presents the downlink transmission resources are being shared with D2D users. In this case, D2D receivers will receive interference coming from base station. Cellular users, which share the same resources as D2D users, will also have interference because of D2D transmissions. Selecting the cellular users for resource sharing is important because of these interferences. Since cellular communications is the primary service, quality of service in cellular downlink transmissions needs to be guaranteed. For this purpose interference limited area method is used to select a group of users for resource sharing that would not face harmful interference from D2D transmissions. To minimize the interference on D2D link, we select the user with minimum transmit power from the group of users selected in ILA (Interference-limited-area) method. System model of D2D communication with downlink resource reuse. In the system model, A_1 and A_2 are interference limited areas for D2D users D_1 and D_2 and radius of these areas are presented by d_1 and d_2 respectively refer Fig. 6. The rates in the system can be written as

$$Z_C = \sum_{i=1,i\neq j}^{M} \log_2(1 + \gamma_i) \quad (12)$$

$$Z_{Cj,HD} = \sum_{j=1}^{M} \log_2(1 + \gamma_{j,HD}) \quad (13)$$

$$Z_{Cj,FD} = \sum_{j=1}^{M} \log_2(1 + \gamma_{j,FD}) \qquad (14)$$

When D2D users operate in half-duplex mode, D2D user D_2 is transmitting and D2D user D_1 is receiving. SINR of D2D user D_l is denoted as γ_{Dl}. Rate of D2D link is

$$Z_{D,HD} = \log_2(1 + \gamma_{Dl}) \qquad (15)$$

When D2D users use full-duplex, both of D2D users transmit and receive at the same time and D2D link rate is

$$Z_{D,FD} = \sum_{l=1}^{2} \log_2(1 + \gamma_{Dl}) \qquad (16)$$

In SINR equations for cellular transmissions, we consider P_{Ci} to be the transmit power of CU_i and $G_{BS,Ci}$channel gain between BS andCU_i.P_j is the transmit power of cellular user that is using the same resources as D2D users and$G_{BS,Cj}$is the channel gain between BS and CU_j, and$I_{Di,Cj}$is interference from D2D transmissions toCU_i. ICI is the Inter-cell interference. SINR for the cellular users in downlink without interference from D2D is

$$\gamma_i = \frac{P_{Ci} \cdot G_{BS,Ci}}{N_0 + ICI} \qquad (17)$$

SINR for cellular users with half-duplex D2D resource sharing is

$$\gamma_{j,HD} = \frac{P_{Cj} \cdot G_{BS,Cj}}{N_0 + I_{D2,Cj} + ICI} \qquad (18)$$

SINR for cellular users with full-duplex D2D resource sharing is

$$\gamma_{j,FD} = \frac{P_{Cj} \cdot G_{BS,Cj}}{N_0 + I_{D1,Cj} + I_{D2,Cj} + ICI} \qquad (19)$$

VI. M2M FADING CHANNELS UNDER

A. *LINE OF SIGHT (LOS)*

Modelling of M2M channels with line-of-sight (LOS) components have motivations behind this comes from the fact that such models are flexible enough to accommodate asymmetric channel conditions. Besides, LOS fading channel models easily reduce to those models that correspond to NLOS propagation conditions. Modelling M2M fading channels with LOS components is more reasonable, since such models can be reduced to those associated with NLOS propagation conditions. It is not necessary that LOS propagation conditions are available in all the transmission links. However, LOS M2M models provide reasonable flexibility to accommodate mixed LOS and NLOS conditions in different machines.

B. *NON LINE OF SIGHT (NLOS)*

The M2M communications describe under non-line of sight (NLOS) propagation conditions. This channel models can be developed based on the geometry of the scattering environment. The multipath propagation channel in any mobile system and wireless communication system efficiently described with the help of proper statistical models. For example, the Rayleigh distribution is considered to be suitable for model fading channels under NLOS propagation conditions in classical cellular networks. NLOS propagation conditions are considered for all transmission links. It is further assumed that there is no direct transmission link between the source mobile station and the destination mobile station.

TABLE I
SUMMARY OF LITERATURE

Proposal	Work
Samad Ali	Full-duplex device-to-device communication. The self-interference cancelation requirements used for full-duplex radios to be implemented in device-to-device communication are investigated.
Afif et.al	Introduced two concepts which have not been present in cellular systems for IMT-Advanced so far: Device-to-device (D2D) communication and network coding.
Asadi et al.	Introduced and survey on classification of device-to-device communication such as in-band and out-band.
S. Shalmashi et al.	A cooperative device-to-device communications in order to combat the problem of congestion in crowded communication areas such as shopping mall and open air festivals.
Batool Talha	Modelled and analysed narrowband M2M fading channels in cooperative network systems under line-of-sight (LOS) as well as non-line-of-sight (NLOS) propagation conditions.
Andrius et al.	Proposed a new approach which is called as Clone-to-Clone (C2C) has the potential to reduce the traffic between end points, improve network performance and reduce power consumption of device.
Prasad et al.	Introduced Energy Efficient and Reliable (EER) and all research issues related with the deployment of M2M architecture of M2M communication.
Booysen et al.	Described M2M communications in the vehicular networking context and The author Booysen investigated areas where M2M principles can improve vehicular networking.
Taranekar et al.	Blocking probability in cellular cells as well as formation of D2D groups.

VII. CONCLUSION

In this paper, we described concepts key to the development of M2M and D2D communications systems. In this paper we communicate two devices directly without going to BS and later into M2M communication in cellular networks. Providing direct communication between devices will decreases latency and also offload of data from BS. A D2D user provides higher spectral efficiency but also causes mutual interference between cellular and D2D users by using full-duplex technique.

VIII. REFERENCES

[1] Afif OSSEIRAN1, Klaus DOPPLER2, Cassio RIBEIRO2, Ming XIAO3, MikaelSKOGLUND3, Jawad MANSSOUR1. "Advances in Device-to-Device Communications and Network Coding for IMT-Advanced". 1Ericsson Research, Stockholm, Sweden. ICT-Mobile Summit 2009 Conference Proceedings Paul Cunningham and Miriam Cunningham (Eds) IIMC International Information Management Corporation, 2009 ISBN: 978-1-905824-12-0.8p.

[2] Ali S. "Full Duplex Device-to-Device Communication in Cellular Networks", University of Oulu, Department of Communications Engineering Master's Degree Program in Wireless Communications Engineering. Master's thesis, 47 p.October 2014.

[3] M.J. Booysen1, J.S. Gilmore1, S. Zeadally2 and G.J.van Rooyen1, "Machine-to-Machine (M2M) Communications in Vehicular Networks", 1MIH Media Lab, Dept. of Electrical and Electronic Engineering, South Africa, KSII TRANSACTIONS ON INTERNET AND INFORMATION SYSTEMS VOL. 6, NO. 2, Feb 2012.

[4] https://www.google.co.in/search?q=m2m+communication&biw=1366&bih=634&tbm=isch&tbo=u&source=univ&sa=X&ved=0CD4QsARqFQoTCKzfmOSikcgCFYgfjgodNZwBqQ#imgrc=m94JDL9Pm5O3DM%3A.

[5] Zhang, Y.; Yu, R.; Xie, S.; Yao, W.; Xiao, Y.; Guizani, M. "Home M2M networks: Architectures, standards, and QoS improvement". IEEE Commun. Mag. 2011, 49, 44–52.

[6] S. Shalmashi, S. Ben, "Cooperative Device-to-Device Communications in the Downlink of Cellular Networks", IEEE WCNC'14 Track 3 (Mobile and Wireless Networks), 978-1-4799-3083-8/14/$31.00 c_2014 IEEE.

[7] Pankil P. Taranekar, V. V. Dixit, "Device-to-Device (D2D) Cellular Communication: Group Formation of Devices", International Journal of Advanced Research in Computer and Communication Engineering Vol. 4, Issue 6, June 2015.

[8] Arash Asadi, Student Member, Qing Wang, Student Member, and Vincenzo Mancuso, Member."A Survey on Device-to-Device Communication in Cellular Networks" IEEE, 18p. 29 April 2014.

[9] BatoolTalha, "Mobile-to-Mobile Cooperative Communication Systems: Channel Modelling and System Performance Analysis", Degree Philosophise Doctor (PhD) in Information and Communication Technology, 60p. September 2010.

[10] Marwat, S.; Potsch, T.; Zaki, Y.; Weera wardane, T.; Gorg, C. "Addressing the Challenges of E-Healthcare in Future Mobile Networks". Lect. Notes Computer. Sci. 2013, 8115, 90–99.

[11] Andrius Aucinas and Jon Crowcroft, Pan Hui, "Energy efficient mobile M2M communications", University of Cambridge, UK, Deutsche Telekom Labs Berlin, Germany.6p.

[12] Shyam Sundar Prasad, Chanakya Kumar, "A Methodology for an Efficient and Reliable M2M Communication", International Journal of Soft Computing and Engineering (IJSCE) ISSN: 2231-2307, Volume-3, Issue-4, September 2013.

[13] Carlos Pereira and Ana Aguiar, "Towards Efficient Mobile M2M Communications: Survey and Open Challenges", Sensors 2014, 14, 19582-19608; doi: 10.3390/s141019582, 1-27p.

[14] ETSI. ETSI TS 102 690 V1.2.1 (2013-06) "Machine-to-Machine communications (M2M); Functional Architecture". Available online:http://www.etsi.org/deliver/etsi_ts/102600_102699/102690/01.02.01_60/ts_102690v010201p.pdf (accessed on 15 March 2014).

[15] ETSI. ETSI TS 102 689 V2.1.1 (2013-07) "Machine-to-Machine communications (M2M); M2M Service Requirements". Available online: http://www.etsi.org/deliver/etsi_ts/102600_102699/102689/02.01.01_60/ts_102689v020101p.pdf (accessed on 15 March 2014).

[16] ETSI. ETSI TR 102 898 V1.1.1 (2013-04) "Machine-to-Machine Communications (M2M);Use Cases of Automotive Applications in M2M Capable Networks". Available

[17] Chen, M.; Wan, J.; Gonzalez, S.; Liao, X.; Leung, V. "A Survey of Recent Developments in Home M2M Networks". IEEE Commun. Surv. Tutor. 2014, 16, 98–114.

[18] Lu, R.; Li, X.; Liang, X.; Shen, X.; Lin, X. GRS: "The green, reliability, and security of emerging machine to machine communications". IEEE Commun. Mag. 2011, 49, 28–35.

[19] Kwang-Cheng Chen, "Machine-to-Machine Communications for Healthcare".Journal of Computing Science and Engineering,Vol. 6, No. 2, June 2012, pp. 119-126.

[20] B. Talha and M. Patzold, "On the statistical properties of mobile-to-mobile fading channels in cooperative networks under line-of-sight conditions," in Proc. 10thInt.Symp. on Wireless Personal Multimedia Communications, WPMC 2007, Jaipur, India, Dec. 2007, pp. 388-393.

[21] C-H. Yu, K. Doppler, C. Ribeiro, and O. Tirkkonen, "Performance impact of fading interference to device-to-device communication undelaying cellular networks," in Proceeding of IEEE PIMRC, 2009, pp. 858-862.

[22] Chanakya Kumar1, Rajeev Paulus2,"A prospective towards M2M Communication" 1*Research Scholar,Department of ECE, SHIATS-DU, Allahabad, India, chanakya@ieee.org 2 *Department of ECE, SHITAS-DU, Allahabad, India, rajeev.paulus@shiats.edu.in2.

KIET IJCE KIET International Journal of Communications & Electronics

Volume. No. 4, Issue No. 1, January-June 2016, ISSN: 2320 - 8996

CSRR Loaded UWB Monopole Antenna with Tri - Notch Characteristics for WLAN, WiMax and X Band Applications

Chhavi Gupta[1], Monika[2] and Jyoti Mishra[3]

M.Tech Student[1, 3], Assistant Professor[2]

Department of Electronics and communication Engineering, Jaypee Institute of Information Technology, Noida - 201307, India

[1]Chhavi01gupta@gmail.com, [2]moniktronics@gmail.com, [3]jyotimishra13@rediffmail.com

Abstract - **In this work, a ultra-wideband planar monopole antenna with tri notch along with a metamaterial structure has been proposed with substrate height of 0.8mm.The antenna consist of semicircular radiating patch and a CSRR loaded ground plane. For verifying the implemented metamaterial structure possess the negative value of permeability and permittivity, Nicolson Ross Weir Method (NRW) has been used. By etching round shape slots on patch we get the characteristics at WLAN band(2.4-2.483GHz),(5.470-5.725GHz), WiMax band(2.5-2.69GHz),(5.25-5.85GHz) and C-band at uplink frequency of (5.9-6.4GHz).To get the notches at X-band having uplink and downlink(7.9-8.4GHz),(7.25-7.55GHz) respectively a pair of CSRR has been loaded on ground plane. The measured impedance bandwidth ranges is from 2.4-11.94GHz having the return loss of less than 10dB. The proposed antenna exhibits omnidirectional radiation pattern in the H-Plane and dipole like Radiation Pattern in E-Plane. The simulated Gain observed is stable output at UWB application. Software HFSS version 16 has been used for Simulation purpose.**

Keywords - **Complimentary Split Ring Resonator (CSRR) Nicolson Ross Weir, Ultra Wide Band (UWB), Microstrip antenna, Metamaterial Antenna (MTM).**

I. INTRODUCTION

Although, the Microstrip patch Antenna have various advantages (low profile, low cost and Omni - directional radiation pattern),it exhibits some disadvantage like narrow bandwidth and low gain[4],[5]. To overcome this concept of metamaterials have been evolved by Veselgo. These materials do not exist in nature but their properties do exists. The simulated result of metamaterial structures has been implemented on MS-Excel approaching NRW Method, in which the negative value of permittivity and permeability has been shown. After that, this structure has been loaded on the ground of proposed patch antenna .As to enhance the data rate in wireless communication UWB antenna has been taken as the wide interest and the Federal Communication Commission(FCC) has released 3.1 to 10.6GHz as an unlicensed band for radio Communication[1].Due to low power emission level UWB can be easily interfered with WiMax band (2.5-2.69GHz), (5.25-5.85GHz), WLAN band (2.4-2.483GHz), (5.470-5.725GHz), C-band at uplink frequency of (5.9-6.4GHz) and X band uplink and downlink (7.9-8.4GHz), (7.25-7.55GHz) respectively. By the literature survey we came to know that by etching different slots on radiating patch and ground plane single, double, triple notch can been attain in UWB region. The notch band characteristics are obtained by radiating two round shape slots on patch and a pair of CSRR loaded on ground plane[3].The dimension of slot has been varied and the optimized result has been shown. The proposed Antenna exhibits nearly omnidirectional radiation pattern in H-Plane and dipole like radiation pattern in E-Plane.

II. NRW APPROACH

To find the value of permeability and permittivity, NRW method has been used. The value of Mu and epsilon is evaluated using equation 1,2and3. To extract the value of S-

parameter the structure is placed in a waveguide. To create the internal environment of waveguide Perfect Electric and Magnetic boundaries have been formed around the structure [7], [8].The simulated S-parameters has been exported on Ms-Excel for verifying the properties of metamaterial structure.

Equations for calculating permittivity and permeability using NRW Method.

$$\mu_r = \frac{2c(1-v_2)}{\omega di(1+v_2)} \quad (1)$$

$$\varepsilon_r = \mu_r + \frac{2S_{11}ci}{\omega d} \quad (2)$$

$$v_2 = S_{21} - S_{11} \quad (3)$$

Where

ε_r = Permittivity

μ_r = Permeability

ω =Frequency in Radian

d=Thickness of the Substrate

c=Speed of Light

v_2=Voltage Minima

III. ANALYSIS OF METAMATERIAL STRUCTURE

This structure has been analyzed on 7x7mm^2 Patch with the 0.8mm FR-4 Substrate Thickness. The width of the slot has been taken as 0.7mm.The simulated value of S11 and S21 has been exported on Ms-Excel and the negative value of permittivity and permeability has been verified by the above stated formulas.

Table 1.Dimensions of Unit Cell

Parameter	Dimension in mm
L	7
W	7
X	6
Y	6
g	0.7

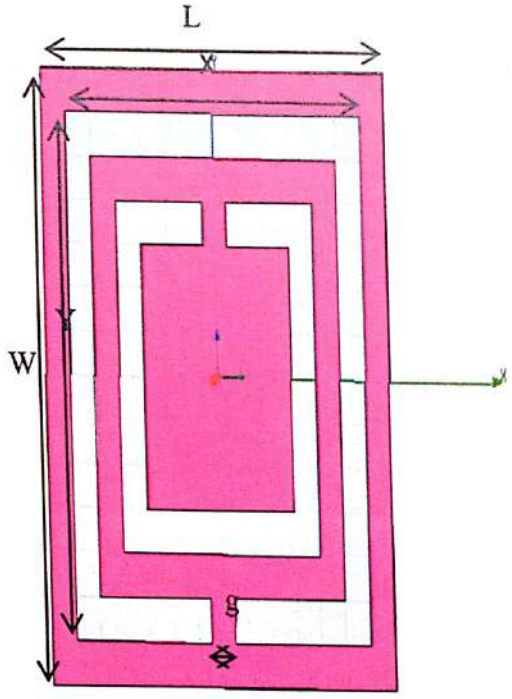

Figure 1: Design of Metamaterial Structure

Table2. Obtained valueof Permeability versus Frequency from the MS-Excel program.

S.No.	Frequency(GHz)	Permeability
1	4	1030511794
2	4.1	-949859018.7
3	4.2	-495348491.9
4	4.3	-334692726
5	4.4	-253966697.6
6	4.5	-205273597.2
7	4.6	-172541014.5
8	4.7	-148907874.3
9	4.8	-130960167.3
10	4.9	-116808649.7
11	5	-105322784.4
12	5.1	-95784114.14
13	5.2	-87713708.7
14	5.3	-80779615.91
15	5.4	-74744151.65
16	5.5	-69432357.05
17	5.6	-64712319.48
18	5.7	-60482447.29
19	5.8	-56662976.96
20	5.9	-53190138.68
21	6	-50012033.63

Table3. Obtained value of Permittivity versus Frequency from the MS-Excel program

S.No.	Frequency(GHz)	Permittivity
1	4	995420565.8
2	4.1	-980368390.5
3	4.2	-521739162.2
4	4.3	-357351258.1
5	4.4	-273219130.1
6	4.5	-221397777.1
7	4.6	-185776041.6
8	4.7	-159461354.1
9	4.8	-139013811.6
10	4.9	-122522628
11	5	-108839126.1
12	5.1	-97229381.24
13	5.2	-87201102.12
14	5.3	-78410633.29
15	5.4	-7060983.89
16	5.5	-63614484.69
17	5.6	-57283850.74
18	5.7	-51508222.54
19	5.8	-46199948.78
20	5.9	-41287420.57
21	6	-36710691.8

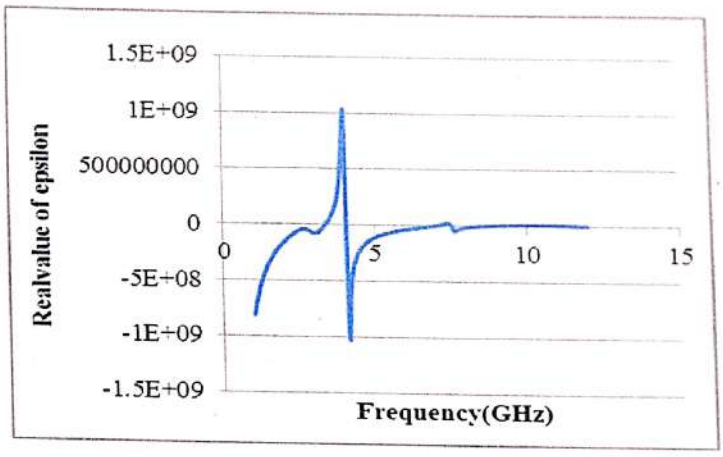

Figure 2: Permeability versus Frequency Graph

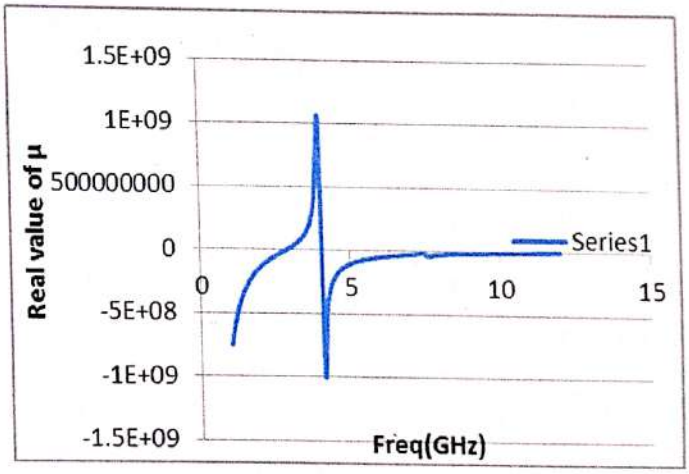

Figure 3: Permeability versus Frequency Graph

IV. DESIGN AND ANALYSIS LOADED WITH METAMATERIAL STRUCTURE

The Antenna has a size of 27x25mm^2.The antenna is designed on FR-4 Substrate of 0.8mm thickness having dielectric constant 0f 4.4 and loss tangent 0.02.The proposed antenna shows the advancement made in design[1].

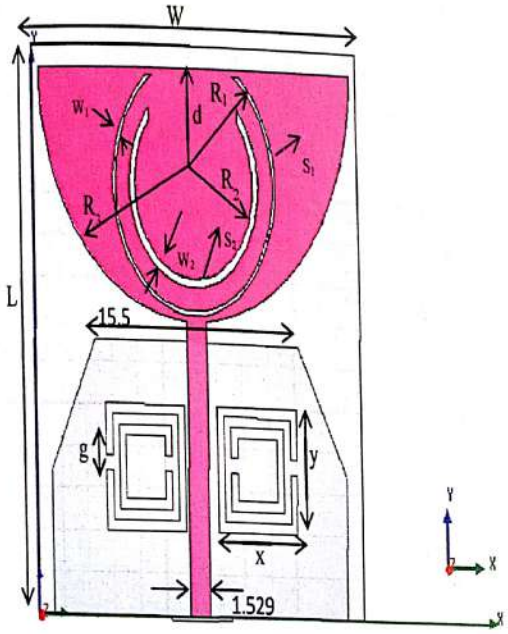

Figure 4:Proposed Antenna

Table 4.Dimensions of proposed Antenna

Parameter	Dimension(mm)
L	27
W	25
D	5.5
R_1	6
R_2	4.5
R_3	12
W_1	0.2
W_2	0.4
X	6
Y	6
G	0.7

V. RESULTS AND DISCUSSION

The Simulation has been done on Ansoft HFSS version 16.Two round slot S1 and S2 has been etched on a radiating patch, with a pair of CSRR Loaded on ground plane shown in fig.4.CSRR dimensions are taken same as described in NRW approach. The band in WiMax and WLAN range is achieved due to S1 and S2 Slot on radiating patch, the band achieved in X band and C band uplink range is due to CSRR loaded on ground plane. The gap of CSRR has been optimized using the e and d as optimizing variables shown in fig 5.The fig.6 shows the optimized simulated results. Fig.7 shows the gain vs frequency plot, which provides the stable gain while fig.8 shows the graph of radiation efficiency in upto 85% efficiency is attain in X band while 95% efficiency in WLAN, WiMax frequency ranges. The Radiation Pattern has been plotted in in different pass band frequencies like 2.5GHz, 3.3GHz, 4.4GHz, 5.5 GHz, 7.5GHz, 8.5GHz which provides bidirectional radiation pattern in E-plane and Omnidirectional in H-Plane. Current distribution has been observed at frequency ranges of our antenna applications. At 2.4GHz and 5.5 GHz surface current is distributed is over slot s1 and s2 while a very high current is observed at CSRR around 7.5GHz and 9.4GHz.

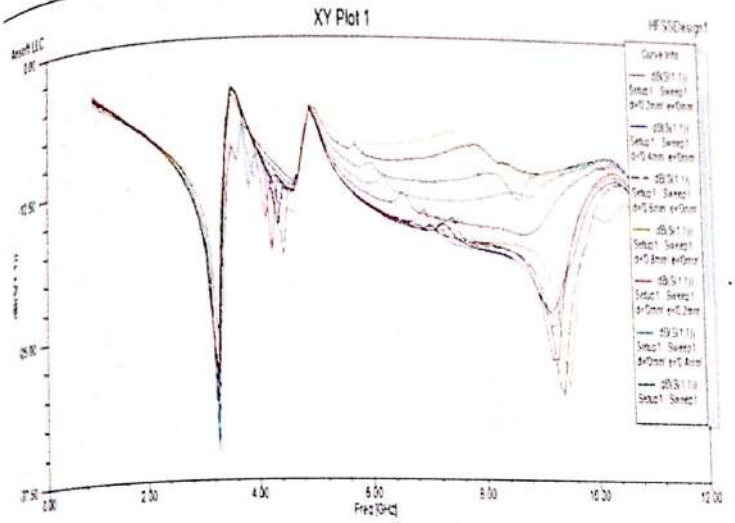

Figure 5:S11 with optimizing variable

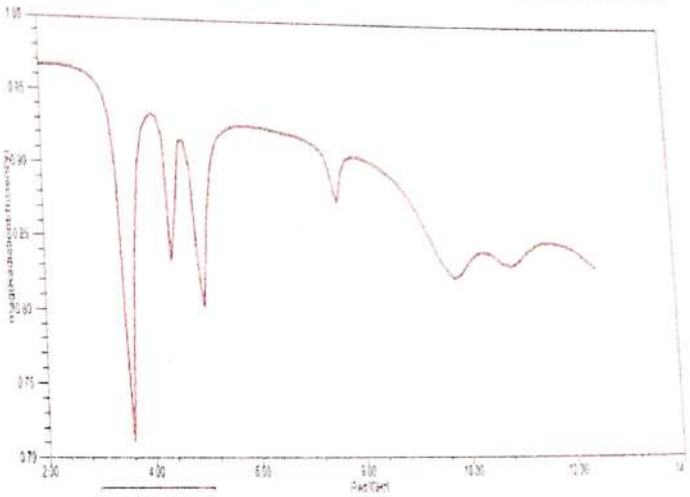

Figure 8: Radiation efficiency plot

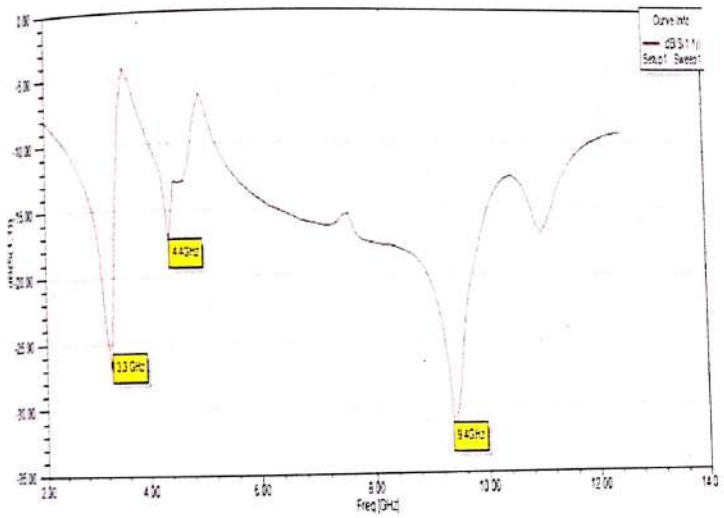

Figure 6:S11 with optimized variable

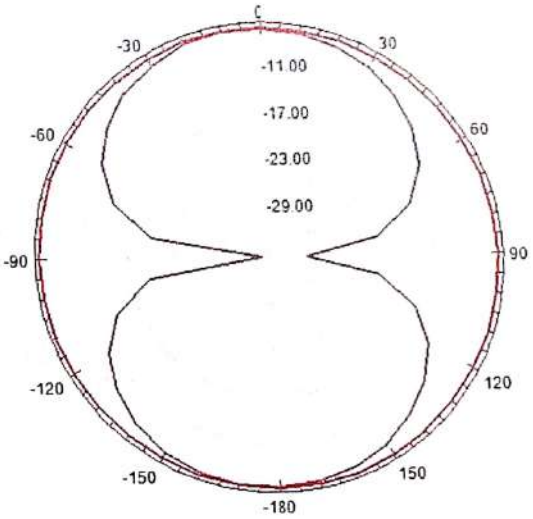

Figure 9: At 2.5GHz

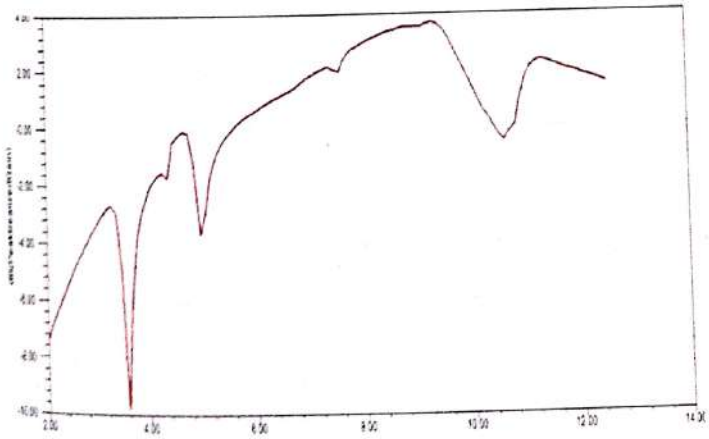

Figure 7:Gain vs Frequency

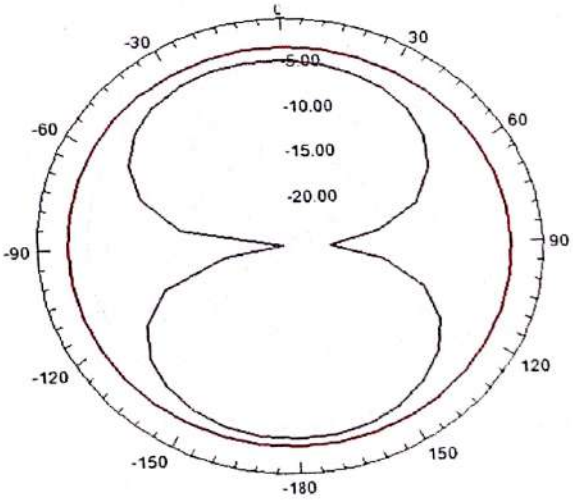

Figure 10: At 4.4GHz

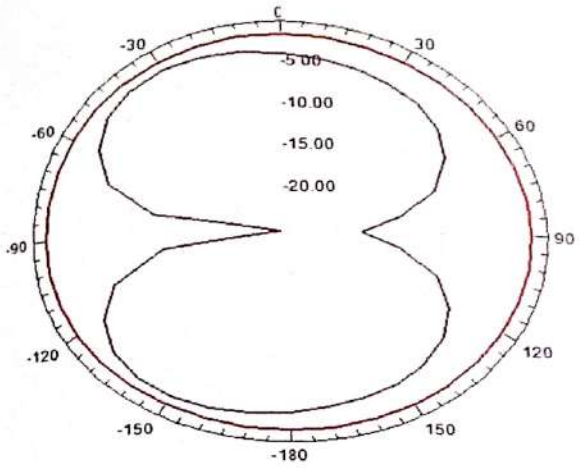

Figure 12: At 5.5GHz

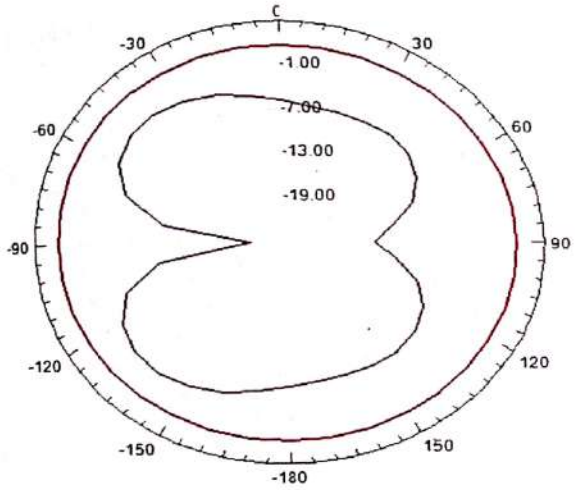

Figure 13: At 7.5GHz

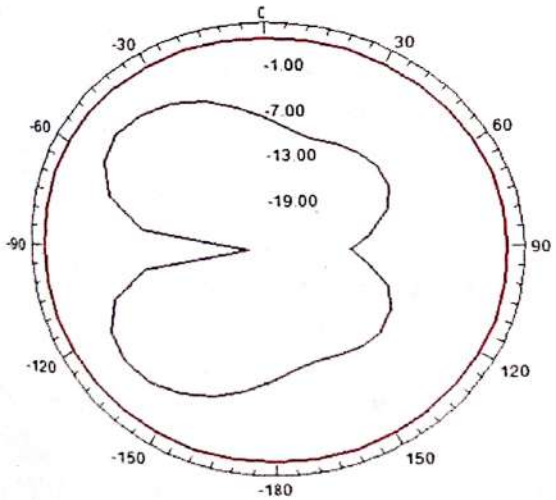

Figure 14: At 8.5GHz

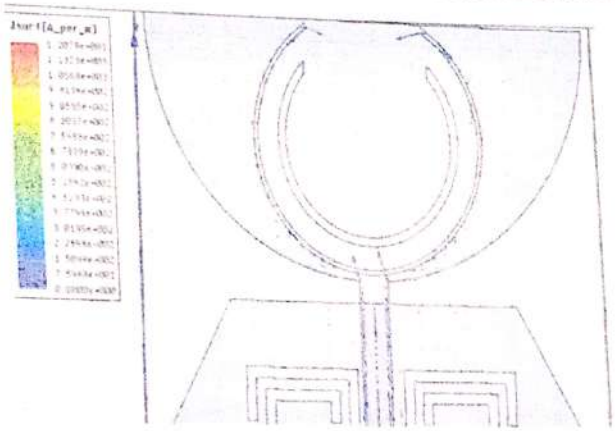

Figure 15: Current Distribution at 2.5GHz

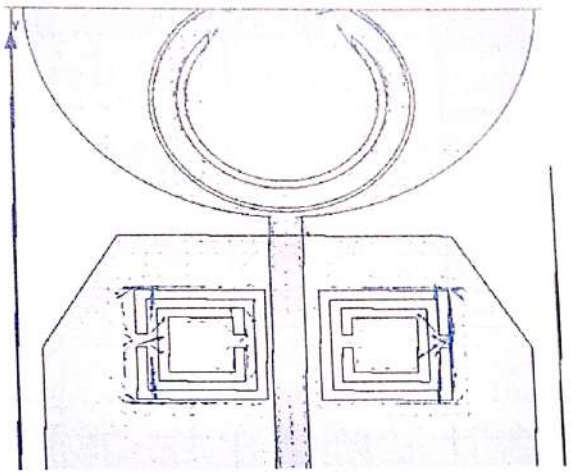

Figure 16: Current Distribution at 5.5GHz

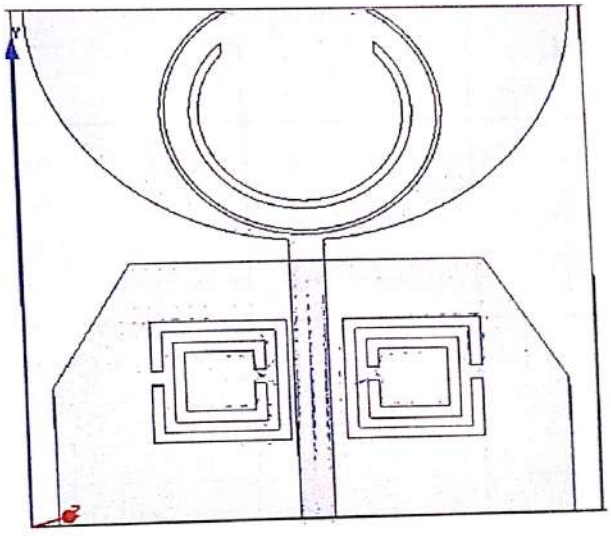

Figure 17: Current Distribution at 7.5 GHz

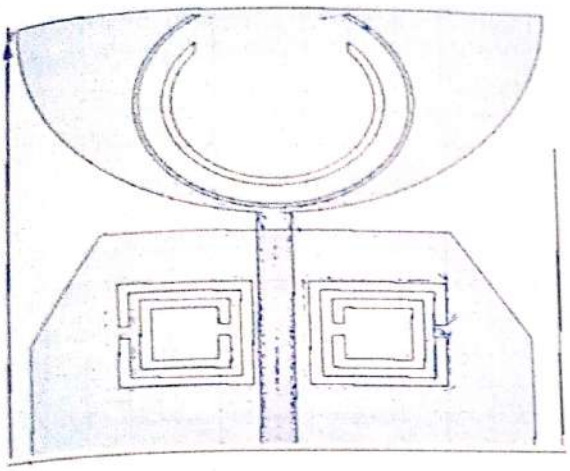

Figure 18: Current Distribution at 9.4 GHz

Table 4: List of Parameter extracted from simulated result at mid frequency of the applications covered by design antenna

Freq (GHz)	S11(dB)	VSWR	Gain(dB)	Directivity(dB)	Efficiency
2.5	-10.47	1.8	-5	-4.5	96%
5.5	-11.79	1.6	0	0.035	92%
6	-14.07	1.4	0.6	1	92.7%
7.5	-15.45	1.4	2.05	2.6	89%
8	-17.56	1.3	3.15	3.4	90%

VI. CONCLUSION

On the basis of simulated results, it is observed that we attain better results by loading CSRR on ground as compare to[1].The proposed design covers the WLAN and WiMax ranges as in[1],as well as it covers the whole X band including C band uplink frequency range. Improvement in return loss of -20 dB at 9.4GHz and -7dB at 4.4 GHz has been observed. It has been observed that by changing the width of CSRR slot, modification in notches can be made,without affecting the UWB band. The observed radiation pattern in H and E plane provides stable far field radiation pattern .The simulated radiation efficiency.75% to 96% Radiation efficiency is observed in different bands. The proposed antenna is suitable for UWB applications.

VII. REFERENCES

[1] SaiK.Venkata, MuktikantaRana, PritamS.Bakariya," Planar UWB Monopole antenna with Tri-Notch band Characteristics, "*Progress in Electromagnetics Research C*", vol.46, pp.163-170, 2014.

[2] Yuandan Dong, Hiroshi Toyao and Tatsuo Itoh, "Design and Characterization of miniaturized patch antenna loaded with complimentary split-ring resonator", *IEEE Trans.Antenna and Propagation.*vol.60, pp.no.20-27, February 2012.

[3] Ricardo Marques, Ferran Martin and Mario Sorolla, "*Metamaterial with Negative Parameters*", first ed., Willey Series in Microwave and Optical Engineering, pp.155-172, 2007.

[4] Constantine A.Balanis, "*Antenna Theory Analysis and Design*", 3rd ed., Willey Student Edition, pp.1-24,811-876.

[5] Matthew N.O Sadiku, "*Principles of Electromagnetics*",4thed.,Oxford International student Edition,pp.479-480.

[6] Ramesh Garg, PrakashBhartia, InderBahl, ApisakIttipiboon,"*Microstrip Antenna Design*", first ed., Artec House Boston, London, pp.1-28.

[7] Shridhar E. Mendhe1 &Yogeshwar Prasad Kosta,"Metamaterial Properties and Applications", *International Journal of Information Technology and Knowledge Management,*January-June 2011, vol.4,no.1, pp. 85-89.

[8] BimalGarg, AnkitSamadhiya, Rahul DevVerma, "Analysis and design of microstrip patch antenna loaded with innovative metamaterial structure", *Research Journal of Physics and Applied Science,* vol.1, pp.013-019, August 2012.

[9] BimalGarg, AnkitSamadhiya, Rahul DevVerma,"Design of Rectangular Microstrip Patch Antenna Incorporated Metamaterial Structure for Dual band Operation and Amelioration in patch Antenna Parameter with Negative μ and ε ", *International Journal of Engineering and Technology*, vol.1, no.3, pp.205-216, 2012.

[10] S.Arslanagic,T.V.Hansen,N.A.Mortensen,A.H.Gregersen, O.Sigmud,R.W.Ziolkowski,andO.Breinbjerg,"A Review of the Scattering-parameter Extraction Method with Clarification of Ambiguity issues in Relation to Metamaterial Homogenization",*IEEE Antennas and Propagation Magazine*,vol.55,no.2,April 2013.

[11] A.M.Nicolson, G.F.Ross, "Measurement of the intrinsic Properties of Materials by Time-Domain Techniques", *IEEE Transaction on Instrumentation and Measurement*, vol.IM-19, no.4, November 1970.

[12] Chieh-Sen Lee and Chin-Lung Yang,"Single-Compound Complimentary Split-Ring Resonator for Simultaneously Measuring the Permittivity and Thickness of Dual-Layer Dielectric-Materials",*IEEE Transaction on Microwave Theory and Techniques*,vol.63,no.6,june 2015.

[13] Olli Luukkonen, StanislavI.Maslovski and Sergei A.Tretyakov, "A Stepwise Nicolson Ross Weir Based Material Parameter Extraction Method",*Antennas and Wireless Propagation Letters*, vol.10, 2011.

[14] Yuandan Dong and Tatsuo Itoh,"Metamaterial-Based Antennas",*Proceedings of the IEEE*,vol. 100, no.7, July 2012.

[15] Kaushal Gangwarl, Dr. Paras and Dr. R.P.S. Gangwar, "Metamaterials Characteristics, Process and Applications", *Advance in Electronic and Electric Engineering*,vol. 4, no.1, pp. 97-106, 2014.

[16] GyanPrakash, Sadhana Pal,"WiMax Technology and its Application", *International Journal of Engineering Research and Application*,vol.1,no.2,pp.327-336.

KIET IJCE KIET International Journal of Communications & Electronics

Volume. No. 4, Issue No. 1, January-June 2016, ISSN: 2320 - 8996

Patch Antenna Loaded With Meander Line and Partially Defected Ground for Satellite Communication

Jyoti Mishra[1], Monika[2] and Chhavi Gupta[3]

M.Tech Student[1, 3], Assistant Professor[2]

Department of Electronics and communication Engineering, Jaypee Institute of Information Technology, Noida - 201307, India

[1]jyotimishra13@rediffmail.com, [2]moniktronics@gmail.com, [3]chhavi01gupta@gmail.com

Abstract- **This paper presents the design of proposed antenna for X-band and Wi-Max (Worldwide Interoperability for Microwave Access, 3.2–3.8 GHz) applications. In proposed antenna slots created in ground plane and top patch provides wide bandwidth (4.6GHz) in X-band. This design approach is meant for satellite communication, amateur radio, military communication and middle band of Wi-Max applications.**

Keywords- **Satellite Communication, Wi-Max Defected ground structure, circular polarized antenna.**

I. Introduction

Presently microstrip patch antennas became the most famous due to their applications and merits like less fabrication cost, light weight, compact shape and covers wide range of frequencies. Moreover it has some drawbacks such as narrow bandwidth, low gain and low efficiency etc. Many researchers preformed to overcome these demerits. In this paper microstrip fed dual band antenna is designed by loaded with meander line in the radiating patch and introducing partially defected ground (PDGS) in the ground plane to enhance the bandwidth. The proposed patch antenna is operating in middle band of Wi-max frequency range (3.2-3.8GHz) and X-band (8-12GHz). In this paper, a good bandwidth is achieved for X-band using partial defect in ground. Moreover radiation characteristics, realised gain, axial ratio and VSWR are obtained by using HFSS with satisfying result values. To design an efficient microstrip patch antenna (MPAs) for satellite communication required to design at specific range of frequency as C band, X, Ka, Ku and S-band with suitable feeding techniques and dielectric substrate[6]. Circular polarisation is often needed for satellite communication application for reduction of any orientation related problem of the receiving based station antennas. In our design AR < 3 is achieved, which is necessary condition for circular polarization.

II. Antenna Geometry and Design

The geometry of the proposed antenna with microstrip feed line is shown in the figure 1. In this paper the proposed antenna is printed on an FR-4 (dielectric constant is 4.4 and loss tangent is 0.02) substrate with size $22 \times 28.8 \times 1.6$ mm^3.To achieve 50 Ω characteristic impedance, the width of the microstrip line is 1.4mm.

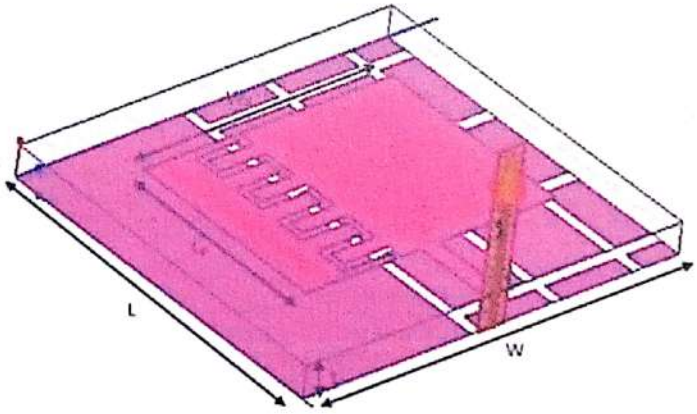

Fig 1: Schematic diagram of microwave-fed meander line loaded MPA placed over PDGS

Length and width of the ground for the proposed microstrip patch antenna is calculated as:

$$L = Lp + 6 \quad (1)$$

$$W = Wp + 6 \quad (2)$$

In this paper, meander line is etched on the radiating patch and the crossed strip line are etched on the ground plane of

the Microstrip patch antenna creating partially defect in ground plane fig 2.

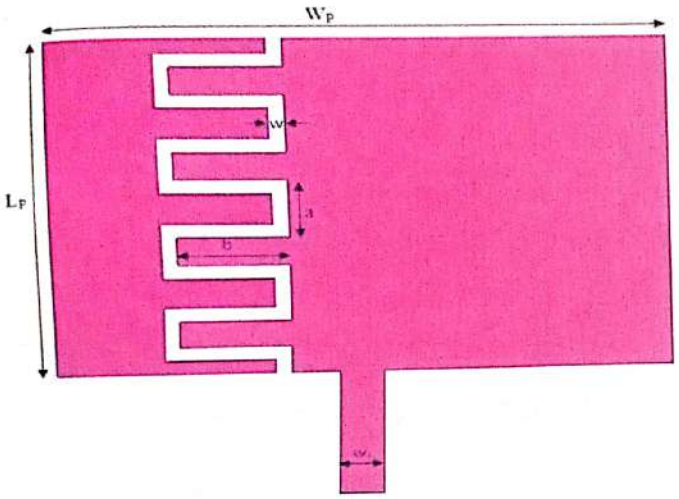

Fig 2: (a) design parameters of meander line: L_P=19.2mm, W_p=12.4mm, w=0.5mm, a=3mm, b=4mm

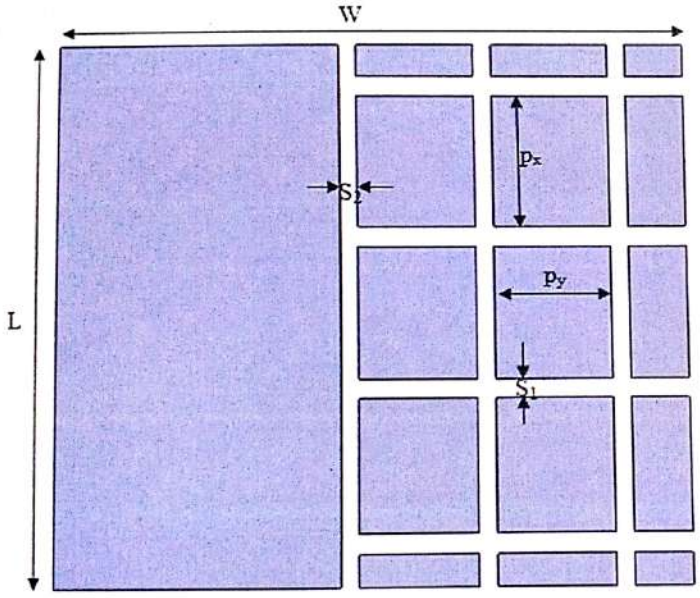

Fig 2: (b) design parameters of PDGS: S_1=0.8mm, S_2=0.7mm, p_x=4.6mm, p_y=4.2mm

III. Simulation and Result

The all results of proposed antenna were simulated by HFSS (high frequency simulator structure) version 16. The simulated return loss and VSWR versus frequency of the proposed antenna is depicted in fig 3. It is observed from the result that microstrip patch antenna resonate at the 3.37-3.49GHz which encompasses the middle range of WiMAX (3.2-3.8GHz) and 6.78-11.3GHz which covers the entire X band (Uplink 7.9-8.4GHz and Downlink 7.25-7.75GHz) as well as Amateur Radio band (10.450-10.50GHz) and Military communication band (8.5-10.5GHz), this shows that MPA is working in two bands.

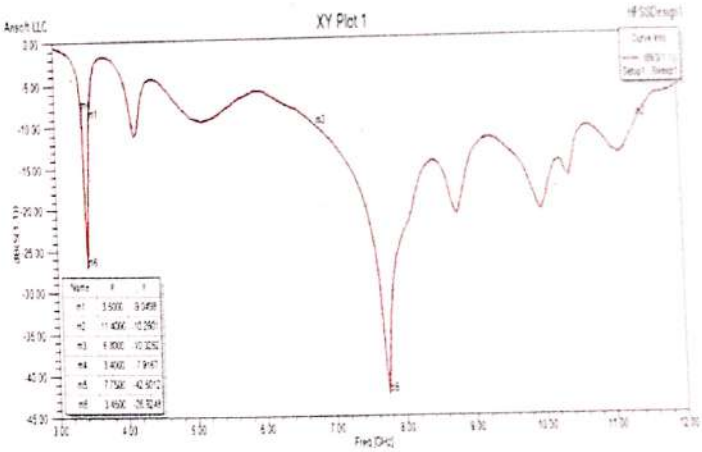

(a)

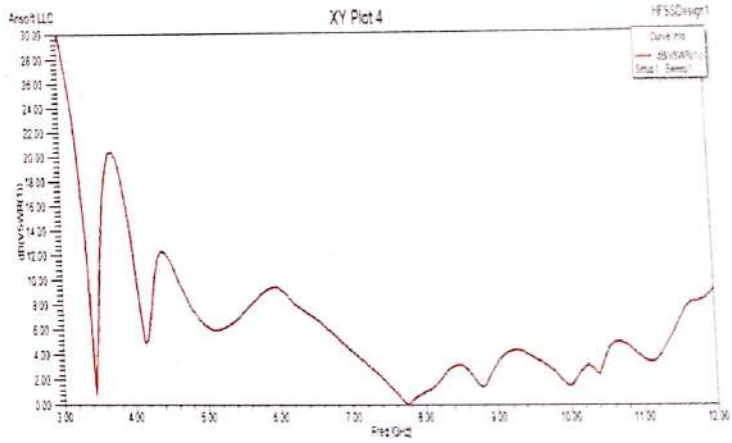

(b)

Fig 3 (a) return loss versus frequency (b) VSWR versus frequency

The radiation characteristics of proposed MPA such as realised gain, axial ratio, radiation pattern, efficiency and directivity have also been measured in a far field range. The realised gain, shown in fig 4(a) of the proposed antenna at 7.5GHz is 2.03dB and at 8.05GHz is 2.61dB. For Amateur communication region (10.45-10.50GHz), it is 1 dB. The efficiency of the proposed antenna is approximately one which is shown in fig 4(b). Fig 4 (c) shows the axial ratio of the MPA with respect to the frequency. From graph it is observed that at uplink and downlink frequencies of the proposed antenna is optimized for best CP radiation (AR < 3).

Volume. No. 4, Issue No. 1, January-June 2016, ISSN: 2320 - 8996

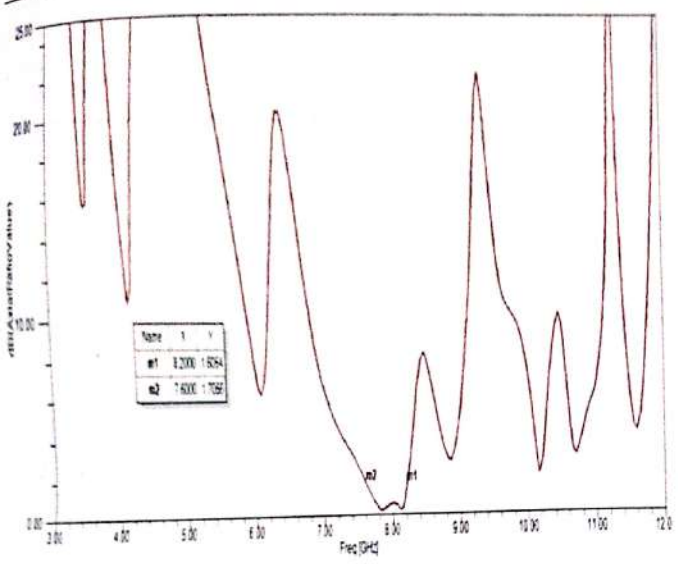

Fig 4(a): Realised Gain Vs frequency

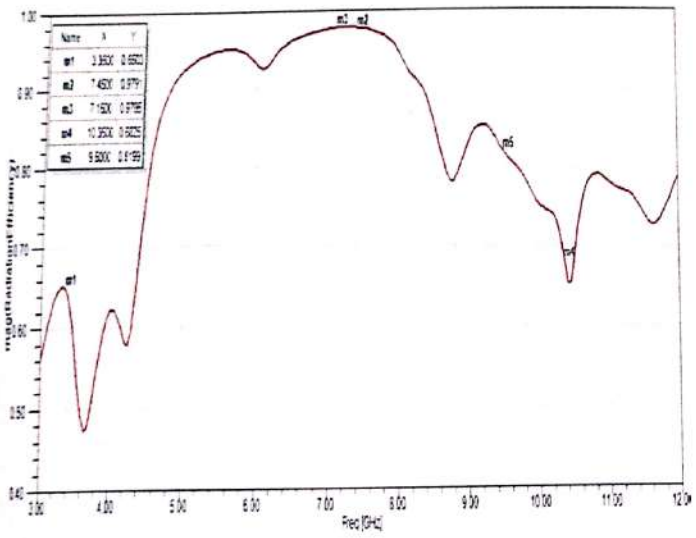

Fig 4(b): Efficiency of proposed MPA

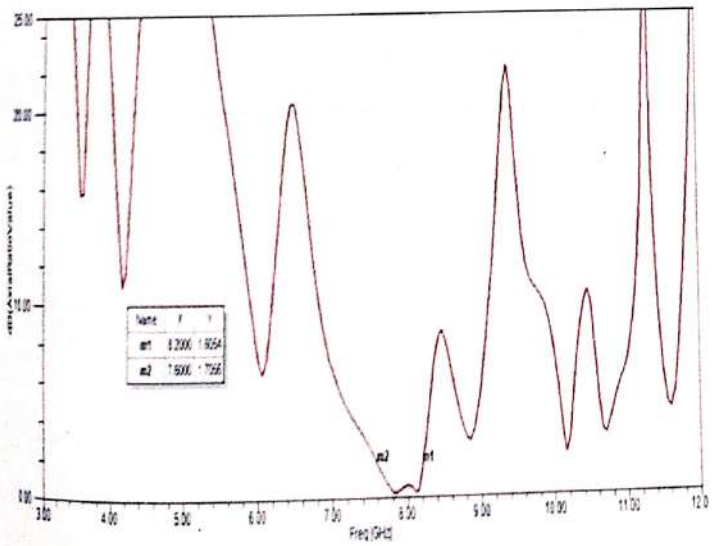

Fig 4(c): Axial Ratio of proposed MPA

The radiation pattern at (a) 3.4GHz (b) 7.5GHz (c) 10.5GHz have plotted in fig 5. And fig 6 shows the 3-D radiation pattern for the above resonant frequencies.

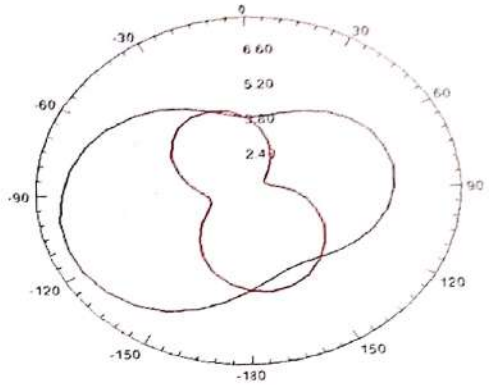

(a)

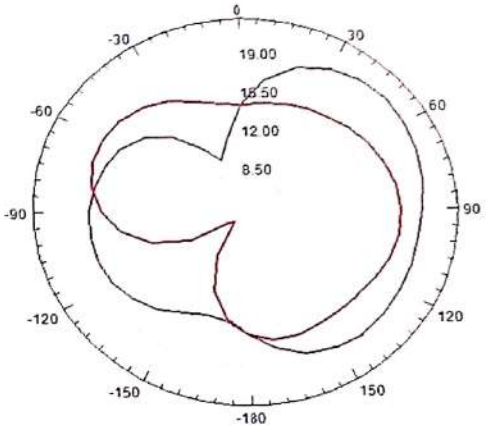

(b)

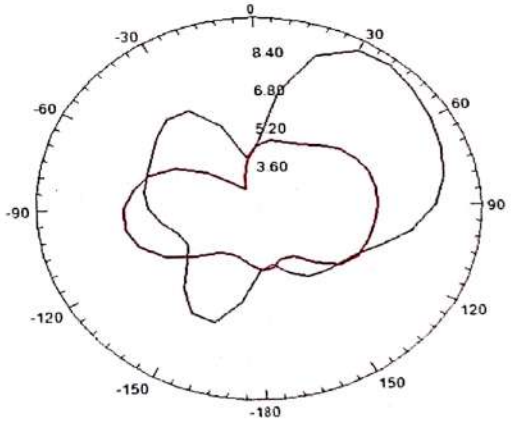

(c)

Fig 5: Radiation Pattern of proposed MPA at

(a) 3.4GHz (b) 7.5GHz (c) 10.5GHz

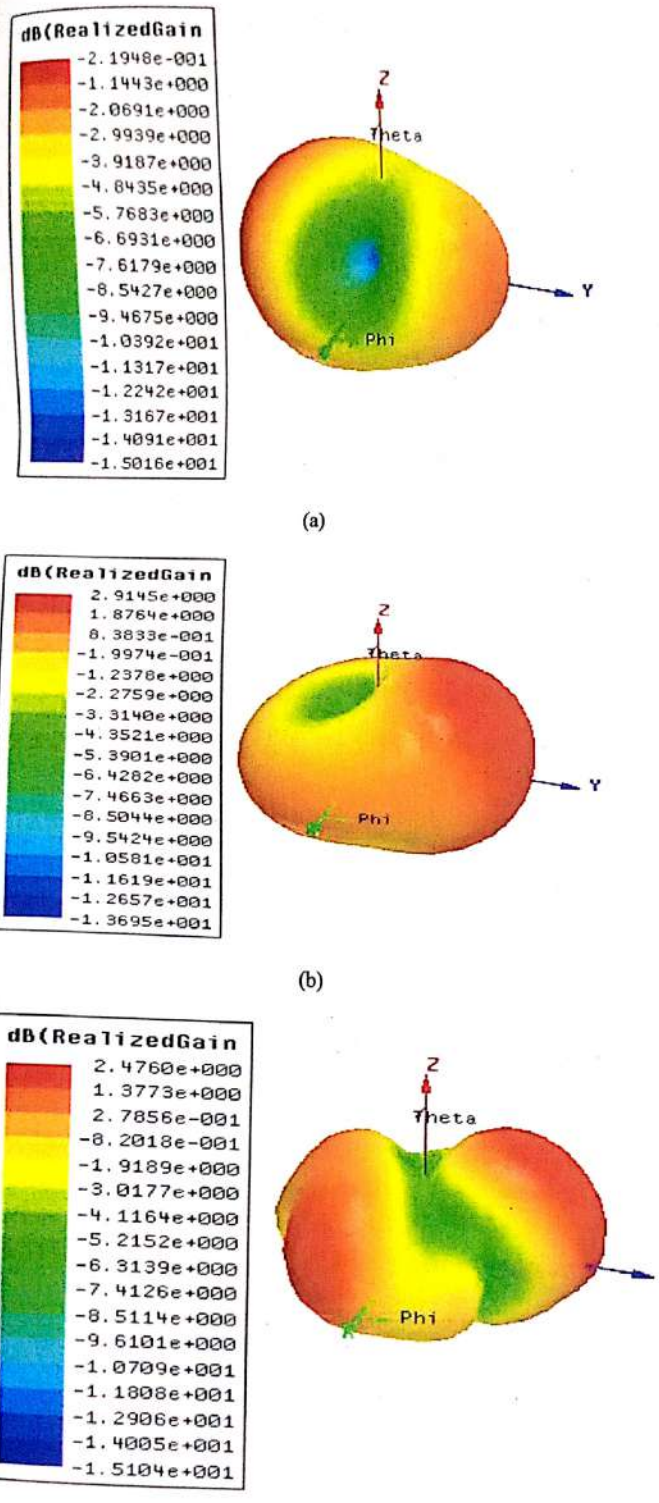

Fig 6: 3-D polar plot of proposed MPA at

(a) 3.4GHz (b) 7.5GHz (c) 10.5GHz

IV. Conclusion

In this paper we designed a dual band microstrip patch antenna. By introducing crossed strip lines in ground plane and meander line at patch we improved the return loss (S_{11}) and VSWR with amazing bandwidth (4.6GHz) in comparison with reference antenna [2]. This antenna also works in middle range of Wi-Max applications. We also analyse the axial ratio, radiation pattern, gain and polar plot for all resonant frequencies. We observed from graph for uplink (7.9-8.4GHz) and downlink (7.25-7.75GHz) frequencies the average gain in 1.5dBi and the axial ratio is near to one that implies circular polarisation in this range (X-band).

V. References

[1]. Constantine A.Balanis,"*Antenna Theory Analysis and Design,*"3rd ed.,Willey Student Edition,pp.1-24,811-876.

[2]. D. Sarkar, K. Saurav, and K. V. Srivastava, "Design of a novel dualband microstrip patch antenna for WLAN/WiMAX applications using complementary split ring resonators and partially defected ground structure," *Proceedings of Progress in Electromagnetics Research Symposium,Taipei, Taiwan,* 854-858, March 2013.

[3]. D. Sarkar, K. Saurav, and K. V. Srivastava, "A Novel Dual-Band Microstrip Patch Antenna Loaded with Fractal CSRR and Partially Defected Ground Structures," *IEEE International Conference on Recent Advances and Innovations in Engineering, 2013.*

[4]. L. H. Weng, Y. C. Guo, X. W. Shi, and X. Q. Chen, "An Overview on Defected Ground Structure," *Progress In Electromagnetic Research B*, Vol. 7, 173–189, 2008.

[5]. Mosallaei, H. and K. Sarabandi, "Antenna miniaturization and bandwidth enhancement using a reactive impedance substrate," *IEEE Transactions on Antennas Propagation*, Vol. 52, No. 9, 2403-2414, 2004.

[6]. G. Jegan, G. Ashok Kumar, A.Vimala Juliet, "Multi Band Microstrip Patch Antenna for Satellite Communication," 978-1- 4244-9182-7/10 ©2010 IEEE.

KIET IJCE KIET International Journal of Communications & Electronics

Volume. No. 4, Issue No. 1, January-June 2016, ISSN: 2320 - 8996

Metamaterial- Inspired Dual- Mode Antenna using Rectangular Type CSRR

Mukul Gupta[1],Monika[2]

M.Tech Student[1], Assistant Professor[2]

Electronics and Communication Department, JAYPEE Institute of Information & Technology, Noida, India

[1]mukuljiit2016@gmail.com, [2]moniktronics@gmail.com

***Abstract*-In this paper a metamaterial-inspired dual-mode antenna using rectangular type CSRR is proposed, Here it is seen that an increase in series capacitance will decrease the resonant frequency at which ZOR mode is achieved using rectangular type CSRR .The resonant frequency of antenna is 2.10 GHz with reflection coefficient up to 21 dB. The electrical size of antenna is $0.531\lambda 0\times 0.272\lambda_0\times 0.010\lambda_0$and ZOR mode is observed at 1.25 GHz. The proposed antenna has gain of 0.8 dB with radiation efficiency of 63%.**

I. INTRODUCTION

ZOR is an attractive feature of CRLH transmission line to miniaturize the antenna size [3, 4].MTM antenna is a class of antennas which use the properties of metamaterial to enhance antenna performance and size reduction. A lot of research is reported based on CRLH TL's in [6, 9] and It is observed that bandwidth can be increased by combining different radiating modes. Several CPW-fed ZOR antennas with extended bandwidth are demonstrated. A compact ZOR antenna using CSRR was proposed which includes an interdigital capacitor loaded on patch of antenna and rectangular type CSRR etched on ground plane [5].

II. ANTENNA DESIGN AND ANALYSIS

The geometry of the proposed MTM antenna using interdigital capacitor and rectangular type CSRR as shown in Figure 1. This structure comprises a patch on which interdigital capacitor loaded and arectangular CSRR etched on the ground plane. The entire structure is implemented on an FR4 epoxyglass substrate (ε_r= 4.4, tan δ = 0.02) with 1.6mm thickness. Analysis is carried out inorder to achieve optimized design dimensions of the proposed antenna. The optimal design parametersof the proposed MTM antenna are shown in Table1.

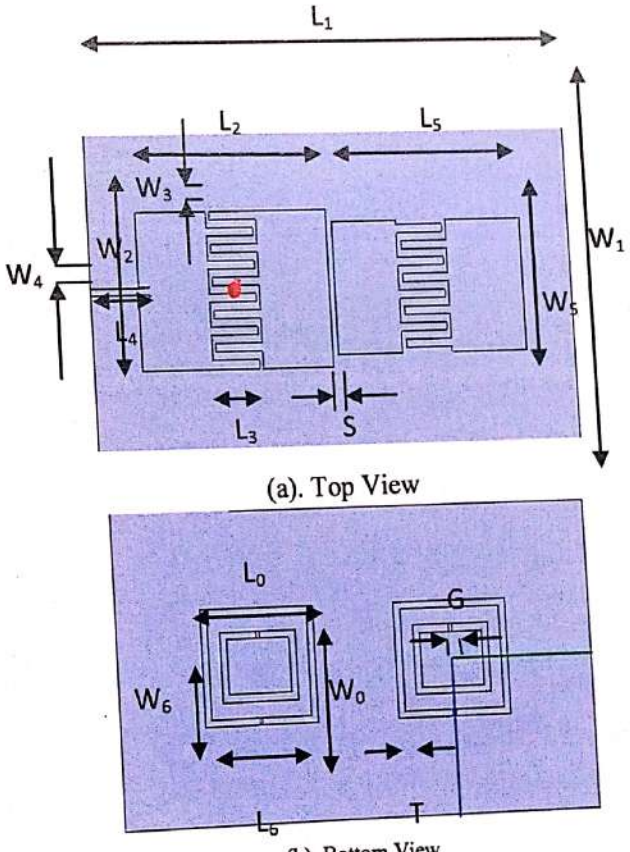

Figure 1: Geometry of proposed antenna, (a) Top view, (b) Bottom view

Table 1: Dimensions of proposed antenna

Parameter	Unit(mm)	Parameter	Unit(mm)
L_1	76	W_5	17
W_1	40	L_6	12
L_2	30	W_6	9
W_2	20	L_0	18
L_3	7.3	W_0	15
W_3	1	G	0.4
L_4	9.25	S	0.8
W_4	1	H	1.6
L_5	30	T	1

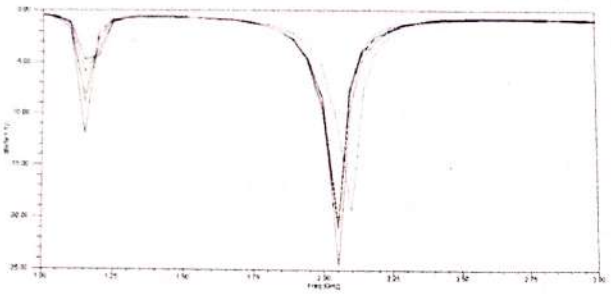

Figure2: Simulated input reflection coefficients of proposed antenna by varying interdigital capacitor finger length L_3

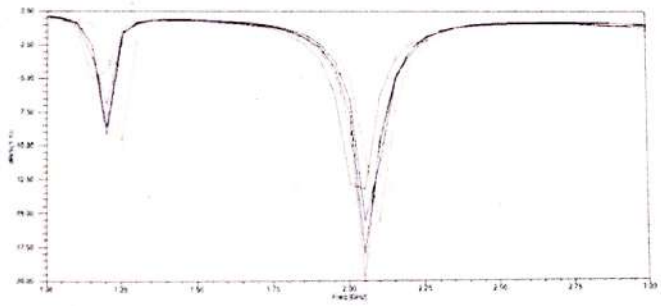

Figure 3: Simulated input reflection coefficients of proposed antenna by varying CSRR thickness T

This antenna design is based on CRLH metamaterial transmission line structure which has two modes by using IDC and CSRR. By using analysis get that n=0 mode is found due to rectangular type CSRR as shown in Figure 2 and n=1 mode is due to coupling between interdigital capacitor and rectangular type CSRR. Figure 3 shows that first order resonant frequency can be tuned by varying the length of inter-digital capacitor while ZOR frequency remains unchanged. This is because increase in length of interdigital capacitor responds to decreases our antenna resonant frequency (increase series capacitance, decrease series inductance). Similarly, by increasing CSRR thickness, ZOR frequency increased (decreases the shunt capacitance, increases shunt inductance) .coupling capacitance act between patch and ground also play a great role in varying the ZOR frequency.

III.ANTENNA THEORY

Equivalent circuit model of the proposed antenna is shown in Figure4 in which Interdigital capacitor is modeled by series capacitance, L_R is modeled by inductance associated with Interdigital capacitor and feed line, which make series LC circuit. CSRR forms the parallel LC tank circuit. C_C represents the coupling capacitance between patch and ground. These parameters are used in tuning the resonant frequency and electrical size of the antenna. It is realized that ZOR frequency can be tuned by C_C , L_L and C_R while first order frequency can be controlled by series parameters i.e. L_R , C_L and C_C .Therefore, it can increase the bandwidth of antenna by introducing a high shunt inductance and a small shunt capacitance.

Generally it has been seen, ZOR antennas have narrow bandwidth; this is because Q-factor of a ZOR antenna is depends only on C_R and L_L .The narrow bandwidth is due to small L_L and large C_R ,To solve this problem or to extend bandwidth a thick substrate having low permittivity is used but this causes more complex fabrication and reduces design freedom. All these can be overcome by proposed antenna design which is based on large L_L and small C_R, which enhanced bandwidth without decreasing radiation efficiency. This structure provides easy fabrication and offers more design freedom. The dispersion relation for proposed antenna can be obtained by [13]

$$\beta_d = \cos^{-1}\left[\frac{1-S_{11}S_{22}+S_{21}S_{12}}{2S_{21}}\right] \quad (1)$$

Figure 5 shows dispersion diagram of the proposed antenna based on β_d variation with respect to frequency .dispersion diagram has two regions 1. RH region (β>0),2.LH region (β<0). It is found that RH modes achieve after 2.10 GHz and LH modes may be achieved below 1.25 GHz.

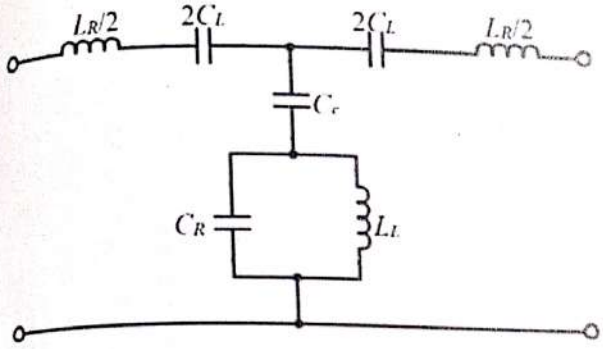

Figure 4: Equivalent Circuit of proposed antenna

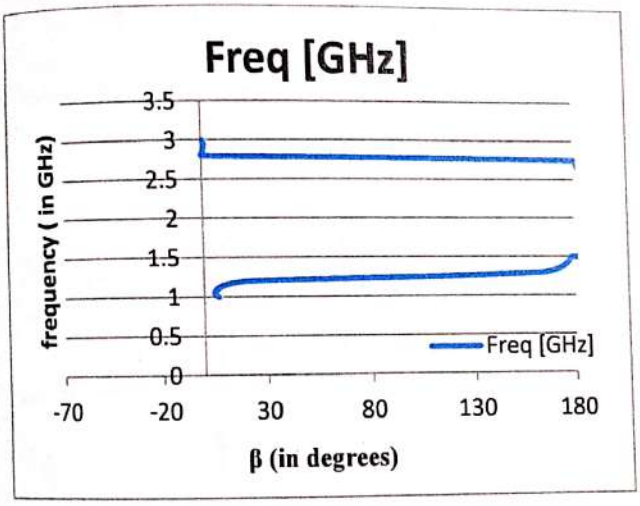

Figure5: Dispersion diagram of the proposed MTM antenna

IV.RESULTS

The simulated reflection coefficient of the proposed antenna is shown in Figure 7. Showing fractional bandwidth of 5.9 % (at the centre frequency 2.08GHz) is found with an extension from 2.02GHz to 2.14GHz. Figure 9 shows the E-field distribution of the proposed MTM antenna at 2.10GHz.It can be clearly seen that first order resonating frequency is due to coupling between Interdigital capacitor and ground plane. It is also seen that ZOR frequency is due to the rectangular type CSRR. The overall electrical size of the antenna is $0.531\lambda_0 \times 0.272\lambda_0 \times 0.010\lambda_0$.Figure 6 shows the simulated reflection coefficients where the resonant frequency is at 2.10 GHz.

Moreover, the bandwidth, radiation efficiency and gain are 5.9%, 63% and 0.8 dBrespectively. From Figure 7, the resonance frequency is 2.10 GHz, the frequencies f_1 and f_2 are given by 2.0210GHz and 2.1440 GHz respectively. Then, the fractional bandwidth can be calculated as 5.9% by using the expression

$$BW\% = \frac{f_2-f_1}{f_c} X100 \quad (2)$$

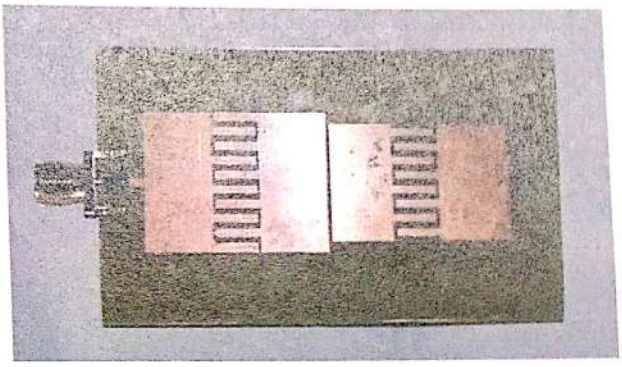

(a). Top View

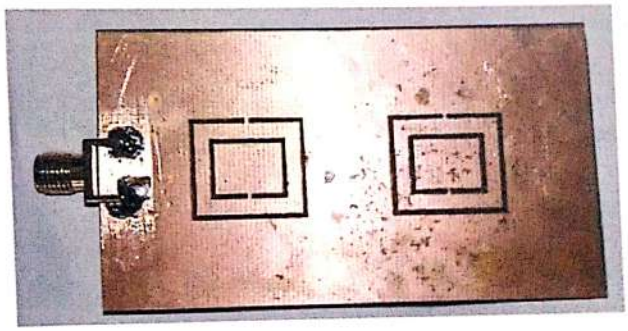

(b). Bottom View

Figure 6: Prototype of fabricated antenna, (a) Top view, (b) Bottom view

KIET IJCE KIET International Journal of Communications & Electronics

Volume. No. 4, Issue No. 1, January-June 2016, ISSN: 2320 - 8996

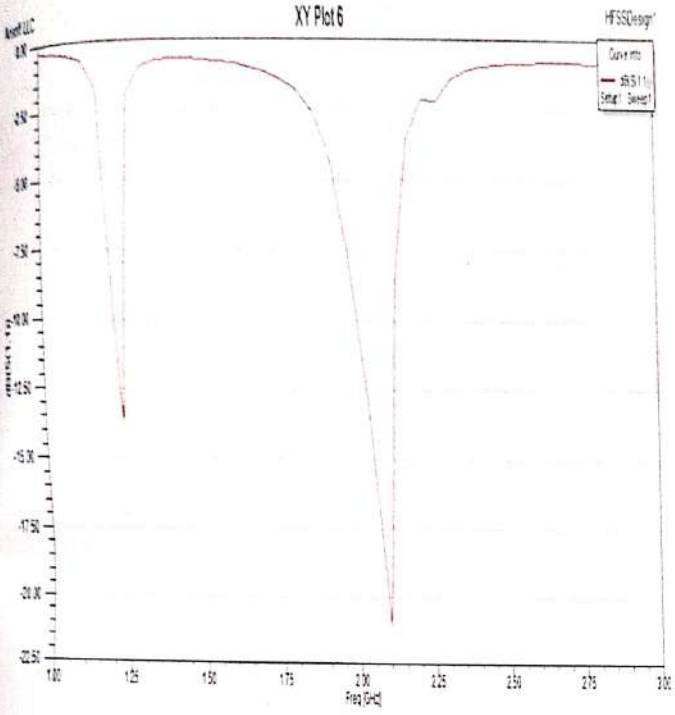

Figure 7: Simulated input reflection coefficient of the proposed antenna

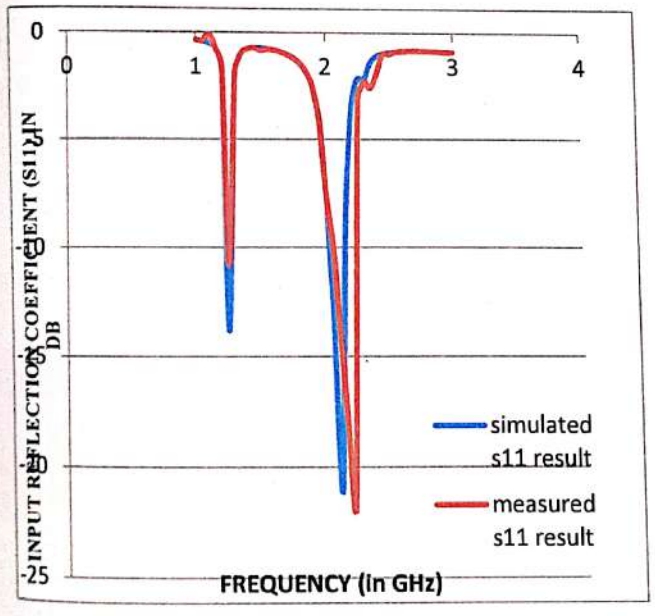

Figure 8: Comparison of simulated and measured input reflection coefficient of proposed antenna

Table 2: Summary of the proposed ZOR antenna at two resonant frequencies

Frequency (GHz)	1.25	2.10
Bandwidth (%)	3.2	5.9
Gain (dB)	-13.66	-0.81
Efficiency (%)	28	63

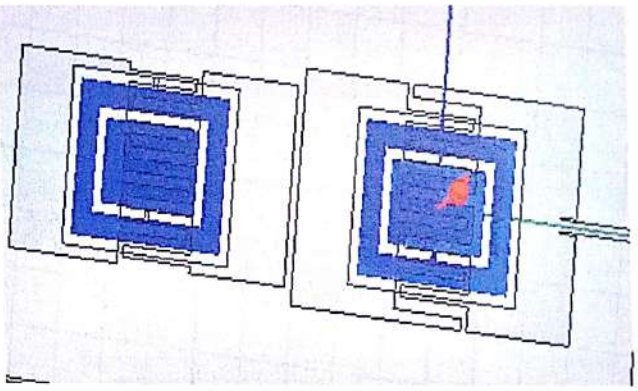

(a)

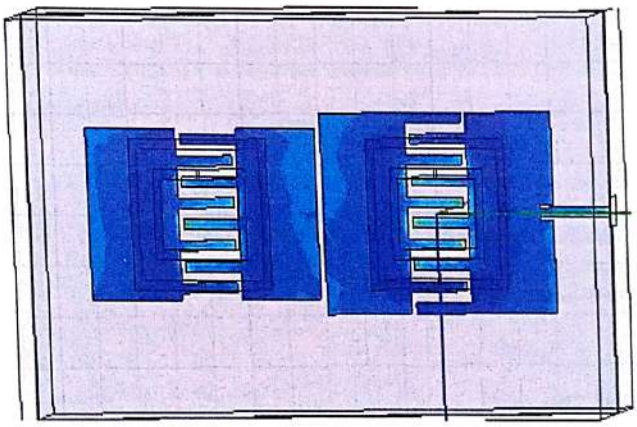

(b)

Figure 9: E-field distribution of proposed antenna, (a) for CSRR, (b)) for interdigital capacitor at 2.10 GHz

Table 3: Comparison with earlier published work

Design and Feeding Technique	Frequency (GHz)	Bandwidth (%)	Electrical size of the whole antenna	Feeding Technique
This work	2.10	5.9	$0.531\lambda0 \times 0.272\lambda0 \times 0.010\lambda0$	Microstrip
[5]	2.14	5.3	$0.321\lambda0 \times 0.285\lambda0 \times 0.011\lambda0$	Microstrip
[10]	3.82	4.9	$0.505\lambda0 \times 0.442\lambda0 \times 0.02\lambda0$	Microstrip
[19]	2.66	4.1	$0.35\lambda0 \times 0.35\lambda0 \times 0.013\lambda0$	CPS-like

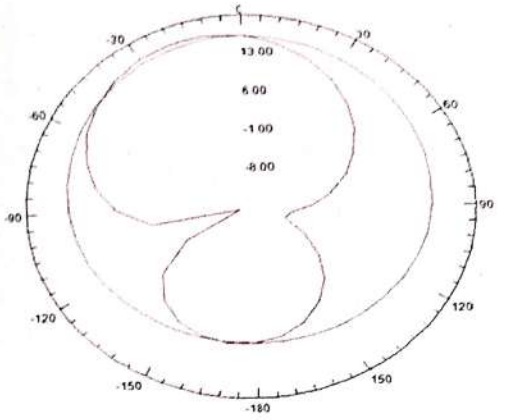

(a)

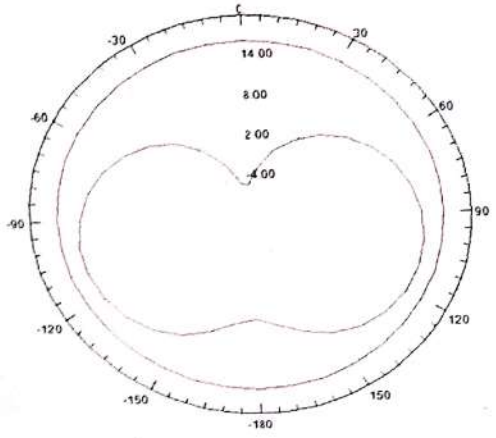

(b)

Figure 10: Simulated radiation pattern of the proposed antenna at 2.10 GHz, (a) at xz-plane, (b) at yz plane

V. CONCLUSION

A MTM antenna using rectangular type CSRR and Interdigital capacitor is proposed here. It is seen that dimensions (size) of antenna can be miniaturized by varying the length of Interdigital capacitor. It is observed that operating frequency of antenna can be tuned by varying CSRR thickness. Dispersion relations are found by calculating β_d. The overall size of the antenna is $0.531\lambda_0 \times 0.272\lambda_0 \times 0.010\lambda_0$. Impedance matching is achieved at 21 dB with fractional bandwidth of 5.9%. The proposed antenna has antenna gain of 0.8dB with 63 % simulated antenna radiation efficiency at the operating frequency of 2.10 GHz. The proposed metamaterial antenna exhibits dual-band behavior with first band centered at 1.25GHz and second band centered at 2.10 GHz. Radiation patterns of field are consistent throughout the antenna working band shown in Figure 10. With all these features, proposed antenna can be operated at various wireless standards such as GPS, UTMS, and CNSS.

VI. REFERENCES

[1]. Shelby, R. A., D. R. Smith, and S. Schultz, "Experimental verification of a negative index of refraction," *Science*, Vol. 292, No. 5514, 77–79, 2001.

[2]. Caloz, C. and T. Itoh, "Novel microwave devices and structures based on the transmission line approach of metamaterials," *IEEE-MTT Int. Symp.*, Vol. 1, 195–198, Philadelphia, PA, USA,Jun. 2003.

[3]. Sanada, A., C. Caloz, and T. Itoh, "Novel zeroth order resonance in composite right/left-handed transmission line resonators," *Asia-Pacific Microwave Conference*, Seoul, Korea, Nov. 2003.

[4]. Niu, B. J. and Q. Fang, "Bandwidth enhancement of CPW-fed antenna based on epsilon negative zeroth and first-order resonators," *IEEE Antennas and Wireless Propagation Letters*, Vol. 12, 1125–1128, 2013.

[5]. Sharma, S. K., A. Gupta, and R. K. Chaudhary, "A compact dual-mode metamaterial-inspired antenna using rectangular type CSRR," *ProgressIn Electromagnetics Research Letters*, Vol. 57, 35–42, 2015.

[6]. Kim, T. G. and B. Lee, "Metamaterial based compact zeroth order resonant antenna," *Electronics Letters*, Vol. 45, No. 1, 12–13, 2009.

[7]. Dong, Y. and T. Itoh, "Miniaturized substrate integrated waveguide slot antennas based on negative zeroth order resonance," *IEEE Transactions on Antennas and Propagation*, Vol. 58, No. 12, 3856–3864, 2010.

[8]. Antoniades, M. A. and G. V. Eleftheriades, "A folded-monopole model for electrically small NRITL metamaterial antennas," *IEEE Antennas and Wireless Propagation Letters*, Vol. 7, 425–428,2008.

[9]. Schubler, M., J. Freese, and R. Jakoby, "Design of compact planar antennas using LH-transmission lines," *IEEE MTT-S Int. Microw. Symp. Dig.*, 209–212, Fort Worth, TX, Jun. 2004.

[10]. Ha, J., K. Kwon, Y. Lee, and J. Choi, "Hybrid mode wideband patch antenna loaded with aplanar metamaterial unit cell," *IEEE Transactions on Antennas and Propagation*, Vol. 60, No. 2, 1143–1147, 2012.

[11]. Jang, T., J. Choi, and S. Lim, "Compact coplanar waveguide (CPW)-fed zeroth-order resonant antennas with extended bandwidth and high efficiency on a vialess single layer," *IEEE Transactionson Antennas and Propagation*, Vol. 59, No. 2, 363–372, 2011.

[12]. Niu, B. J. and Q. Y. Feng, "Bandwidth enhancement of asymmetric coplanar waveguide (ACPW)-fed antenna based on composite right/left handed transmission line," *IEEE Antennas and WirelessPropagation Letters*, Vol. 12, 563–566, 2013.

[13]. Singh, G. K., R. K. Chaudhary, and K. V. Shrivastava, "A compact zeroth order resonating antenna using complementary split ring resonator with mushroom type of structure," *ProgressIn Electromagnetics Research Letters*, Vol. 28, 139–148, 2012.

[14]. Mart´ınez, F. J. H., G. Zamora, F. Paredes, F. Mart´ın, and J. Bonache, "Multiband printed monopole antennas loaded with OCSRRs for PANs and WLANs," *IEEE Antennas and WirelessPropagation Letters*, Vol. 10, 1528–1531, 2011.

[15]. Sharma, S. K., A. Gupta, and R. K. Chaudhary, "Compact CPW-fed CHSSR antenna for WLAN," *IEEE International Microwave and RF Conference (IMaRC)*, 115–117, Bangalore, 2014.

[16]. Baena, J. D., J. Bonache, J. F. Martin, et al., "Equivalent-circuit models for split-ring resonators and complementary split-ring resonators coupled to planar transmission lines," *IEEE Transactionson Microwave Theory and Techniques*, Vol. 53, No. 4, 1451–1461, 2005.

[17]. Si, L.-M. and X. Lv, "CPW-fed multi-band omni-directional planar microstrip antenna using composite metamaterial resonators for wireless communications," *Progress In ElectromagneticsResearch*, Vol. 83, 133–146, 2008.

[18]. Lai, A., K. M. K. H. Leong, and T. Itoh, "Infinite wavelength resonant antennas with monopolar radiation pattern based on periodic structures," *IEEE Transactions on Antennas and Propagation*, Vol. 55, No. 3, 868–876, 2007.

[19]. Majedi, M. S. and A. R. Attari, "A compact broadband metamaterial-inspired antenna," *IEEE Antennas and Wireless Propagation Letters*, Vol. 12, 345–348, 2013.